Report #24-UR-146

NSTSCE

National Surface Transportation Safety Center for Excellence

Traffic Sign Characteristics for Machine Vision Safety Benefits

• Andrew Kassing • Ronald Gibbons • Eric Li • Matthew Palmer • Johann Hamen • Alejandra Medina

Submitted: July 3, 2024

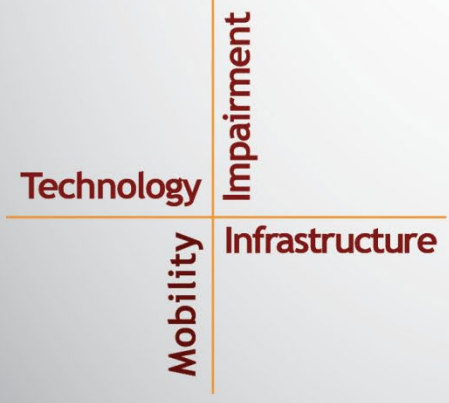

Housed at the Virginia Tech Transportation Institute
3500 Transportation Research Plaza • Blacksburg, Virginia 24061

ACKNOWLEDGMENTS

The authors of this report would like to acknowledge the support of the stakeholders of the National Surface Transportation Safety Center for Excellence (NSTSCE): Zac Doerzaph from the Virginia Tech Transportation Institute; John Capp from General Motors Corporation; Terri Hallquist from the Federal Motor Carrier Safety Administration; Mike Fontaine from the Virginia Department of Transportation and the Virginia Transportation Research Council; and Melissa Miles from State Farm Insurance.

The NSTSCE stakeholders have jointly funded this research for the purpose of developing and disseminating advanced transportation safety techniques and innovations.

EXECUTIVE SUMMARY

Machine vision has become a central technology for the development of automated driving systems and advanced driver assistance systems. To support safe navigation, machine vision must be able to read and interpret roadway signs, which provide regulatory, warning, and guidance information for all road users. Complicating this task, transportation agencies use a large variety of signs, which can have significantly different shapes, sizes, contents, installation methods, and retroreflectivity levels. Additionally, many environmental factors, such as precipitation, fog, dew, and lighting, also affect the visibility and legibility of roadway signs.

While industry has been devoting effort to sign detection and recognition, understanding how environmental factors and sign conditions affect machine vision performance will be important for transportation agencies to maximize the technology's safety benefits. Recognizing this significance, the National Surface Transportation Safety Center for Excellence (NSTSCE) stakeholders funded the research presented in this report to study the environmental factors affecting sign visibility and legibility relevant to vehicle vision performance.

The research team began by conducting a literature review cataloguing current research concerning roadway sign and visual performance, vehicle vision systems, and sign significance for automated driving. Information and insight gained during the literature review process informed the design and system development of data collection systems. Field data collection was then performed over the course of 3 months in late spring to early summer in 2021. Simultaneously, sign data were harvested using Google Street View and mapped using ArcGIS. Data collected during the experimental trips were then reduced and carefully prepared for analysis. Researchers conducted a thorough data analysis, particularly looking at sign location, viewing distance, sign color, font size, sun position, and illumination, to assess the impact of many environmental and infrastructure factors on the legibility of sign characters.

The results of the analysis showed the following:

- Blue and brown signage with white legend text, which commonly appeared on supplemental guide signage, provided the best chance of sign character legibility during the daytime. These color schemes have restricted use cases, and consideration should be given to moving vehicle vision system information onto signage with dark background and white legend text, especially for small letters.

- Sign characters were easy to read during the day at all three experimental distances (200, 400, and 500 ft), with small characters becoming less legible as view distance increased. Nighttime data suggested that increasing font size would help vehicle vision systems identify sign characters at 500 ft.

- Daytime legibility decreased as light levels decreased. Sign images captured at nighttime illumination levels had poor legibility results.

- Font size increases correspond to an increase in legibility rating and the odds of being legible. Daytime legibility plateaus around a 12-inch letter size, and font sizes beyond 12-

inches were found to offer no improvement in the expected legibility of sign characters for vehicle vision systems.

- Sign characters on overhead signage were found to be more legible and are expected to be identified at a higher rate by vehicle vision systems. Systems not designed for high-speed image capture will struggle to read roadside signage at highway speeds. In addition, overhead signage may suffer from less dynamic visual obstruction, as only very tall vehicles would obscure them, but heavy traffic flow was found to frequently block camera vision for roadside signage.

- Data collection efforts found that vehicle vision systems should use a high-quality camera capable of taking pictures at night without motion blur. Experimental images suffered from unexpected quality issues that impacted nighttime legibility assessments.

Based on the experience gained from this effort, the research team has the following recommendations to advance future research into machine sign vision:

- Conduct controlled testing using a variety of capable and established machine vision tools to assess the visibility needs of roadway signage. Studying the most common sign locations and types would help to standardize lighting practice for automated vehicle technologies.

- Subsequent research should consider the stroke width of the sign characters in addition to the font size.

- Sign image quality was limited by the image capturing technologies used in the data collection. Future data collection efforts should look to employ a high-sensitivity camera that allows for high shutter speed images and performs at low lighting levels. Consideration should be given to vehicle speed, as this may be a limiting factor for shutter speed. In addition, cameras must be able to capture the full range of sign locations, whether vertically or horizontally offset.

- Future research should assess the influence of weather conditions. This effort was limited by the naturalistic approach of the study, which did not encounter much inclement weather. Additionally, further investigations should consider conditions where dew and condensation are evident on the sign surface.

- Future research efforts should study the influence of sun position under more controlled conditions. Sun position analyses were limited by the naturalistic approach of this study. Additional research should look to identify problematic sun positions and consider if lighting design needs should adapt.

- Future research should evaluate sign lighting needs for machine vision applications. This study was limited by the practical implementation of signage by the *Manual on Uniform Traffic Control Devices*. Consideration of alternative sign character sizes, sign locations, and color schemes could lend insight into the lighting needs of sign machine vision.

TABLE OF CONTENTS

LIST OF FIGURES

LIST OF TABLES

LIST OF ABBREVIATIONS AND SYMBOLS

AASHTO	American Association of State Highway Transportation Officials
ANOVA	analysis of variance
CAN	Controller Area Network
CART	classification and regression tree
CCD	charge-coupled device
CMOS	complementary metal oxide semiconductor
CMS	changeable message sign
CNN	convolutional neural network
CSV	comma separated value
GLM	generalized linear modeling
GPS	Global Positioning System
HAV	highly automated vehicle
HOG	histogram of oriented gradients
HSI	Hue Saturation Intensity
HSV	Hue Saturation Value
INNC	iterative nearest neighbors classifier
IVC	International Visibility Code
LIDAR	light detection and ranging
MOR	Meteorological Optical Range
MUTCD	Manual on Uniform Traffic Control Devices
NCHRP	National Cooperative Highway Research Program
NHTSA	National Highway Traffic Safety Administration
NOAA	National Oceanic and Atmospheric Administration
NSTSCE	National Surface Transportation Safety Center for Excellence
OCR	optical character recognition
REIMS	Roadway and Environment Information Measurement System
RFID	Radio-Frequency Identification
RLMMS	Roadway Lighting Mobile Measurement System
ROI	regions of interest
SIFT	Scale Invariant Feature Transform

SHS	Standard Highway Signs
SNR	signal noise ratio
SVM	support vector machine
TSR	transportation safety research
VTTI	Virginia Tech Transportation Institute

CHAPTER 1. INTRODUCTION

BACKGROUND

The development and deployment of automated and advanced vehicle functions are progressing quickly. Regardless of their primary focuses, advanced vehicle safety and navigational features require abundant external information relevant to the roadway and traffic, of which 90% is obtained visually.[1] As the roadways are configured to provide visual information, vehicle vision systems become a vital part of modern vehicles for collecting information needed to support automated decision-making or provide driver guidance.

As an integral part of the roadway environment, roadway signs provide regulatory, warning, and guidance information for all road users. Transportation agencies use a large variety of signs, which can have significantly different shapes, sizes, contents, installation methods, and retroreflectivity levels. Many environmental factors, such as precipitation, fog, dew, and lighting can also affect the visibility and legibility of roadway signs. The reliable detection and recognition of such signs therefore becomes a major challenge for vehicle vision systems.

The automotive and related industries have been devoting significant efforts to sign detection and recognition. Understanding how environmental factors and sign conditions affect machine vision performance, however, can be important for transportation agencies to take actions to maximize machine vision safety benefits. Recognizing the significance, the National Surface Transportation Safety Center for Excellence (NSTSCE) stakeholders funded this research to study the environmental factors affecting sign visibility and legibility relevant to vehicle vision performance.

RESEARCH TASKS AND REPORT ORGANIZATION

This report is presented chronologically to highlight the major research tasks completed. The research team began by conducting a literature review cataloguing current research concerning roadway sign and visual performance, vehicle vision systems, and sign significance for automated driving. Information and insight gained during the literature review process informed the design and system development of data collection systems. Field data collection was then performed over the course of 3 months in late spring to early summer in 2021. Simultaneously, sign data were harvested using Google Street View and mapped using ArcGIS. Data collected during the experimental trips was then reduced and carefully prepared for analysis. Researchers conducted a thorough data analysis to assess the impact of many environmental and infrastructure factors on the legibility of sign characters. The research effort concluded with the creation of this report.

CHAPTER 2. LITERATURE REVIEW

ROADWAY SIGNS AND VISUAL PERFORMANCE

Introduction to Roadway Signs

The *Manual on Uniform Traffic Control Devices* (MUTCD) and *Standard Highway Signs* (SHS) contain detailed inventory and guidelines for the design, placement, operation, and maintenance of traffic signs.[2,3] This section, therefore, is developed largely based on these two references and is mostly applicable to signs used in the U.S. The MUTCD defines signs based on their functions into regularity, warning, and guide signs. Based on their applications, the manual organizes roadway signs into the following groups:

- Regulatory signs, barricades, and gates
- Warning signs and object markers
- Guide signs for conventional roads
- Guide signs for freeways and expressways
- Toll road signs
- Preferential and managed lane signs
- General information signs
- General service signs
- Specific service signs
- Tourist-oriented directional signs
- Changeable message signs
- Recreational and cultural interest area signs
- Emergency management signs

The following sections summarize the major characteristics of roadway signs that have implications to vehicle vision performance on the detection and reorganization of signs. Note that although most signs on major roadways follow relevant standards and guidelines for the design and installation, many signs, particularly those installed earlier and/or on local/private roadways, can deviate significantly from current standards.

Shape

A sign, depending on its type, can have one of the following shapes:[2]

- Octagon, exclusively for stop signs
- Equilateral triangle pointed down, exclusively for yield signs
- Circle, exclusively for grade crossing advance warning signs

- Pennant shape/isosceles triangle, exclusively for no passing zone signs
- Pentagon pointed up with squared bottom corners, exclusively for school advance warning signs
- Pentagon pointed up with tapered bottom corners, exclusively for county route signs
- Crossbuck, exclusively for grade crossing signs
- Diamond, for warning signs
- Rectangle (including square), for regulatory, guide, and warning signs
- Interstate shield and U.S. highway shield, for route signs
- Trapezoid, for recreational and cultural interest area signs and national forest route signs

In addition to these standard sign shapes, different states/localities may use unique shapes for certain types of signs. Examples of such cases include route marker signs on state highways, signs on private roads, and signs installed prior to the current MUTCD.

Color

Roadways signs use a variety of colors for their legends and background. Table 1 summarizes the commonly used colors for sign legend and background based on MUTCD.

Table 1. Common sign colors by sign type.[(2)]

Sign Type	Legend								Background										
	Black	Green	Red	White	Yellow	Orange	Fluorescent Yellow-Green	Fluorescent Pink	Black	Blue	Brown	Green	Orange[1]	Red[1]	White	Yellow[1]	Purple	Fluorescent Yellow-Green	Fluorescent Pink
Regulatory	X		X	X					X					X	X				
Prohibitive			X	X										X	X				
Permissive		X													X				
Warning	X															X			
Pedestrian	X															X		X	
Bicycle	X															X		X	
Guide				X								X							
Interstate Route				X						X				X					
State Route	X														X				
U.S. Route	X														X				
County Route					X					X									
Forest Route				X							X								
Street Name				X								X							
Destination				X								X							
Reference Location				X								X							
Information				X						X		X							
Evacuation Route				X						X									
Road User Service				X						X									
Recreational				X							X	X							
Temporary Traffic Control	X												X						
Incident Management	X												X						X
School	X																	X	
ETC-Account Only	X																X[2]		
Changeable Message Signs																			
Regulatory			X[3]	X					X										
Warning					X				X										
Temporary Traffic Control					X	X			X										
Guide				X					X			X[4]							
Motorist Services				X					X	X[4]									
Incident Management					X			X	X										
School, Pedestrian, Bicycle					X		X		X										

[1]Fluorescent versions of these background colors may also be used.
[2]The use of the color purple on signs is restricted per the provisions of Section 2F.03 in MUTCD.
[3]Red is used only for the circle and slash or other red elements of a similar static regulatory sign.
[4]These alternative background colors would be provided by blue or green lighted pixels such that the entire changeable message sign (CMS) would be lighted, not just the legend.

Letters and Symbols

Word messages on the majority of the roadway signs currently used in the nation are of two types of fonts: the Highway Gothic series (commonly known as the Standard Alphabets for

Highway Signs) and the less commonly used Clearview font series.[4] The Standard Alphabets contains six letter series with increasingly wider letter forms and letter strokes designed for rapid viewing and recognition in a driving environment. MUTCD assumes a minimum specific ratio of 1 inch of letter height per 30 feet of legibility distance for letter size selection. On conventional roadways, MUTCD requires sign letter sizes at least 6 in. in height for upper case letters except for low-volume roadways with a speed limit of 25 mph or lower, where letters need to be at least 4 in. in height. On freeways and express ways, MUTCD requires a minimum letter height of 8 in. The manual also specifies that the height (defined as the nominal loop height) of lower-case letters should be ¾ of the height of the upper-case letters for signs with messages of mixed cases.[2]

In addition to word messages, roadway signs use a large variety of symbols to graphically convey messages that would otherwise be difficult to describe using limited words. The *United States Road Symbol Signs* contains a catalog of symbol signs commonly used in the country and approved by the current MUTCD.[5] New symbol designs are, however, continuously adopted by FHWA based on research evaluations.

Retroreflectivity

The MUTCD requires that roadway signs be either retroreflective or illuminated to show their shape and color in both daytime and nighttime. Retroreflective signs can reflect vehicle headlight back to drivers, and therefore are more visible during the nighttime or other conditions with lower visibility. The retroreflectivity of sign materials is enabled by special paints consisting of glass beads or microprisms (Figure 1). The ASTM D4956 standard categorizes sign sheeting materials into 11 types based on their retroreflection capability, with type XI having the highest retroreflectivity level.[6] At a given observation angle of 0.2° and entrance angle of -4°, the type XI sheeting can be 11 times brighter than the type I sheeting for white color legends. Sign sheeting of higher quality (with a higher grade of retroreflectivity) is associated with lower life-cycle costs as well as higher safety benefits.[7,8]

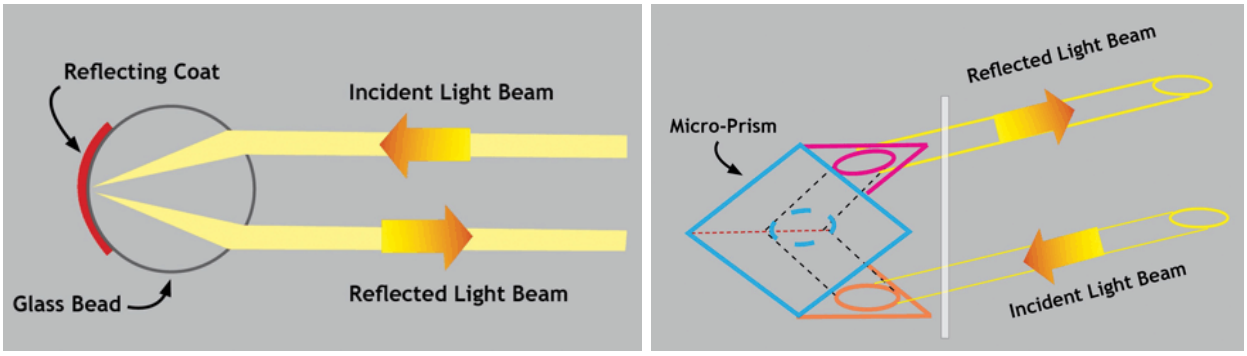

Figure 1. Diagram. Retroreflection mechanism of glass beads and micro-prisms.[9]

The retroreflectivity of sign sheeting degrades over time. The degradation rate depends on multiple factors such as installation orientation, elevation, solar radiation levels, temperature, precipitation, color, and air pollutants.[10-13] The MUTCD requires transportation agencies to maintain sign retroreflectivity at or above the minimum levels specified in Table 2. However, it is not rare for signs, including some on major arterials, to not meet the specified minimum levels.

Table 2. Minimum maintained retroreflectivity levels.[2]

Sign Color	Sheeting Type (ASTM D4956-04)				Additional Criteria
	Beaded Sheeting			Prismatic Sheeting	
	I	II	III	III, IV, VI, VII, VIII, IX, X	
White (W) on Green (G)	W*; G ≥ 7	W*; G ≥ 15	W*; G ≥ 25	W ≥250; G ≥ 25	Overhead
	W*; G ≥ 7	W ≥ 120; G ≥ 15			Post-mounted
Black on Yellow (Y) or Black on Orange (O)	Y*; O*	Y ≥ 50; O ≥ 50			[1]
	Y*; O*	Y ≥ 75; O ≥ 75			[2]
White on Red (R)	W ≥ 35; R ≥ 7				[3]
Black on White	W ≥ 50				-

The minimum maintained retroreflectivity levels shown in this table are in units of cd/lx/m^2 measured at an observation angle of 0.2° and an entrance angle of -4.0°
[1]For text and fine symbol signs measuring at least 48 inches and for all sizes of bold symbol signs.
[2]For text and fine symbol signs measuring less than 48 inches.
[3]Minimum sign contrast ratio ≥ 3:1 (white retroreflectivity ÷ red retroreflectivity)
*This sheeting type is not used for this color for this application.

Illumination

The current MUTCD does not contain detailed guidelines or requirements on sign illumination and, therefore, different states frequently have different practices for illuminating highway signs. As almost all highway signs are made with retroreflective materials, transportation agencies typically only provide illumination to certain types of signs, such as overhead signs on freeways and overhead street name signs.(14) Sign illumination can be provided either externally or internally. Internally illuminated signs are generally overhead street name signs with lights enclosed within the sign to illuminate the sign message, utilizing the different colors and transparency levels of the sign face materials. The latest American Association of State Highway Transportation Officials (AASHTO) *Roadway Lighting Design Guide* provides guidelines for establishing a threshold level of legend luminance based on specific levels of visual complexity to accommodate the needs of nighttime motorists.(14) To sufficiently and uniformly illuminate sign faces, the luminaires may be located on either the top of the sign, the bottom of the sign, or an adjacent support. Note that, depending on the types of lighting source and color temperatures, sign illumination may alter the original color of the illuminated signs.

Placement

Depending on the type of the roadway, the type of the signs, and right-of-way constraints, the standardization of roadway signs is in many cases impractical. Signs can be installed on an overhead structure, either or both sides of the roadway, and on the median, channelization, or centerline of the roadway. The latest MUTCD contains the following guidelines regarding sign height:

- A minimum of 5 ft. vertical clearance from the pavement for signs at the side of rural roads
- A minimum of 7 ft. vertical clearance from the curb for signs at the side of urban roads

- For collocated signs at the side of roadways, the vertical clearance of the lowest sign may be 1 ft. less
- A minimum of 7 ft. vertical clearance from the pavement for signs at the side of freeways
- A minimum of 5 ft. vertical clearance from the pavement for signs installed below another sign at the side of freeways
- A minimum of 17 ft. vertical clearance from the pavement for overhead signs except where the structures on which the sign is to be mounted have a lower vertical clearance

The lateral clearance of the signs can be subject to many factors, such as right-of-way constraints, type of roadway, presence of clearance zones, roadside objects/obstructions, and other cross section elements. In general, the placement of traffic signs needs to meet sign visibility, safety, and practicality. The MUTCD also recommends that the placement of signs be longitudinal far enough from the intended action location so that drivers can react and make corresponding maneuvers in advance. For example, destination signs should be placed 200 ft or more prior to intersections, which corresponds to 2.0 s reaction time at a 65-mph highway. For more critical warning signs, such as LANE END or MERGE, the sign placement should provide extra time for drivers to adjust the speed or change lanes in heavy traffic, considering possibly existing complex driving situations, which is around 14.0 to14.5 s. In addition, signs are often placed slightly more than perpendicular to the roadway direction to relieve the effect of direct sunlight and specular glare.[2,7,9]

Sign Conspicuity Enhancement

It is a common practice for transportation agencies to use a variety of methods to enhance the conspicuity of standard signs. While such methods can be effective in drawing the attention of human drivers to the signs, some enhancements may result in reduced sign legibility and alteration of the original sign shapes. The following are examples of some commonly used sign enhancement methods:[2]

- Adding a yellow rectangular header panel (with a legend such as notice, new, or state law) above a standard sign
- Adding red or orange flags above a standard sign
- Adding solid or striped strip around the border of a standard sign
- Adding flashing beacons to a standard sign
- Adding steady or flashing LEDs outlining the legend or border of a regular sign
- Adding retroreflective strips on signposts.

Environmental Factors Affecting Sign Visibility and Legibility

Many environmental factors temporarily or permanently affect sign visibility, retroreflectivity, and/or legibility regardless of how long they have been in service. The following are a list of commonly seen factors:

- Sign damage and deterioration. Damage due to environmental deterioration, vehicle collisions, and vandalism can cause signs to become bent, with cracks in sheeting materials, fading, and peeling of sheeting materials, which can significantly reduce sign retroreflectivity levels and cause premature sign failures.[15] The loss of retroreflectivity and the fading of the colors are known to be the primary mechanisms of sign deterioration. As the retroreflective properties deteriorate, the sign becomes less detectable and legible at night. When the colors fade, the sign loses a distinguishing feature, and the contrast between legend and background is reduced, which can make the sign less detectable and legible even during the daytime. Factors such as harsh environmental conditions, time in service, and poor workmanship can all contribute to sign deterioration.[16] While some agencies may routinely inspect their signs, most states and localities do not do so due to staffing and resource constraints.
- Dirt and dust. The presence of dirt, dust, and other materials on the face of signs can affect sign legibility. Dirt and dust on signs may be caused by wind, precipitation, insect/bird activities, emissions and other airborne pollutants, and nearby construction/maintenance/mowing activities. For example, a previous study in Utah showed that signs placed in areas with higher ground elevation that experience frequent snowfall, signs very close to ground, and signs installed in areas with higher concentration of air pollutants were prone to dirt and dust impacts.[17]
- Frost and dew. Sign visibility and retroreflectivity can be significantly affected by adverse weather conditions, such as rain, snow, and fog. For example, a previous study found that the presence of frost and dew on traffic signs could cause an average reduction of 79% and 60%, respectively, in retroreflectivity levels for Type I sign sheeting, and 83% and 40% for Type III sheeting.[18,19]
- Frost can form due to a combination of factors.[20] Clear skies (condition for fast and radiational cooling), calm to light winds (for super-cooled temperatures to develop at surface), and cool temperatures (lower than 42 °F) are generally required for the formation of frost. In addition, frost tends to form in valleys, where cold air tends to settle. Similarly, dew is common in conditions with clear skies, light to no wind, moist soil (due to recent rains), and low nighttime dew point depressions.[21]
- Glare. Sign legibility can also be affected by glare due to strong light from external sources reflected off the sign into a driver's eyes. The retroreflective sheeting on signs themselves sometimes can cause glare during nighttime due to approaching headlamps.

SIGN PERFORMANCE CONSIDERATIONS AND IMPLICATIONS

Traditionally, roadway sign performance is generally evaluated based on human drivers. Driving and navigation is a dynamic visual task significantly affected by sign visibility, vehicle speed, and the driving environment. As the driving environment (e.g., traffic, roadway, and atmospheric conditions) becomes more complex, drivers would naturally concentrate less on detecting and understanding signs. In addition, a driver's peripheral vision degrades as speed increases. Sign performance for human drivers, therefore, takes into account metrics such as ease and time relevant to sign detection and reading, decision-making and responding, and maneuvering.

High-level automated vehicle functions that make decisions and maneuvers in place of human drivers detect and recognize signs instantaneously as soon as it becomes possible to do so. The required maneuvers (e.g., changing lanes, stopping, braking, or turning), therefore, can be initiated instantaneously subject to constraints from roadway, traffic, and/or mechanical performance. Although the execution of non-safety-critical maneuvers by automated systems needs to take into consideration passenger comfort, the overall time required should be much shorter compared to that taken by a human driver.

Machine vision systems primarily intended to provide relevant warning/notification to human drivers, however, would need to enable sufficient time for human drivers to make decisions and complete the appropriate actions. In this regard, decision, reaction, and maneuvering times are still relevant in vehicle vision-based sign detection. Based on a previous literature review[22], a study found that the 85th-percentile decision time for a braking situation ranged between 0.7 and 2.6 s (Table 3). The same literature review also showed a 50th-percentile decision time for a braking situation of 0.50 s and an 85th-percentile decision time of 0.85 s. A study based on 401 simulated lane changes on a multi-lane highway showed an average of 5.14 s for a single lane change.[23] McGee suggested a set of values for decision and maneuvering based on a literature review validated with controlled experiment (Table 4) in a decision in a hazard avoidance situation.[24]

Table 3. 85th-Percentile decision time for braking situation.[22]

Information (bits)	Decision Time (s)	
	Expected	Unexpected
1	0.7	1.0
2	1.3	1.6
3	2.0	2.6

Table 4. Decision and maneuvering times in a hazard avoidance situation.[24]

Design Speed (km/h)	Decision and Initiation of Response (s)	Lane Change (s)
80	4.2 - 6.5	4.5
100	4.7 - 7.0	4.3
120	4.7 - 7.0	4.0
140	4.7 - 7.0	4.0

When combining decision, reaction, and maneuvering, the latest green book recommends durations ranging between 10 and 15 s based on design speeds and maneuvers required (Table 5).

Table 5. AASHTO decision and maneuvering times in a hazard avoidance situation (derived based on decision distances).[25]

Design Speed (mph)	55	60	65	70	75
Speed/path/direction change on rural road	10.72	11.25	11.01	10.76	10.73
Speed/path/direction change on suburban road or street	12.15	12.78	12.80	12.42	12.41
Speed/path/direction change on urban, urban, urban core, or rural town road or street	14.07	14.55	14.32	14.07	14.05

VEHICLE VISION SYSTEMS

Vehicle Vision Technologies Overview

Automation and connectivity have been two major trends for the modern development of transportation. Highly automated vehicle (HAV) technologies are becoming increasingly mature and implementable. Based on the levels of automation defined by the National Highway Traffic Safety Administration (NHTSA)[26], many vehicle models on today's roadways have already been equipped with functions falling into Level 2 (Partial Automation) and Level 3 (Conditional Automation). While providing a multitude of opportunities for improved safety, efficiency, and comfort, such technologies also impose unique needs and requirements for transportation infrastructure.

Automated vehicle functions utilize a variety of sensors to detect, recognize, and track obstacles surrounding a vehicle. Recent advances in software and hardware technologies, combined with increasingly affordable costs, have enabled a boom in vehicle vision applications, propelling the development of HAV functions. Most automated vehicle functions rely on individual or a combination of technologies, such as camera-, lidar-, and radar-based systems (Figure 2).

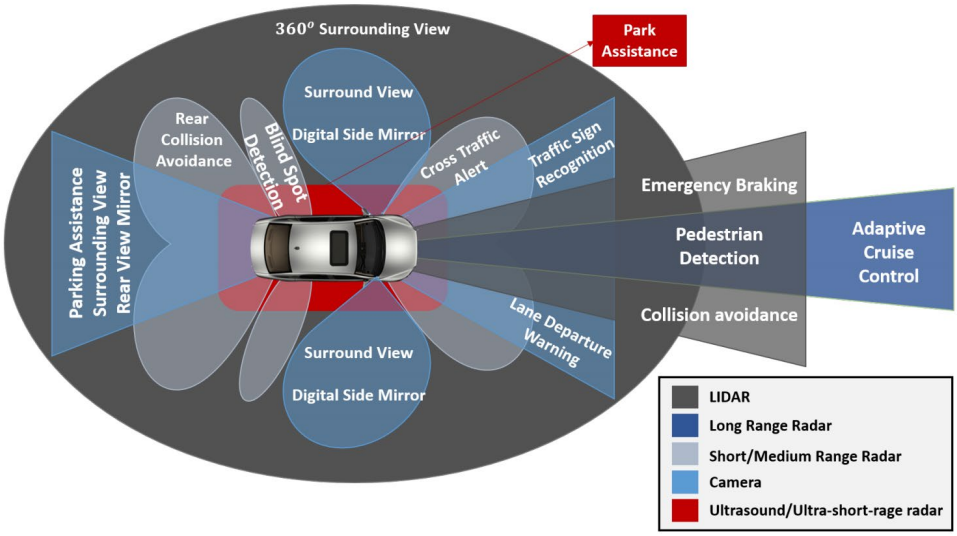

Figure 2. Diagram. Vehicle sensing systems and corresponding functions.[27]

Although vehicle automation technologies are maturing fast, autonomous vehicles are hardly expected to replace human drivers in the near future. Based on a survey conducted in Texas, a study estimated the following adoption rate for various connected and automated vehicle (CAV) technologies by 2045:[28]

- Blind-spot monitoring and emergency automated braking: 59.4%
- Connectivity (for basic safety messaging): 57.9%
- Full self-driving: 38.5%
- Traffic sign recognition: 2% (least desired)

Although it is hard to foresee if such rates are an accurate reflection of future CAV adoption rate, they clearly indicate a significant period of coexistence of automated vehicles and human drivers on the nation's transportation system.

Camera-based Machine Vision

Image Sensing Basics

Among the various sensing technologies used by automated vehicle functions, lidar- and camera-based systems are most relevant to sign detection and recognition. Lidar allows the mapping of the environment surrounding the vehicle, including the physical locations and shapes of traffic signs. For example, researchers previously demonstrated algorithms that took advantage of the high retroreflectivity of sign sheeting materials and used lidar data to map signs in 3D.[29,30] Currently, however, sign detection and particularly recognition for automated vehicle functions are mostly achieved through camera-based systems.

Modern cameras use an aperture or lens to sample the light from objects, then expose the sampled light to a sensor chip made with semiconductor materials with a photoelectric effect. The received light intensities are represented by charges accumulated in each pixel cell due to the photoelectric effect, which are then amplified, stored, and read out by other electric components.[31] The digital image obtained is inherently a numerical matrix consisting of values representing color and brightness for each pixel (e.g., grey value for one-channel camera and RGB values for three-channel cameras).

Most modern cameras use charge-coupled device (CCD) or complementary metal oxide semiconductor (CMOS) image sensors. In a CCD image sensor, pixels are represented by an array of capacitors that allow the conversion of incoming photons into electron charges at the semiconductor-oxide interface when exposed to light. Images are projected through a lens onto the capacitors, making each capacitor accumulate electric charges proportional to the light intensity. A control circuit operates each capacitor to transfer its content to the neighboring capacitor and ultimately to a charge amplifier, which converts the charge into a voltage. By repeating this process, the CCD sensor converts the entire contents of the array to a sequence of voltages, which are then further processed and interpreted. CMOS image sensors are active-pixel sensors with integrated circuits constructed with the CMOS technology (a technology for constructing integrated circuits such as those used in microprocessors and microcontrollers). CMOS image sensors typically contain multiple transistors that amplify and move capacitor charges using more traditional wires.[32,33]

CMOS sensors are manufactured using traditional manufacturing processes for microchips, while CCD sensors require a specialized and expensive manufacturing process. CMOS image sensors are known to be associated with lower cost and higher speed. However, due to their designs, CMOS sensors have lower light sensitivity and are more susceptible to noise. CMOS is becoming increasingly popular due to consumer cameras and certain professional cameras that do not require extremely high-quality images. CCD sensors, however, are typically used for medical and scientific applications. The quality superiority of CCD sensors is increasingly challenged as the CMOS image sensing technology continuously advances.[33] Table 6, for

example, lists some common characteristics of commercially available cameras used for vehicle vision.

Table 6. Technical specifications of common commercially available cameras.[31]

Camera Element	Specification
Number of pixels	640×480 - 4800×3200
Size of pixel	2×2 μm2 - 10×10 μm2
Electronic shutter speed (exposure time)	10 μs - several seconds
Frame rate (decreased for increasing imaging size)	3 Hz - 200 Hz
Signal noise ratio (SNR)	50 dB - 60 dB

Cameras are capable of providing long-range and high-resolution information in ideal weather and illumination conditions, but the image quality can severely deteriorate during low-visibility conditions. In addition, dirt, dust, precipitation, and fog on windshields (if installed inside) or camera lenses (if installed outside) affect camera performance considerably.

Sign Detection and Recognition

Camera-based sign detection and recognition is the process of identifying signs from digital images and then extracting the information that the signs convey using computer algorithms. In the process of sign detection, algorithms first determine a number of regions of interest (ROIs), and then verify the hypothesis of sign presence in each ROI. Based on the techniques of searching ROI, the detection process can be grouped as shape-based or color-based, taking advantage of the fact that signs have relatively regular shapes and uniform designs compared to other outdoor objects.[34] The color-based method, for example, segments the incoming image pixels into different regions based on a number of thresholds. ROIs are determined by looking up the color combinations that determine the characteristics of traffic signs.[35] Many researchers use the RGB color space to implement the color-based technique. However, the accuracy of the detection results based on the RGB method is sensitive to factors such as varying lighting intensities. Some studies therefore use the Hue-Saturation-Intensity/Hue-Saturation-Value (HSI/HSV) color space, CIELUV (CIE 1976 L*, u*, v*) color space, and/or normalized color to identify ROIs.[34]

Many factors can affect colors and therefore the reliability of color-based methods, such as adverse weather conditions, shadow, and sunlight intensity and angle. Shape-based techniques, therefore, can be used in combination to improve sign detection accuracy. Common image processing techniques that are based on object shapes and that search for ROIs with shapes of interest include Hough transform, canny edge detection, and corner detection.[34] During the sign detection process, many researchers utilize machine learning techniques to improve accuracy. For example, Bahmann et al. used Haar-like feature extraction in RGB color space for sign detection[36], and Shi and Lin used support vector machine (SVM) classifiers trained with histogram of oriented gradients (HOG) features to identify ROIs with signs.[37]

Sign classification can be achieved with either a non-learning, template matching method or a machine learning method, with the latter often having more robust performance. The most commonly used template matching method is the normalized cross-correlation to measure the similarity between subject sign image and a sign image template.[38] Examples of such methods

include matching signs by comparing horizontal and vertical color ratios[39] or statistically determine identifying sign characteristics (e.g., using principle component analysis).[40] Machine learning methods, on the other hand, typically apply a feature vector extracting method to the ROI first and then use a machine learning classifier trained with the feature vectors to classify the subject sign. Examples of commonly used feature vector extracting methods in sign recognition algorithms include Haar-like feature, HOG feature, and scale invariant feature transform (SIFT) feature. Examples of machine learning classifiers include SVM, Adaboost, neural network, and classification and regression tree (CART). For example, studies using machine learning methods showed an accuracy rate as high as 99% for sign classification.[41-43] Table 7 summarizes some recent roadway sign recognition studies that are based on machine learning methods.

Table 7. State-of-art transportation safety research (TSR) works.

Study	Method
Shi and Lin, 2017[37]	SVM and HOG shape detection techniques and the hue information based on the HSI color space for sign detection, and neural network for sign recognition. The algorithm obtained a 90% detection rate and 84% classification rate for images captured by cameras behind the windshield.
Bahlmana et al., 2005[36]	Adaboost with Haar-like feature based on the RGB color space for sign detection and linear discrimination analysis for sign classification. The algorithm obtained a 94% classification rate for isolated sign patches and an 85% recognition rate for video tests.
Shustanov and Yakimov, 2017[41]	Convolutional neural network (CNN) based on the color information from the HSI color space for sign detection and reorganization. The algorithm obtained a 99.94% classification accuracy at a detection distance up to 50 m when applied to sample testing data.
Ciresan et al., 2012[42]	CNN. The algorithm reached a 99.46% classification rate with testing data.
Zhou and Deng, 2014[29]	Combining 2D image and 3D lidar data. Signs detected with a combination of the 3D location, 2D color, and lidar intensity. Sign recognition is based on SVM and HOG. The algorithm achieved a 95.78% detection rate and 95.07% recognition at a distance up to 100 m.
Mathias et al., 2013[44]	Weighted linear combination of boosted 2-depth decision trees for sign detection and iterative nearest neighbors classifier (INNC) among others for sign recognition. Best performance reached an average classification rate of 95.73%.
Lasson and Felsberg, 2011[45]	Fourier descriptor based on sign shapes as the feature vector for detection and classification. The algorithm showed a 70%-90% accuracy rate based on different testing data.
Shustanov and Yakimov, 2017[46]	Extraction of blue and red pixels based on the HSV color space for sign detection and CNN for sign classification. The algorithm reached a 99.94% accuracy rate for signs with required shapes and red contours.

SIGN SIGNIFICANCE FOR AUTOMATED DRIVING

Signing for HAVs

In an ideal HAV environment, traffic signs (as well as most, if not all, other traffic control devices currently used) may be completely replaced by digital navigation data and traffic control information communicated individually and wirelessly to vehicles. However, the technology and infrastructure developments must address the challenges due to the gradual implementation nature of HAV technologies and the foreseeable prolonged coexistence of increased automated vehicles and human-driven vehicles. Currently, research and developments are mostly focused

on the following areas, which are highly likely to be merged in the future as HAVs become more dominant:

- Image recognition is based on traditional signs. Relevant research experience and informal conversations with vehicle technology vendors point to a practitioner opinion that "infrastructure improvements good for human drivers are also good for HAVs." Based on this opinion, traditional traffic signs with standardized design and installation; improved retroreflectivity, size, and legibility; and better illumination would likely play a significant role in the transportation system for the foreseeable future to benefit both human drivers and automated vehicles.
- Machine vision-oriented signs. Many automated vehicle functions use image recognition for reading road signs. However, a much more reliable approach would be machine-readable signs. Examples of such signs are those designed with radio-frequency identification (RFID) systems or machine-readable codes (e.g., QR codes) using special sheeting designs to enable short-range sign-to-vehicle communication or facilitate machine vision systems.[47,48,49]
- Digital/virtual signs. Traffic information conveyed by traditional signs can theoretically all be communicated wirelessly to HAVs in a future connected environment.[50] The advances in cellular and short-range communication technologies, combined with geospatial sensing and analysis techniques, make it possible to communicate traffic sign information to individual vehicles in need. When receiving such information, onboard processors would process the information, based on which driving and navigation decisions are made. It is optional to visualize the digital/virtual sign information in the vehicle to benefit passengers. It is also optional to have physical transmitters/receivers (e.g., via 5G cellular communications to/from vehicles and control centers) at strategic locations along roadways to meet different technological needs.

Currently, there are a number of ongoing or upcoming research efforts to understand and evaluate the implications of HAVs on transportation infrastructure. Examples of the most relevant national research include National Cooperative Highway Research Program (NCHRP) 20-102(15), "Impacts of Connected and Automated Vehicle Technologies on the Highway Infrastructure"; NCHRP 20-102(26), "Dynamic Curbside Management: Keeping Pace with New and Emerging Mobility and Technology in the Public Right of Way"; NCHRP 20-102(24), "Infrastructure Modifications to Improve the Operational Domain of Automated Vehicles"; and NCHRP 20-102(25), "Readiness and Effectiveness of Freeway-Based Corridor V2X Applications for Improving Congestion and Safety."

CHAPTER 3. SYSTEM DEVELOPMENT AND DATA COLLECTION

DATA COLLECTION NEEDS AND SYSTEM REQUIREMENTS

This study required detailed information about environmental factors potentially affecting sign visibility on roadways. For this purpose, the team developed a data collection system to record the following types of data:

- Sign images and locations;
- Light conditions, including horizontal and vertical light levels; and
- Weather conditions, including visibility, humidity, and temperature.

To meet the data collection needs, the project team further expanded the Virginia Tech Transportation Institute (VTTI) roadway lighting mobile measurement system (RLMMS) to include sensors and equipment capable of collecting the aforementioned data elements into an integrated database in an efficient manner.

VTTI ROADWAY LIGHTING MOBILE MEASUREMENT SYSTEM

VTTI previously developed the RLMMS data collection system primarily for in situ collection of roadway lighting data. The system contained the following major components (Figure 3):[51]

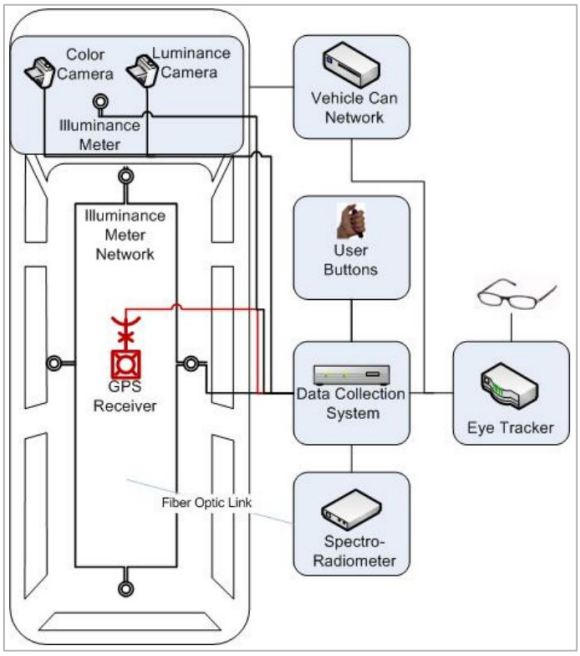

Figure 3. Diagram. RLMMS).[51]

- Illuminance meters. The RLMMS uses four Minolta T-10 illuminance meters[52] mounted directly to the roof of the vehicle facing up for horizontal illuminance measurement. The illuminance meters have a range of 0.01–299,900 lx and allow connections to a personal computer for continuous measurements. The product

specification sheet indicates that the T-10 meters have an operating temperature range of -10 to 40 °C and an operating humidity range of 85% or less at 35 °C with no condensation. The meter is within 6% of the CIE spectral luminous efficiency, has a cosine response within 3% for its receptor, and a linearity of ±2% ±1digit of displayed value. The mean values of the four meter readings are used during data analysis to ensure accuracy and reduce the effects of potential shadows from roadside vegetation and/or overhead objects. A fifth Minolta T-10 illuminance meter is mounted inside the windshield vertically facing forward, measuring the vertical illuminance, which can be used as an indicator for glare to driver's eyes. All five meters are synchronized at a 10 Hz frequency.

Note that the RLMMS allows additional Minolta illuminance meters to be installed as so desired. For example, the team previously used two additional illuminance meters installed on the sides of the RLMMS vehicle vertically facing out to measure the vertical illuminance levels at intersections.(53)

- GPS. The RLMMS uses a NovAtel FlexPak™ GPS receiver with a NovAtel GPS-702L antenna positioned on the vehicle roof in the center of the horizontally mounted illuminance meters. The system has a horizontal position accuracy of 1.2 m and a corrected accuracy of up to 40 cm based on the manufacturer-provided NovAtel CORRECT™ algorithm and the differential GPS method. The GPS antenna operates within a temperature range between -40 °C and +85 °C and a humidity range up to 95% non-condensing. The GPS was directly connected to the data collection computer and provided latitude and longitude measurement readings at a frequency of 10 Hz.
- Machine vision camera system. The camera system uses two Point Gray Flea FL2G 13S2C-C cameras: one black and white, and the other in color. The two cameras both use CCD image sensors and are capable of taking videos at a frequency of up to 30 fps. The color camera has a resolution of 1288 × 964 pixels and the monochrome camera has a resolution of 1624 × 1224 pixels.(54,55)
- Luminance camera. The luminance camera is a VTTI-developed system capable of capturing 12-bit monochrome 1624 × 1224 images of the roadway environment that are calibrated to measure the luminance values on roadways. The camera consists of a Point Gray Grasshopper GRAS-20S4M-C camera fitted with a Computar® 2/3" telephoto lens (12-36 mm). The camera has an operating temperature range of 0° C to 40 °C and a humidity range of 20% to 90%. The luminance camera is mounted behind the windshield vertically facing forward.
- Luminance Meter. The luminance camera measures luminance values of large areas. The RLMMS also includes a Minolta LS-110 luminance meter installed vertically behind the windshield to measure spot luminance values for cross-reference/calibration with the luminance camera. The LS-110 meter has a 9° field of view, a measuring range of 0.01 to 999,900 cd/m^2, and an accuracy of ±2% ±2 digits for measured values that are lower than 1 cd/m^2 or ±1 digit for measure values that are 1 cd/m^2 or above.
- Spectrometer. The RLMMS uses an Ocean Optics HR4000 spectrometer mounted behind the windshield with a fiber optic cable linking a sphere receptor on the vehicle

roof to capture spectroradiometric data. The HR4000 spectrometer has a detection range of 200-1100 nm and a corrected linearity > 99.8%.[56]

- Tilt sensor. The RLMMS uses a Rieker Seika N3C-0.5 inclinometer mounted on top of the vehicle and connected via a National Instruments USB-6218 data acquisition system for the measurement of vehicle inclination. The inclinometer has a measuring range of ±30° and a precision of 6 mV/degree. The VTTI calibration during system development showed a ±5% accuracy range for the inclinometer when mounted atop the vehicle. The primary purposes of the tilt sensor include identifying lighting measures collected during significant tilts (to therefore possibly adjust the horizontal and vertical illuminance values accordingly), measuring grades on the vertical curves of roadways, and recording vehicle inclination status during an incident. The lateral tilt values measured may also indicate roadway superelevation levels (although not calibrated for this purpose yet).
- Vehicle Controller Area Network (CAN bus) connection. The RLMMS data collection software reads vehicle kinematic data continuously at a 0.3–0.5 Hz frequency from the vehicle's CAN bus. A large number of variables depicting the vehicle's operating status can be collected from the CAN bus, such as vehicle speed and the status of vehicle functions such as the antilock braking system (ABS), brake pedal, and various lights.
- Event push button. The push button serves as an event marker to the data collected. When the button is pushed either by the vehicle operator or any of the additional RLMMS operators, a binary indicator is added to the data row based on synchronized timestamps. This mechanism is used to indicate the occurrence of any incidents during the data collection, such as sudden changes to the vehicle speed or noticeable changes to roadway/traffic conditions that might be of interest to the research project. By adding the indicator, researchers can later revisit the marked epochs of data, including both tabular and video/imagery data, for additional analysis.
- Eye tracker. The RLMMS includes a ViewPoint EyeTracker® developed by Arrington Research, Inc. The eye tracker is used to capture participants' eye movement data for research purposes. The eye-tracking hardware components are mounted to lightweight goggles that fit a variety of participant head sizes.
- Webcam. The RLMMS includes a webcam installed behind the vehicle windshield facing forward. The webcam allows the streaming of lower-resolution videos when activated during data collection activities. The primary purposes of using the webcam include the production of videos for education and outreach activities, and the monitoring of data collection status as needed.

The RLMMS hardware is connected to the data acquisition system and controlled by a specialized software program created in LabVIEW. All components of the system are synchronized and integrated with the GPS data by the central computer into a single database for downloading and analysis. Note that the data collection frequencies of all sensors can be adjusted within the operational ranges using the RLMMS controlling software to fit data collection needs. The RLMMS uses a Cadillac Escalade as the vehicle platform for mobile data collection.

ROADWAY AND ENVIRONMENT INFORMATION MEASUREMENT SYSTEM

During this study, the project team further expanded the RLMMS system to include functions for measuring environmental data and enhancing the machine vision capabilities. In addition to the existing RLMMS sensors/meters, the new data collection system, named Roadway and Environment Information Measurement System (REIMS), now includes the following additional components:

- Humidity/temperature sensor. REIMS uses a Cleware USB-Humi 6-1 sensor with combined humidity and temperature measurement capability mounted on top of the REIMS vehicle. For temperature measurement, the Cleware sensor has a measuring resolution of 0.01 °C, measuring range of -20 °C to 80 °C, and a measuring accuracy of ±0.2 °C. For humidity measurement, the sensor has a measuring resolution of 0.01% at an accuracy of ±2%.[57]
- Visibility module. The visibility module of the REIMS uses a green (550 nm) 50-mW laser (attenuated to ~ 2mW output to prevent accidental harm to human eyes) with two Minolta T-10aSW illuminance meters to measure the initial laser output and the remaining laser output at the receiving terminal 6 ft. (1.83 m) away. The module is mounted 1 ft from the left side of the REIMS vehicle at the rooftop height. This module was previously developed independently by the VTTI research team (Figure 4) for measuring visibility during adverse weather conditions such as rain and fog.

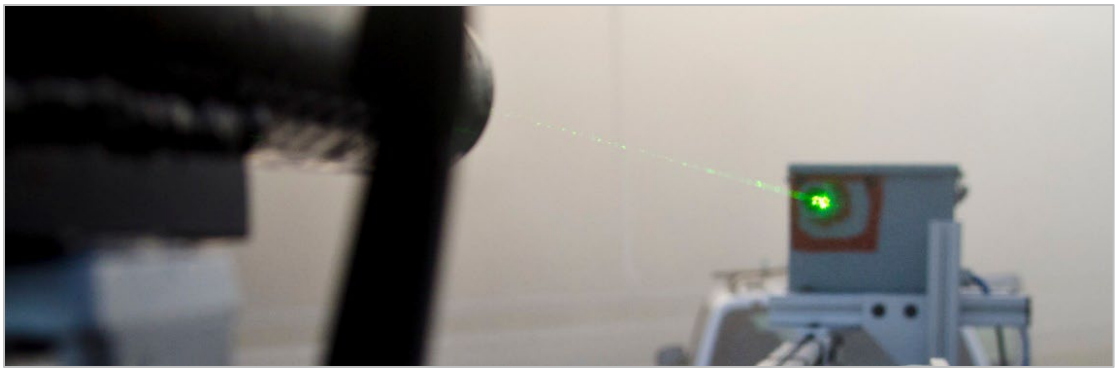

Figure 4. Photo. Visibility module in operation. The laser beam can be seen because of the scatter caused by the fog.

The American Meteorological Society explains surface visibility as "the greatest distance in a given direction at which it is just possible to see and identify, with the unaided eye, a prominent dark object against the sky at the horizon," and more informally "as the clarity with which an object can be seen."[66] Assessments of visibility were made using the meteorological optical range (MOR). MOR is a measure of the density of fog and is defined as the distance through the fog when the contrast of a black object reaches 5% caused by the scattering of 95% of the light. A green laser is used to measure the light loss over a fixed length, as shown in Figure 4. The MOR can then be calculated from the ratio of the foggy sensor *measurement* to the sensor reading with no fog (*calibration*) and the distance (*length*) between the laser emitter and the sensor. The number "negative three" in the numerator is the natural log of 0.05, or 5%, the contrast against which we are comparing

the measured contrast (light loss). The measured laser output loss can be converted to visibility distance using Equation 1, Equation 2, and Equation 3:

Equation 1. MOR calculation equation.

$$MOR = -\frac{3}{\ln\left(\frac{measurement}{calibration}\right)}(measurement\ length)$$

Equation 2. Equation for determining the measurement variable (foggy sensor measurement).

$$measurement = \frac{\left(detector2_{on_i} - \ detector2_{off_i}\right)}{\left(detector2_{on_0} - \ detector2_{off_0}\right)}$$

Equation 3. Equation for determining the calibration variable (without fog sensory measurement).

$$calibration = \frac{(detector1_{on_i} - \ detector1_{off_i})}{(detector1_{on_0} - \ detector1_{off_0})}$$

- Lidar. REIMS includes a Livox Horizon Lidar unit mounted on top of the vehicle.[58] The unit scans a field of view of 81.7° (horizontal) × 25.1° (vertical) using 905-nm laser beams. Different from traditional lidars, the unit uses a non-repetitive scanning technology that results in an average line spacing of 0.2° at 0.1 s in the center and an average line spacing of 0.4° at the left and right ends of the field of view. In comparison, traditional 64-line lidars have an average line spacing between 0.3° and 0.6°. Other key specifications of the lidar are:
  - Detection range: 90 m at 10% reflectivity, 130 m at 20% reflectivity, and 260 m at 80% reflectivity
  - Operational temperature range: -40 °C to 85 °C
  - Distance random error: 1σ (at 20 m) < 2 cm
  - Angular random error: 1σ < 0.05°
  - Point rate: 240,000 points/s for first or strongest return and 480,000 points/s for dual return (the lidar can be set to operate at a dual return mode where it generates a point cloud of up to two returns).

During the expansion of the RLMMS, the project team kept the previous Cadillac Escalade vehicle platform. The original RLMMS software was modified using C and LabVIEW to accommodate the new sensors. All sensor and meter data, with the exception of images from various cameras and the lidar data, are stored in a single, synchronized comma separated value (CSV) file for downloading and analysis.

Figure 5 illustrates the various components of REIMS and the approximate locations where they are mounted relative to the REIMS vehicle. Figure 6 through Figure 9 show pictures of the REIMS components.

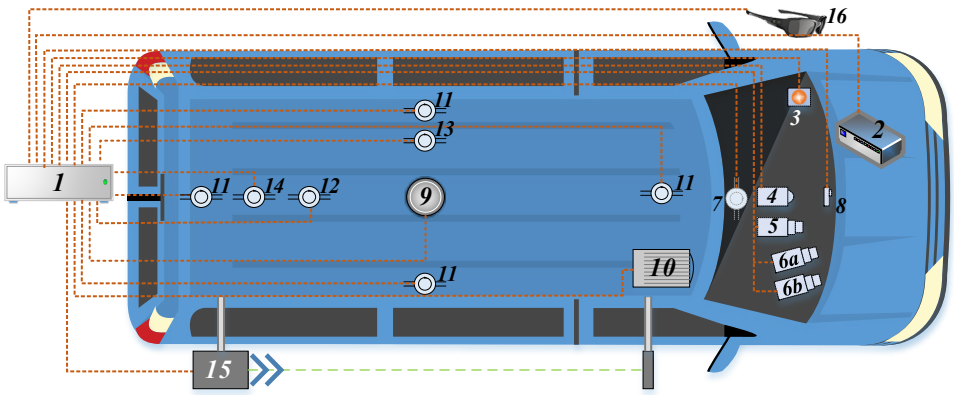

1 Control and data storage
2 Vehicle CAN network
3 Operators push button
4 Luminance meter
5 Luminance camera
6 Machine vision cameras (a. mono; b. color)
7 Illuminance meter for glare
8 Web camera
9 GPS antenna)
10 Lidar
11 Illuminance meters (horizontal)
12 Spectrometer
13 Tilt sensor
14 Humidity/temperature sensor
15 Visibility module
16 Eye tracker

Note: 3-8 are installed inside the vehicle behind the windshield, 9-15 are installed on vehicle rooftop.

Figure 5. Diagram. REIMS components.

Figure 6. Photo. REIMS components – front view.

Figure 7. Photo. REIMS components behind windshield.

Figure 8. Photo. REIMS components mounted on top of vehicle.

Figure 9. Photo. REIMS control and data storage.

SIGN MACHINE VISION IMAGE REDUCTION

During data collection trips to Charlottesville, Virginia, and Greensboro, North Carolina, images were captured using a GoPro Hero 3+ and GoPro Hero. The cameras were mounted on a Cadillac Escalade instrumented with an RLMMS, which facilitated sensor, meter, and GPS data collection. The experimental vehicle and cameras are shown in Figure 10.

Figure 10. Photos. GoPro Hero 3+ and GoPro Hero are shown on the left panel, and the experimental vehicle (Cadillac Escalade) is shown on the right panel.

Images from all eight trips were reviewed by a data reductionist to determine if the target sign was located within the captured image. Images that contained the target sign structures were then evaluated for legibility. Reductionists assessed each sign structure for the number of unique signs located on the same structure. Unique signage was identified as any area containing different background and legend color combinations. This resulted in more unique signs than the number of target sign locations (n = 100). The research team then assigned legibility scores (Table 8) for each unique sign present at all target sign locations. Legibility was scored for all sign character font sizes present on each sign. Sign characters appearing on the same sign structure using identical font size, legend color, and background color were evaluated for legibility score as a group.

Table 8. Legibility score scale with descriptions for each score.

Legibility Score	Description
0	Cannot read sign.
1	Difficult to read but the words can be guessed. Major issues with darkness, blurriness, and/or glare are present.
2	Somewhat difficult to read. The number of characters in each word can be distinguished, however some letters may require guessing. Some significant issues with glare, darkness, and/or blurriness exist.
3	Somewhat easy to read. The characters and letters within each word can be read. Some issues with glare, darkness, and or blurriness appear. The reader can distinguish differences in font size at this score.
4	Easy to read but obstructions due to glare, blurriness, and/or darkness may be present. All characters are clearly visible.
5	Easy to read with no obstructions and all characters visible.

Legibility Score Examples

Five

Figure 11 gives study image examples of signs rated with a 5 legibility score. The letters in each sign are clearly defined and can be clearly read by human eyes. There are no issues with glare, blurriness, or darkness within the image. The research team expects well-developed machine vision algorithms to read most or all characters on signs with a 5 legibility score.

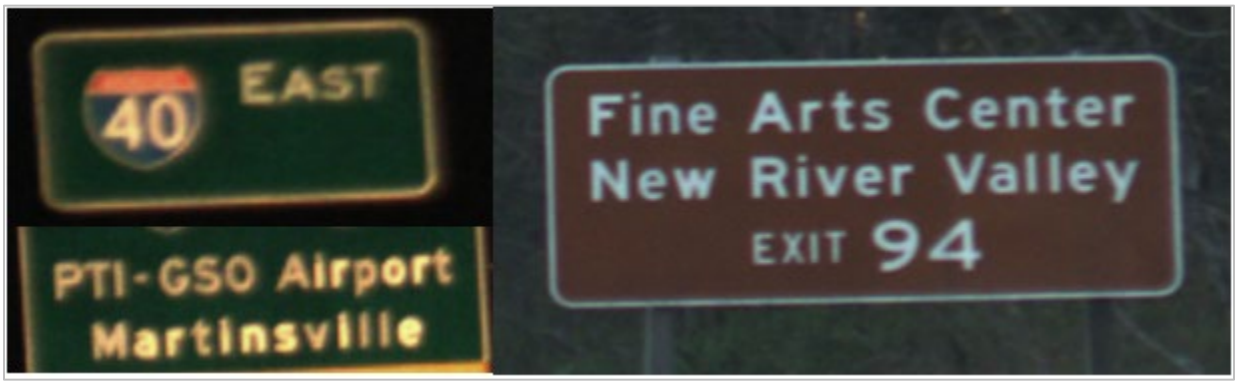

Figure 11. Photo. Signs rated with a legibility score of 5.

Four

Figure 12 gives study image examples of signs rated with a 4 legibility score. The letters on each sign can be read in full even in the presence of glare or blurriness. The number of characters within each word can be easily counted and even small size differences between letters can be identified. The white background sign shows a 4 score during the daytime, and the yellow background sign shows a 4 score during the nighttime. The research team expects well-developed machine vision algorithms to read the majority of characters on signs with a 4 legibility score.

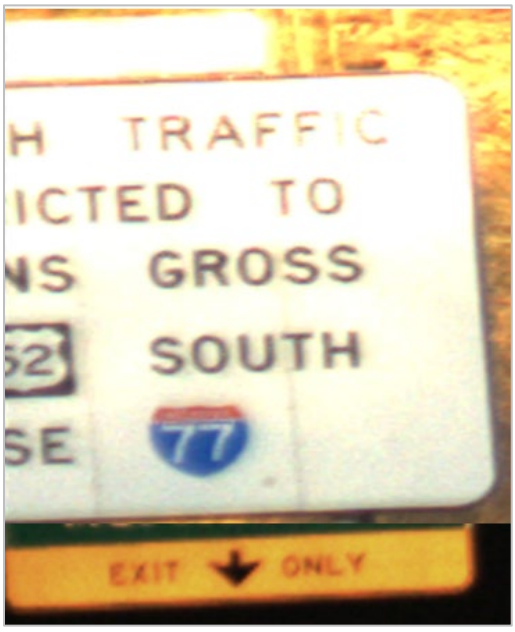

Figure 12. Photo. Signs rated with a legibility score of 4.

Three

Figure 13 gives study image examples of signs rated with a 3 legibility score. The signs' letters can be read individually, and the entire word can be deciphered without any inference. Some letters may appear blurry or be obscured by glare, causing some difficulty in reading the sign. The number of characters within each word is clear, and size differences between the characters can be seen. Both images show signs that scored 3 during the daytime. The research team expects well-developed machine vision algorithms to read some of the characters on signs with a 3 legibility score.

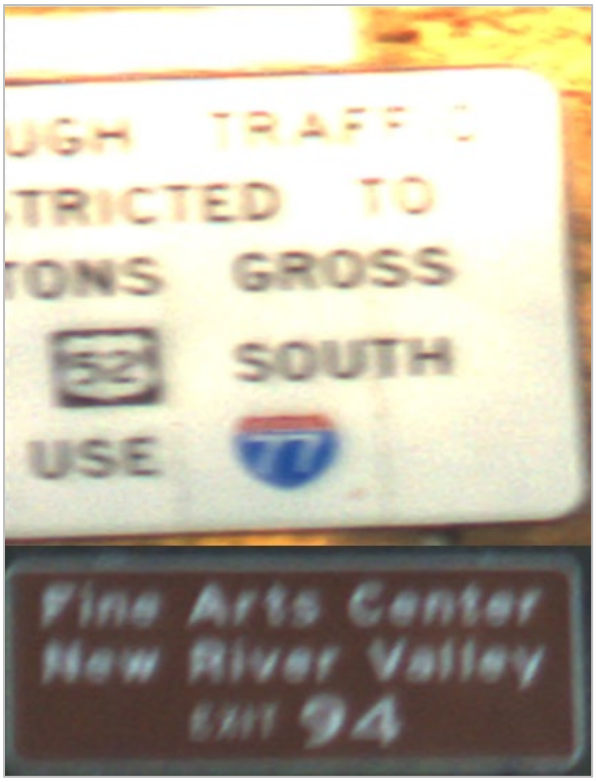

Figure 13. Photo. Signs rated with a legibility score of 3.

Two

Figure 14 gives study image examples of signs rated with a 2 legibility score. The signs have distinct letters that are somewhat difficult to read due to blurriness, glare, or darkness in the image. The number of characters within each word can be distinguished, but some may need to be inferred. The image below on the left is an example of a 2 score during the nighttime, and the image on the right is an example of a 2 score during the day. The research team expects signs with a 2 legibility score to have many of their characters read by machine vision algorithms.

Figure 14. Photo. Signs rated with a legibility score of 2.

One

Figure 15 gives study image examples of signs rated with a 1 legibility score. The signs are very difficult to read, but the words can be inferred, especially with prior knowledge of similar signs. The characters within each word are difficult or impossible to distinguish. Words look to be missing letters or multiple letters in each word are obscured due to blurriness or darkness within the image. Signs with a 1 legibility score are not expected to be read by machine vision algorithms.

Figure 15. Photo. Signs rated with a legibility score of 1.

Zero

Figure 16 gives study image examples of signs rated to have a 0 legibility score. The signs cannot be read from the image at all. Almost no characters are legible, and none of the words can be deciphered. The white background sign on the left in Figure 16 is a daytime example, and the yellow background sign on the right is a nighttime example. Without prior knowledge of the sign, a viewer would not be able to know its message. Signs with a 0 legibility score are not expected to be read by machine vision algorithms.

Figure 16. Photo. Signs rated with a legibility score of 0.

CHAPTER 4. DATA COLLECTION AND ANALYSIS APPROACH

FIELD DATA COLLECTION

Data collection was carried out during April and June 2021 on two selected routes: VTTI headquarters (Blacksburg, Virginia) to Charlottesville, Virginia; and VTTI headquarters to Greensboro, North Carolina (Figure 17 and Figure 18). In total, the team conducted eight data collection trips (Table 9). Data collection trips involved approximately 300 mi of travel (round trip) between VTTI headquarters and either destination. Each data collection trip involved approximately 6 hours of data collection between either 5:00 a.m. and 11:00 a.m. or 5:30 p.m. and 11:30 p.m. The planning of the data collection trips took into consideration the following factors:

- Sufficient data on freeways. Freeways use a large number and variety of signs, and therefore provide abundant opportunity to collect data about signs of different colors and shapes. The two data collection routes included parts of several major freeways in the region, such as I-81, I-64, I-77, and I-74. The route between VTTI and Greensboro covers roadways in both Virginia and North Carolina and therefore potentially reflects different practices relevant to signage and roadways.
- Collection of both daytime and nighttime sign information. All data collection trips were scheduled to leave early in the morning (before dawn) or later in the afternoon to ensure that both nighttime and daytime data were collected. In addition to the different light conditions, the data collection trips also included periods of sun rising or setting, capturing higher probability of sun glare affecting sign visibility.
- Diverse weather conditions. Both the data collection portions on I-81 and I-77 go through mountainous areas where localized rain and foggy weather conditions occur frequently. In addition, the rapid temperature changes in the region frequently result in dew on signs during earlier mornings.
- Trip distance and data collection cost. Both data collection routes required approximately 6 hours of travel for each round trip, eliminating overnight stays during the data collection for reduced data collection costs. In addition, each data collection trip was sufficiently long to capture a variety of lighting conditions.

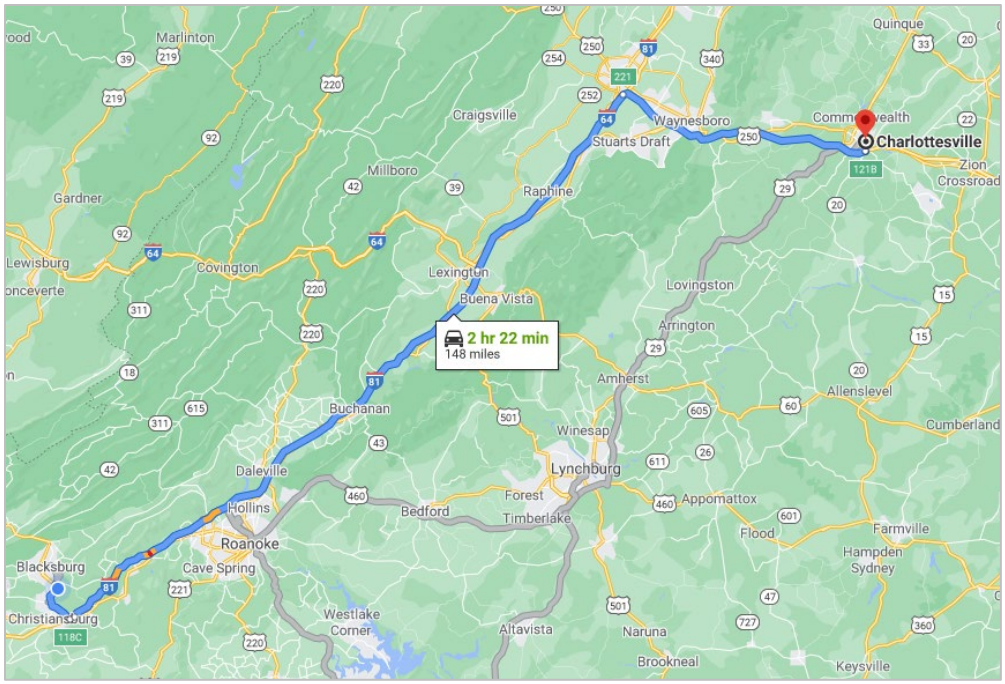

Figure 17. Map. Data collection route between VTTI headquarters and Charlottesville, VA.

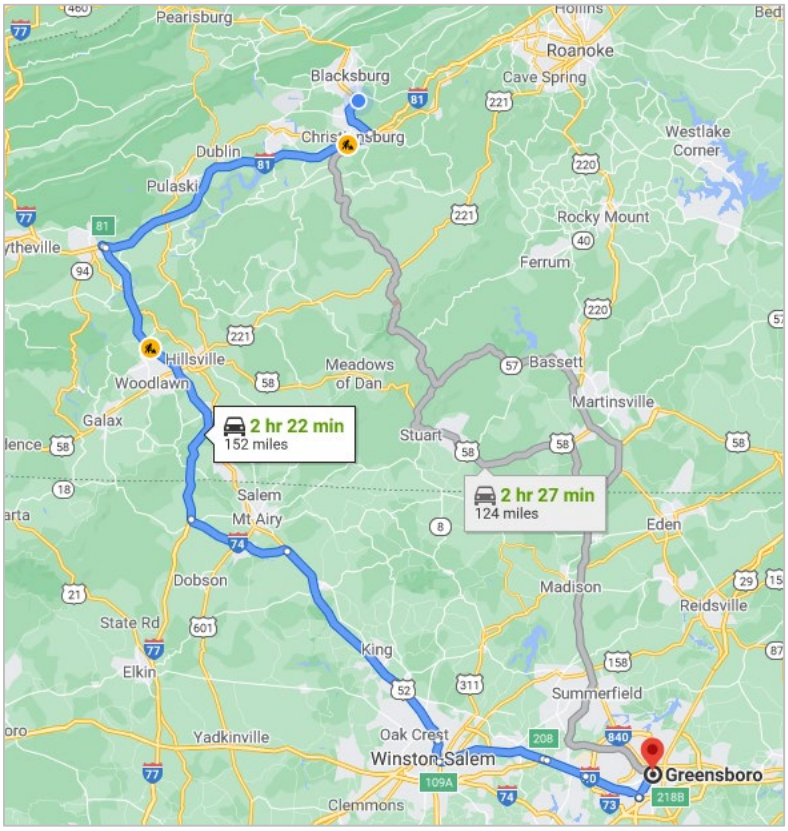

Figure 18. Map. Data collection route between VTTI headquarters and Greensboro, NC.

Table 9. List of data collection trips and time/date.

Time/Date	Trip
5:30-11:30 PM, Tuesday, April 13, 2021	VTTI HQ-Greensboro, NC
5:00-11:00 AM, Thursday, April 15, 2021	VTTI HQ-Charlottesville, VA
5:00-11:00 AM, Tuesday, May 18, 2021	VTTI HQ-Charlottesville, VA
5:30-11:30 PM, Thursday, May 20, 2021	VTTI HQ-Greensboro, NC
5:00-11:00 AM, Tuesday, May 25, 2021	VTTI HQ-Charlottesville, VA
5:30-11:30 PM, Thursday, May 27, 2021	VTTI HQ-Greensboro, NC
5:30-11:30 PM, Tuesday, June 1, 2021	VTTI HQ-Charlottesville, VA
5:00-11:00 AM, Thursday, June 3, 2021	VTTI HQ-Greensboro, NC

SIGN DATA COLLECTION AND PROCESSING

Sign Selection and Identification

For the purpose of this project, the team identified 50 signs per data collection route, with signs located approximately 6 mi apart from each other for each data travel way (i.e., two ways for each data collection route). During the sign selection process, the team made an effort to select signs with different colors and legends:

- Regulatory signs with white/red backgrounds and black/white legends. Figure 19 shows three examples of regulatory signs.

Figure 19. Diagram. Examples of regulatory signs.

- Guide signs with green/yellow backgrounds and white/black legends (including blue and red Interstate route shields). Figure 20 includes three examples of such guide signs.

Figure 20. Diagram. Examples of guide signs.

- Warning signs in many cases have yellow backgrounds and black legends (Figure 21).

Figure 21. Diagram. Examples of warning signs with yellow background and black legend.

- General information, service, and tourist-oriented directional signs typically have a blue/brown background and a white legend (Figure 22).

Figure 22. Diagram. Examples of information signs.

When selecting signs, the project team only selected signs in which the legend contained a fair number of words, regardless of whether the sign contained graphics. This was because the intended data analysis approach of this study relied on optical character recognition (OCR) algorithms for text as a surrogate for machine vision legibility of the signs. In addition, the research team made an effort to select signs with different installation locations (e.g., roadside versus overhead), orientation (i.e., azimuth), and terrain.

The research team performed the selection and location identification of the signs primarily based on Google Maps using the Street View feature. After identifying each sign, its location was then added to a Feature Class file in the Esri ArcGIS platform for further processing. All signage present on the target sign structure was categorized and counted based on color scheme, location, and sign type. Across all 100 sign locations, the research effort identified 182 unique signs throughout all sign structures. The distribution of sign location, type, and color scheme is summarized in Table 10. Additionally, Figure 23 illustrates the distribution and location of all sign structures considered for analysis along the data collection routes.

Table 10. Sign location, type, and color scheme summarized by count for all signs identified during data collection.

Data Category	Location	Count
Sign Location	Overhead	69
	Side of Road	113
Color Scheme (Background Color / Legend Color)	Blue / White	33
	Brown / White	7
	Green / White	56
	White / Black	53
	Yellow / Black	32
	Black / White	1
Sign Type	Guide	109
	Regulatory	24
	Warning	28
	Informational	24

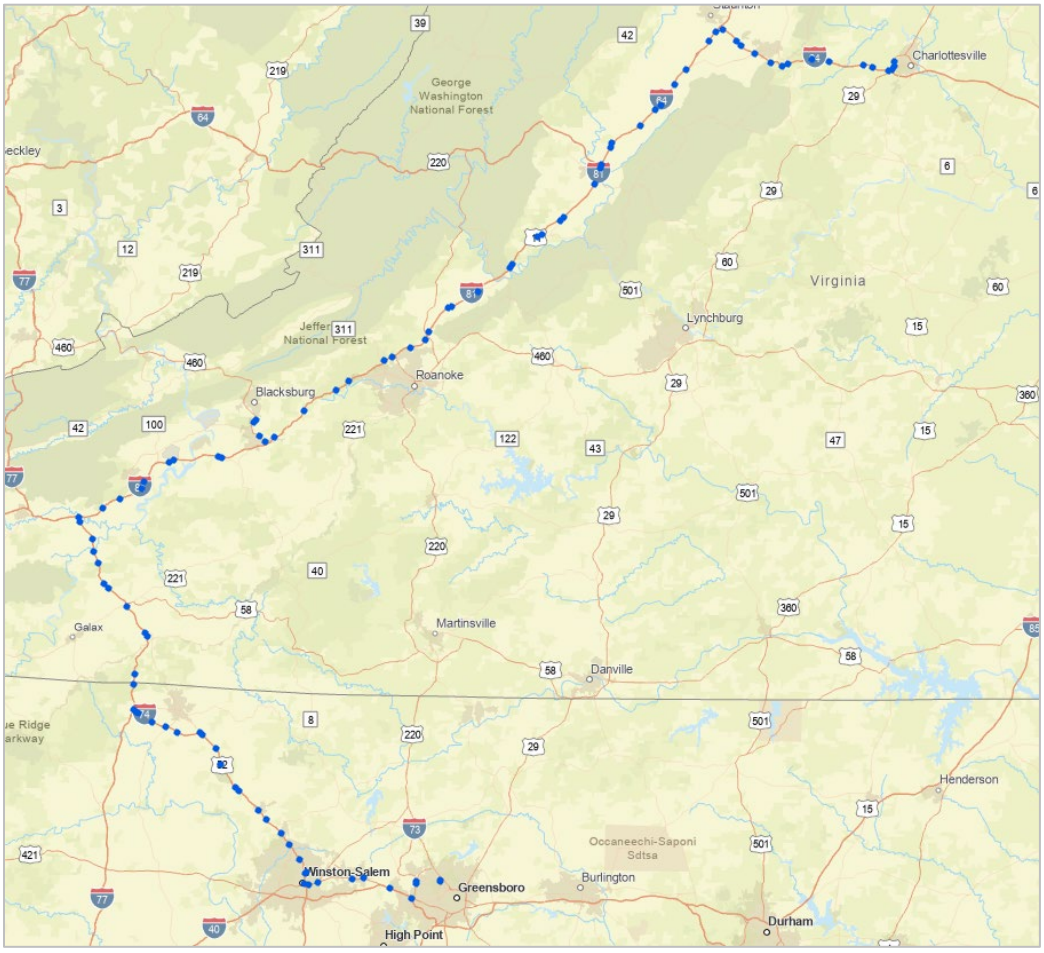

Figure 23. Map. GIS map of sign locations created in ArcGIS.

Data Variables and Analysis Methods

For each sign previously identified along the data collection routes, the project team analyzed the machine vision legibility levels at three distances: 500 ft, 400 ft, and 200 ft. At a speed of 65-70 mph on freeways, the distances correspond to a travel time of approximately 5 s, 4 s, and 2 s, respectively. Note that a freeway guide sign with a 12-inch legend provides an approximately 360 ft legibility distance based on the MUTCD assumption of 30 ft legibility distance per 1 inch of letter height.[2] Combining the three scenarios with data collection trips, the trips between Blacksburg and Charlottesville traveled through a total of 88 signs and provided a total of 1,056 sign visibility data points (i.e., 88 signs × 3 distances × 4 data collection trips). Additionally, the trips between Blacksburg and Greensboro traveled through a total of 98 signs and provided a total of 1,176 sign visibility data points (i.e., 98 signs × 3 distances × 4 data collection trips). Table 11 lists the variables collected and analyzed by the project team during this study. Among the variables:

- Legibility score was obtained during the data reduction. A researcher at VTTI examined each picture taken during data collection. Legibility score was assessed for each of the font sizes, independently, by image, and legibility score was recorded as a single data point representing all characters for each font size (Table 17). Font size varied word to word and within words that contained capitalizations.
- Machine vision legibility. During this project, the team extracted the images of each selected sign, at the three distances, from the data collection trips and fed them into MATLAB for text recognition. Based on the MATLAB OCR tools, the project team calculated a legibility measure (i.e., percentage of characters read correctly) for each sign for a combination of different environmental conditions and distances.

  The image OCR function in MATLAB[59] uses the Tesseract OCR engine for text recognition from images. The Tesseract OCR engine is maintained by Google for text detection on mobile devices, in video, and in Gmail image spam detection.[60,61,62] The MATLAB function allows font-specific training to potentially enable improved OCR performance. During this study, the project team trained Tesseract in MATLAB using the images of the selected signs taken during clear and daylight weather conditions.

  When comparing the OCR results with the original text, the project team treated misrecognized characters with similar shapes as correct, assuming that better OCR algorithms and/or algorithms better trained for recognizing roadway signage would be able to correct such characters according to sign type and legend meanings. Examples of characters with similar shapes include I, l, and 1; and 0, o, and O.
- Sun position variables. Both the sun angle from horizon and the sun azimuth relative to the travel direction were determined based on the National Oceanic and Atmospheric Administration (NOAA) solar calculation algorithms.[63] In order to calculate the sun azimuth relative to the travel direction, the project team calculated the roadway azimuth at each sign location using the ArcGIS software package. The relative sun azimuth was then computed as the azimuth difference between the travel direction and the sun at the time when the sign data was collected.

Table 11. Analysis variables describing sign and environmental conditions.

Variable	Value	Source
Variables Describing the Subject Sign		
Legibility score	Numeric	Camera and video images
Legible	Binary	Camera and video images
Machine vision legibility score	Numeric	Camera and video images
Number of words	Continuous whole numbers	Video images/Google Street View
Number of characters	Continuous whole numbers	Video images/Google Street View
Sign legend	Text	Video images/Google Street View
Sign legend color	White, black	Video images/Google Street View
Sign background color	White, red, yellow, green, blue, and brown	Video images/Google Street View
Sign installation location	Overhead and roadside	Video images/Google Street View
Environmental Condition Variables		
Sun angle from horizon	Continuous numbers in degrees	NOAA solar calculation
Sun azimuth from travel direction	Continuous numbers in degrees	NOAA solar calculation and ArcGIS
Illumination	Continuous numbers in lux	Field data collection
Humidity	Continuous numbers in percent	Field data collection
Temperature	Continuous numbers in degrees Celsius	Field data collection
Weather	Cloudy, overcast, rain, fog, or sunny	Field data collection

The mean legibility analysis used a multiple linear regression analysis to assess the influence that font size, sign color, sign location, view distance, sun position, and illumination level had on the legibility of sign characters during day and night. Data were formatted for use, and all linear regression procedures were performed using SAS. Difference in mean legibility score was assessed across a series of analyses, which are summarized in Chapter 5.

Model assumptions of independent observations, constant variance, and normally distributed residuals were checked for all models. Constant variance was checked using Levene's test, and the distribution of sample residuals was checked using histograms. Post hoc analysis was performed using a least-squares means methodology, adjusting for multiple comparisons with Tukey's least significant difference procedures. The research team chose a significance level (α) of 0.05 (p-value ≤ 0.05) for determining statistical significance.

The data set for all analyses consisted of 1,257 sign legibility measurements across 100 sign structure locations. Overall, 17% ($n = 210$) of the data were for signage at night and 83% ($n = 1,047$) of the data points were for the day. There was a large disparity between the number of nighttime and daytime signs visible in the images collected during experimental trips, which contributed to the difference in sample size. Nighttime images suffered from a lack of lighting at the sign locations, as well as visual blur and distortion from vehicle headlamps, which impacted the number of images that contained signage.

For the sun position and illumination analyses, the research team used logistic regression modeling to assess the odds of legibility of sign characters. Logistic regression was chosen for its usefulness in predicting the odds of a binary event by fitting data to a logit logistic function curve (S-curve). Logistic regression modeled the natural log of the odds of a sign being legible by comparing the odds of a sign being legible with and without exposure to a particular explanatory variable. An odds ratio significantly different from 1 suggests that the variable exposure contributed to sign character legibility. The logistic odds function, odds ratio equation,

and generalized logistic regression model are shown in Equation 4, where *P* is the chance of the event happening.

Equation 4. Odds ratio equation (left), logistic odds function (middle), and generalized logistic regression equation (right).

$$Odds\ Ratio = \frac{a/c}{b/d}; \quad Odds = \frac{P}{1-P}; \quad \ln(Odds) = \beta_0 + \beta_1 X_1 + \beta_2 X_2 + \cdots$$

The logistic odds function can be rewritten in terms of *P* (Equation 5), which allows for computation of the probability of an event. The function inputs are the regression coefficients obtained using SAS (β values) and the independent variable values (X_1, X_2, etc.). Logistic regression results are reported using odds ratios and event probability.

Equation 5. Logistic odds function written in terms of generalized event probability.

$$\mathrm{P} = \frac{e^{(\beta_0+\beta_1 X_1+\beta_2 X_2+\cdots)}}{1+e^{(\beta_0+\beta_1 X_1+\beta_2 X_2+\cdots)}}$$

The null hypothesis for the overall model test is that each β_i equals zero. If every β_i value is zero, the associated independent variables have no effect on the odds of the event occurring ($P = 0.5$), resulting in insignificance. The alternative hypothesis is that at least one β_i is significant. The null hypothesis is checked using a chi-square statistic obtained by comparing a model with only the intercept to the fully fit version and taking the difference. Comparisons between treatment levels are summarized in the analysis of maximum likelihood estimate tables. For modeling, the research team used a significance level of 0.05. Any *p*-value of less than 0.05 indicated the treatment has a significant effect on event likelihood when compared to the reference level. Model assumptions of binary outcome, multicollinearity, independent observations, and linear relationship to log odds were checked using SAS output. Extreme outliers were identified and excluded during data processing.

DATA CHARACTERIZATION

Data collection took place during 2021 between April 13 and June 3, during which the research team completed eight data collection trips. Four trips were made between VTTI and Charlottesville, and four trips were made between VTTI and Greensboro. For reporting purposes, data collection trips are referred to by their date, when possible; however, for visualizations they are reported in chronological trip order, as outlined in Table 12.

Table 12. Data collection trip number assignments for used in analysis reporting.

Date of Trip	Time of Day	Trip Number
Tuesday, April 13, 2021	Night	1
Thursday, April 15, 2021	Day	2
Tuesday, May 18, 2021	Day	3
Thursday, May 20, 2021	Night	4
Tuesday, May 25, 2021	Day	5
Thursday, May 27, 2021	Night	6
Tuesday, June 1, 2021	Night	7
Thursday, June 3, 2021	Day	8

Table 13 presents descriptive statistics of variables obtained during data collection. Humidity, temperature, illuminance, and visibility were collected by the vehicle-based data collection systems. Horizontal and vertical sun angle were both calculated using GPS, date, and time information from each trip. Font size was assessed for each sign by an experimenter using specifications outlined in MUTCD, Chapter 2E: *Guide Signs – Freeways and Expressways.*[65]

The number of characters and the font size of each character on every target sign structure were collected. As previously discussed, the signage on each structure was identified as unique by the background and legend color combinations. Route plaques, informational signs, and supplemental guide signs were considered to be their own sign if the text and background color were different from the rest of the sign. Signs that shared background and legend color and were located on the same sign structure were counted as one.

Table 13. Descriptive statistical summary of important measures.

Variable	Subset	Average	Max	Min	SD	N	Unit Of Measure
Humidity		65.25	86.95	33.41	13.29	605	Percent
Temperature		19.68	28.48	9.68	4.82	605	Celsius
Sun Orientation		90.85	179.74	2.58	50.62	605	Degrees
Sun Elevation		13.86	58.30	-43.49	23.47	605	Degrees
Illuminance	Day	15137.52	68044.18	0.09	14658.73	500	Lux
	Night	2.09	15.14	0.00	4.46	105	Lux
Visibility		620.05	115481.05	2.15	6782.46	579	Kilometers
Font Size Category	Small	3.18	5	0	2.07	530	Legibility Score
	Medium	3.49	5	0	2.12	368	Legibility Score
	Large	3.70	5	0	2.00	359	Legibility Score
Font Size (inches)	8	2.93	5	0	1.99	194	Legibility Score
	10	3.32	5	0	2.10	336	Legibility Score
	12	3.83	5	0	1.95	198	Legibility Score
	13	3.10	5	0	2.25	170	Legibility Score
	15 & 16	3.65	5	0	2.01	271	Legibility Score
	18	3.83	5	0	1.98	88	Legibility Score

Temperature

Data collection trips were evenly balanced between day and night. The morning runs started data collection at dawn, and the night runs started at dusk. Temperature was collected automatically by the experimental vehicle equipped with VTTI's RLMMS. The maximum temperature for all trips was 28.45 °C (83.2 °F) and the minimum temperature was 9.68 °C (49.4 °F). The average temperature across all data collection trips was 19.7 °C ± 4.8 °C (67.4 °F ± 8.7 °F). The April 13, 2021 (trip number one), data collection took an invalid route for the middle section of data collection and thus a significantly lower number of data points were collected that day. Data collection instrumentation operated in error on May 18, 2021 (trip number 3), and very little temperature variation was observed; because of this error, the temperature data from May 18 was excluded in reporting and analysis. Figure 24 visualizes the variation of temperature for each of the eight data collection trips. Data collection trips one and two took place during the middle of April, and the remaining six trips (numbers 3 to 8) took place between May 15, 2021, and June 3,

2021, which may account for the lower temperatures recorded during the April data collection trips.

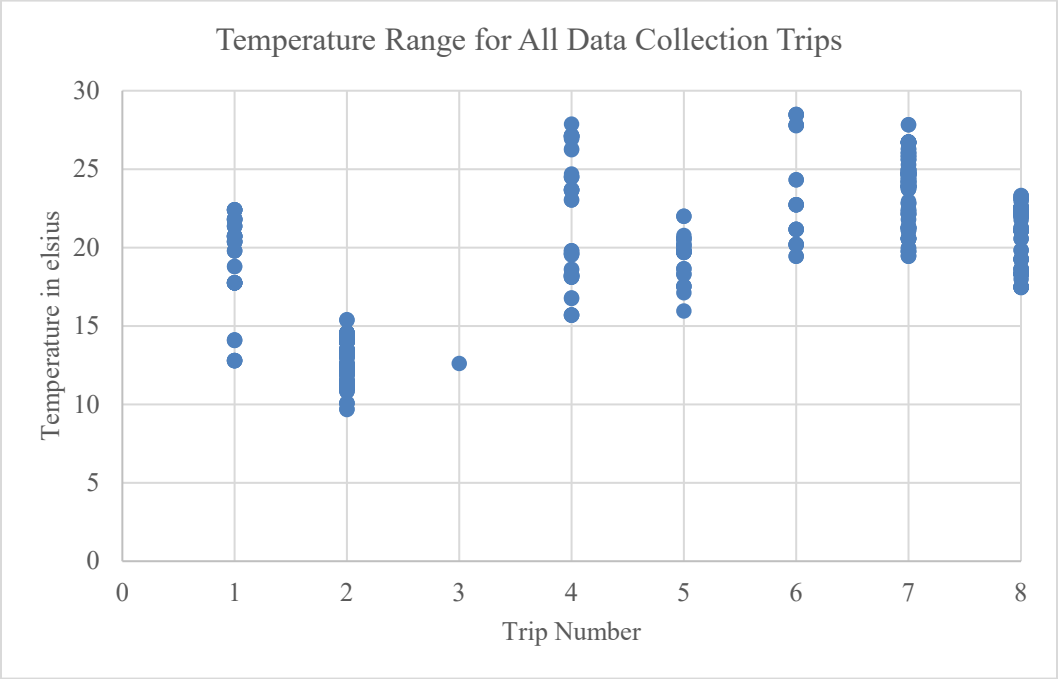

Figure 24. Graph. Temperature range for all data collection trips measured in Celsius.

HUMIDITY

The maximum humidity level for all trips was 86.95%, and the minimum humidity level was 33.41%. The average humidity level across all trips was 65.25% ± 13.29%. The April 13, 2021 (trip number one), effort is underrepresented, as the experimental vehicle took an invalid route for part of the data collection. The May 18, 2021 (trip number 3), effort also saw an error in collecting humidity and was excluded from the data reporting and analysis. Figure 25 visualizes the spread of humidity measurements for each of the eight data collection trips.

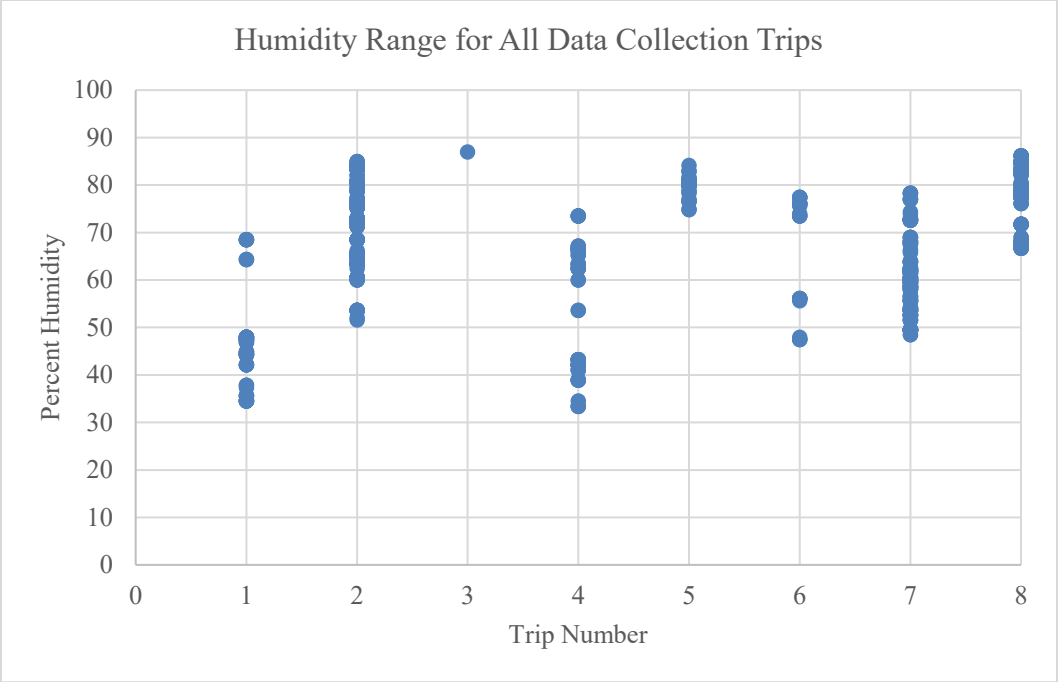

Figure 25. Graph. Humidity range for all data collection trips measured in percentage.

Sun Position

Sun position refers to the location of the sun with respect to the direction the experimental vehicle was traveling as it approached a target sign location. For data reporting and analysis, the sun's position was broken down into vertical and horizontal components. Figure 26 gives a visual representation of the horizontal and vertical components of sun angle. The vertical angle is measured in degrees relative to the horizon, while horizontal angle is measured relative to the experimental vehicle's direction of travel.

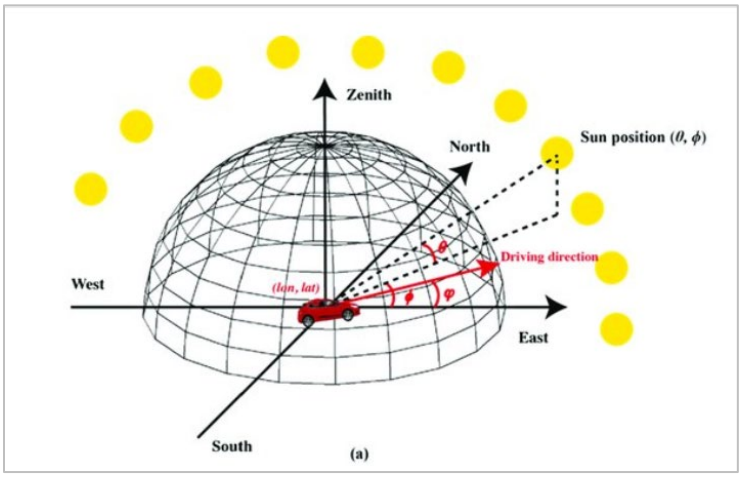

Figure 26. Diagram. Visualization of the vertical and horizontal sun angle in relation to vehicle driving direction.[68]

A solar angle determination spreadsheet was used to establish the sun's position relative to the experimental vehicle. The same spreadsheet was also used to calculate the sun's vertical and horizontal angles for the date and time the data collection trips took place. This process used latitude and longitude in conjunction with the temporal data. The resulting output provided the vertical angle component used for analysis. The horizontal component was reported in degrees clockwise from compass north. A correction was applied to the horizontal component by subtracting the compass angle the experimental vehicle was traveling from the horizontal angle provided by the solar angle determination spreadsheet. This process created a new variable that indicated the position of the sun relative to the car, independent of the direction of travel. The calculated measure represented the position of the sun relative to the direction the driver is facing. The NOAA solar calculator (https://gml.noaa.gov/grad/solcalc/) was used to verify the calculations made in the solar angle determination spreadsheet. A sample of random and representative data points was plugged into the NOAA calculator to verify that the same azimuth and vertical sun angles were given.

The horizontal sun angle varied between zero and 180 degrees. A horizontal sun angle measure of 180 degrees means that the sun was positioned directly behind the experimental vehicle as it passed the sign location. On the other hand, a horizontal sun angle of zero degrees indicates the sun was positioned in front of the vehicle. The final measure used for analysis, horizontal angle, does not indicate whether the sun is oriented to the right or left of the driver's view.

Sun angle components were used in the determination of several categorical variables. Sign location pictures were classified as night or day based on the vertical sun angle. If the vertical angle was -6 degrees below the horizon or higher in the sky (Vertical Angle > -6°), then the data were considered daytime. Any picture taken when the vertical sun angle was less than -6 degrees (Vertical Angle < -6°) was classified as night. The horizontal sun angle was used to create a Sun Orientation variable. If the absolute value of the horizontal sun angle was between zero and 60 degrees, the orientation was marked as front. If the horizontal sun angle was between 60 and 120 degrees, the orientation was marked side; larger than 120 degrees was marked as behind.

Figure 27 shows the distribution of the vertical sun angle by trip number. The maximum vertical angle during collection was 58.3 degrees above the horizon and the minimum was -43.49 degrees below the horizon. The average vertical sun angle was 13.86 ± 23.47 degrees across all trips.

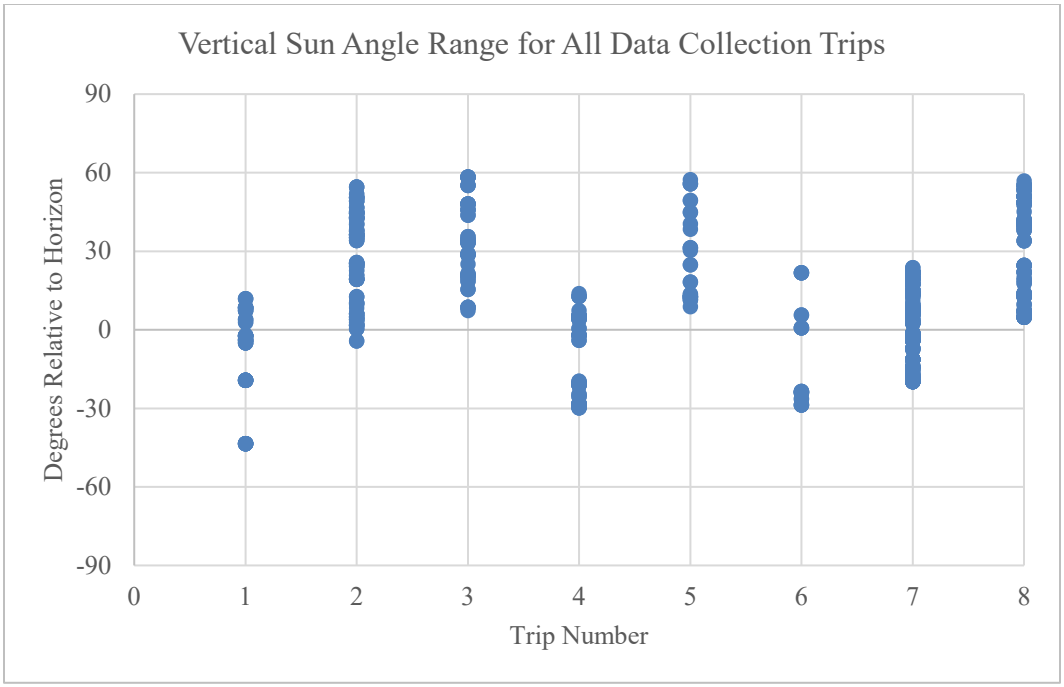

Figure 27. Graph. Vertical sun angle range for all data collection trips measured in degrees relative to the horizon.

Figure 28 shows the spread of the horizontal sun angles by trip number. The maximum horizontal angle collected was 179.74 degrees, and the minimum was 2.58 degrees. The average horizontal sun angle was 90.85 ± 50.62 degrees across all trips.

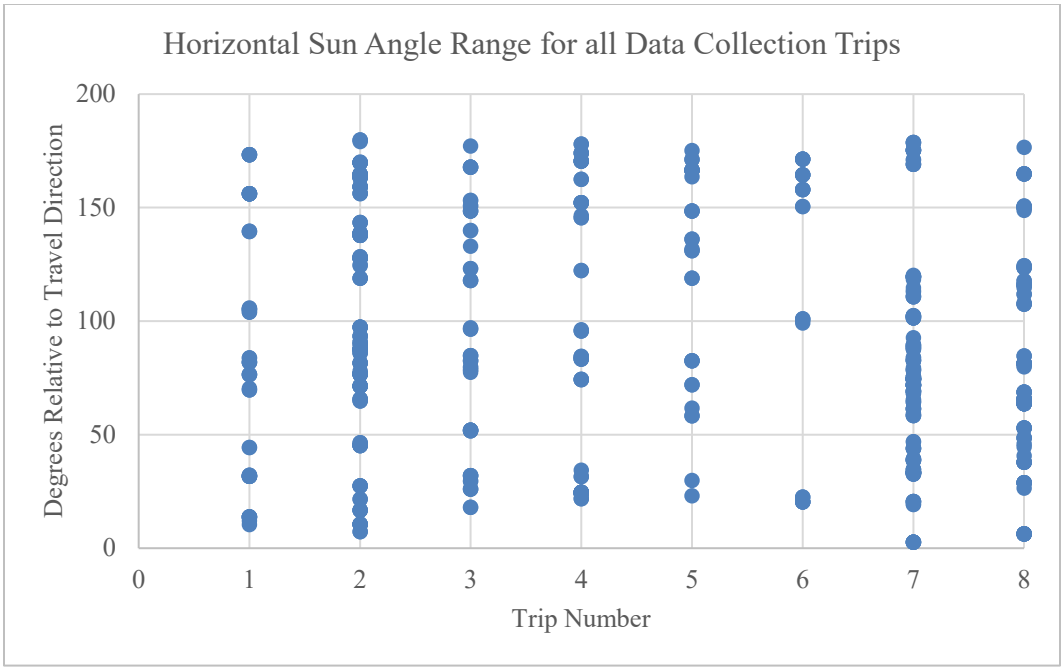

Figure 28. Graph. Horizontal sun angle relative for all data collection trips measured in degrees relative to direction of travel.

Illuminance

Illuminance was measured during data collection trips by the RLMMS at four different points on the vehicle: the driver wheel track, passenger wheel track, middle of lane front, and middle of lane rear. The center of vehicle track measurements were redundant, and therefore at each sign location both middle of lane values were averaged. Subsequently, all three measurement tracks were averaged together to produce the average illuminance used for analysis. The maximum illuminance during the day was 68,044.18 lx, and the minimum was measured at 0.09 lx. Illuminance measurements during the day had an average of 15137.52 ± 14658.73 lx. The maximum illuminance during the evening was 15.14 lx, and the minimum was measured at 0.00. Illuminance measurements at night had an average of 2.15 ± 4.46 lx. Overall, 86% of the nighttime illuminance measurements at the target sign structures were less than 1 lx, as summarized in Figure 29.

Additionally, illumination measurements were converted into a categorical variable for analysis. This process resulted in an illumination category variable that specified four factor levels: night, overcast, sunny, and very sunny. Illuminance measurements categorized as night ranged between 0 and 15.2 lx, overcast measurements were between 15.2 and 1000 lx, sunny measurements were between 1,000 and 10,000 lx, and very sunny measurements were any with a lux greater than 10,000 lx.

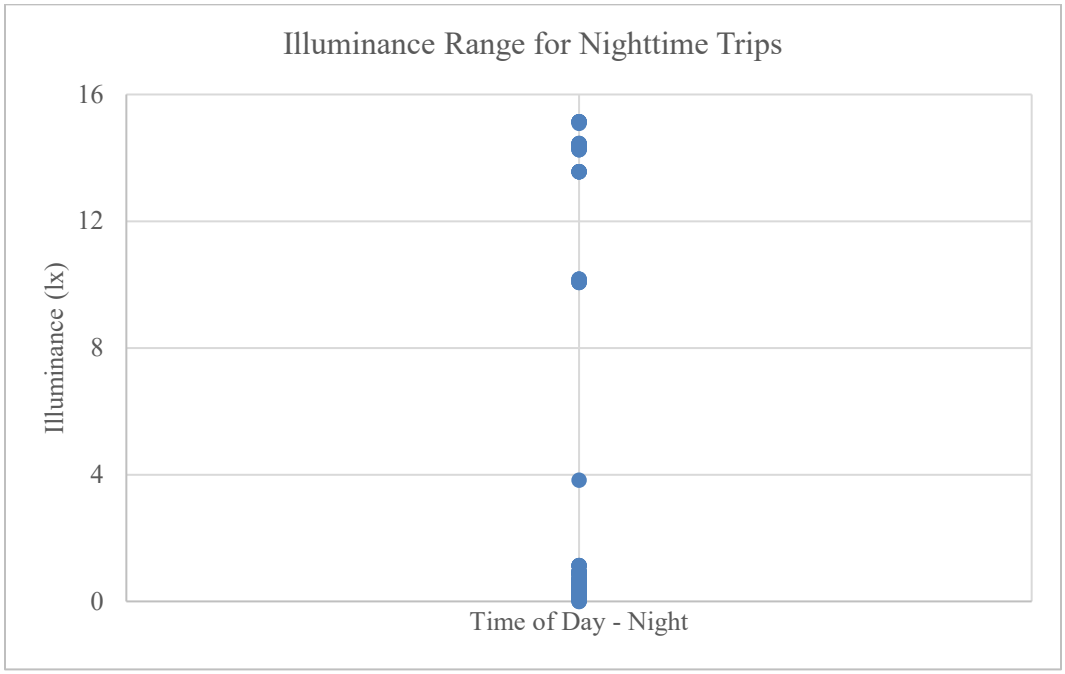

Figure 29. Graph. Nighttime illuminance (lux) across all data collection trips.

VISIBILITY

Visibility was reported using MOR. As previously discussed, MOR is a measure of the density of fog and is defined as the distance through the fog when the contrast of a black object reaches 5% caused by the scattering of 95% of the light. MOR measurements were taken using the

VTTI-developed REIMS system mounted to the roof rack of the experimental vehicle. Measurements were captured at a frequency of 10 Hz. The measurement length used by the VTTI system is 1.83 m. MOR calculations employed Equation 1, Equation 2, and Equation 3. The calibration was calculated using the beginning or end values of a trip where the research team verified that no fog was present.

MOR was calculated for each data point on every trip segment across all trips. A data reductionist selected an initial measurement point to act as the calibration value for each trip. The calibration value represented measurements from the visibility module in known clear conditions. The full data set was processed trip by trip. In total, 2,509,740 MOR values were calculated across all eight data collection efforts. Figure 30 visualizes the range of MOR values for each of the eight data collection trips.

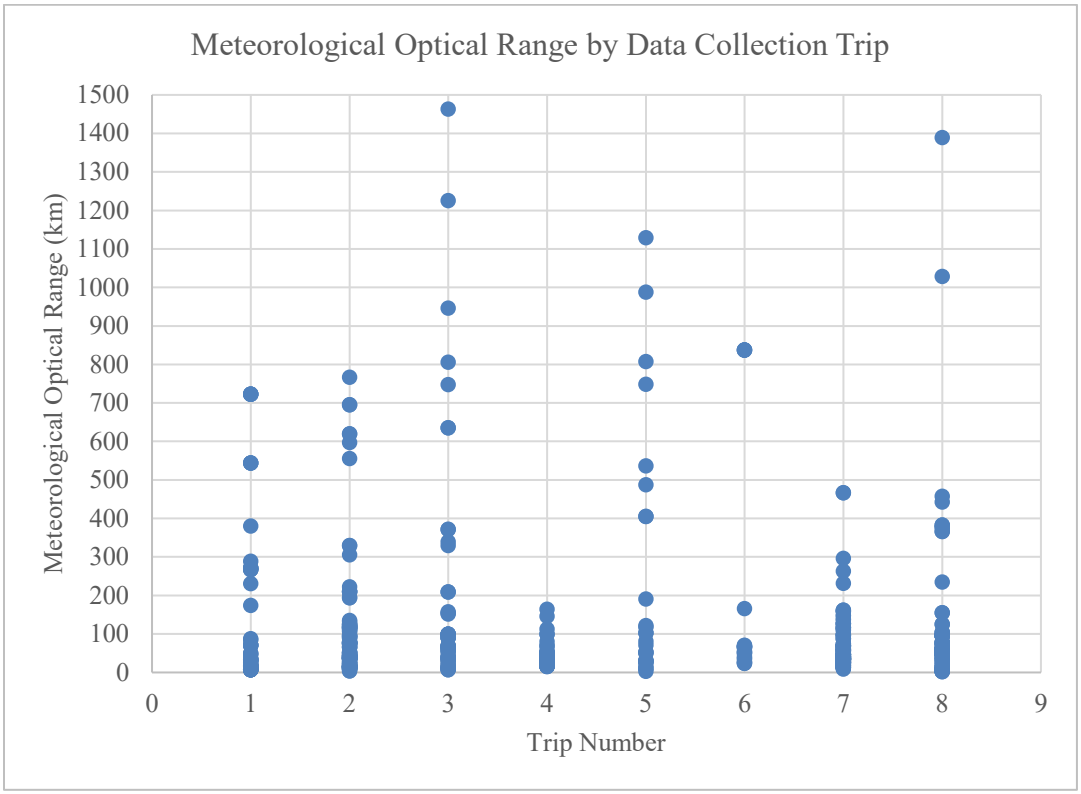

Figure 30. Graph. Meteorological optical range for all data collection trips.

The total number of MOR measurements at sign locations where the sign was present in experimental footage was 1,192. The maximum MOR measured across all sign locations was 115,481, and the minimum was 2.15. The average MOR across all data collection trips was 620.04.

To determine if foggy or hazy conditions were present, the resulting visibility data were trimmed down to only include measurement values that occurred while the experimental vehicle was passing by target sign locations. Using ArcGIS, the research team selected data 200, 400, and 500 ft upstream from target sign structures as reference visibility points. The MOR values at these points were paired with images captured via experimental video to compare sign character

legibility and visibility. In total 1,257 images were paired with a MOR value for the final analysis data set. The research team then assigned a visibility type to all MOR values. Researchers consulted the International Visibility Code (IVC) table for laser beam atmospheric measurements from manned and unmanned aerospace vehicles. The measure ranges shown in Table 14 were used as a template to create a simpler scale to categorize the experimental data.

Table 14. IVC table for laser beam atmospheric measurements from manned and unmanned aerospace vehicles.[64]

Designation	Visibility Distance	Unit of Measure
Dense Fog	0–50	m
Thick Fog	50–200	m
Moderate Fog	200–500	m
Light Fog	500–1	km
Thin Fog	1–2	km
Haze	2–4	km
Light Haze	4–10	km
Clear	10–20	km
Very Clear	20–50	km
Exceptionally Clear	>50	km

Table 15 gives a breakdown of the distribution of MOR value categorization across all data collection trips. Experimental trip routes were selected to go through varying terrain and span significant time periods. Therefore, the MOR data were expected to reflect a variety of visibility conditions. In practice, the routes were all driven in the late spring to early summer on mostly clear days. As Table 15 emphasizes, over 95% of visibility data were collected in clear conditions and less than 0.5% across all trips were collected during foggy conditions.

Table 15. MOR counts for all visibility conditions across all data collection efforts.

Trip Date	Trip Num	MOR Count	Visibility Condition	Visibility Percent
13-Apr	1	264,448	Clear	95.3%
13-Apr	1	11,969	Hazy	4.3%
13-Apr	1	1,080	Foggy	0.4%
15-Apr	2	308,006	Clear	96.1%
15-Apr	2	11,834	Hazy	3.7%
15-Apr	2	746	Foggy	0.2%
18-May	3	315,209	Clear	96.4%
18-May	3	10,947	Hazy	3.3%
18-May	3	714	Foggy	0.2%
20-May	4	320,193	Clear	94.2%
20-May	4	18,422	Hazy	5.4%
20-May	4	1,290	Foggy	0.4%
25-May	5	313,842	Clear	95.9%
25-May	5	12,641	Hazy	3.9%
25-May	5	618	Foggy	0.2%
27-May	6	317,042	Clear	94.6%
27-May	6	17,112	Hazy	5.1%
27-May	6	986	Foggy	0.3%
1-Jun	7	306,633	Clear	96.0%
1-Jun	7	11,868	Hazy	3.7%
1-Jun	7	958	Foggy	0.3%
3-Jun	8	250,670	Clear	95.2%
3-Jun	8	11,950	Hazy	4.5%
3-Jun	8	562	Foggy	0.2%

Table 16 gives the simplified version of the IVC fog-haze-clear table that the research team used to classify MOR measurements. Any MOR value less than 2 was classified as foggy; values greater than 2 and smaller than 10 were classified as hazy; and any MOR value exceeding 10 was classified as clear. Additionally, Table 16 shows the distribution of MOR values for images captured while the experimental vehicle was passing the target sign structures.

Table 16. Simplified version of the IVC scale and data counts for MOR in the experimental images.

Designation	Visibility	Unit of Measure	Count (Proportion)
Fog	0-2	km	0 (0%)
Haze	2-10	km	79 (6.6%)
Clear	> 10	km	1,113 (93.4%)

Font Size

Font size was assessed for each sign structure by a data reductionist following specifications outlined in MUTCD Chapter 2E, *Guide Signs – Freeways and Expressways*.[65] Additionally, the number of characters present for each font size on every target sign structure was collected. Font size and character count were evaluated for each unique sign located on the sign structure. Signs were identified as unique by the combinations of background and legend colors. Characters on signage that shared background and legend color, and were located on the same sign structure, were counted together.

The data collection found that seven font sizes were present on the target sign structures (8, 10, 12, 13, 15, 16, and 18 inches). For all signage, one average legibility score was assigned for each font size present. Arithmetic summarization across all data collection efforts showed that, overall, legibility score increased with font size. Eighteen-inch and 12-inch fonts were rated as having the highest average legibility score, with both font sizes receiving an average legibility score of 3.83 across all trips. The 8-inch sized fonts were found to be the least legible, on average, with an average score of 2.93. Figure 31 visualizes the average legibility score for each of the seven fonts sizes.

Although data showed an increase in mean legibility score as font size increased, the pattern was not uniform. Thirteen-inch font sized characters bucked the trend of mean legibility score increasing with font size. The 13-inch font sized characters were rated as less legible than 12-inch characters and more similarly to 10-inch characters, even though they were 30% larger in size. The difference in mean legibility score between 13-inch characters and similarly sized characters could be due to font size variation and pairings found on the target sign structures. Furthermore, differences in legibility may be confounded by factors not accounted for, such as stroke width. For example, 13-inch fonts were commonly used as capital letters at the beginning of place names on guide signs, and the remaining lower-case characters in the same word were frequently all 10 inches.

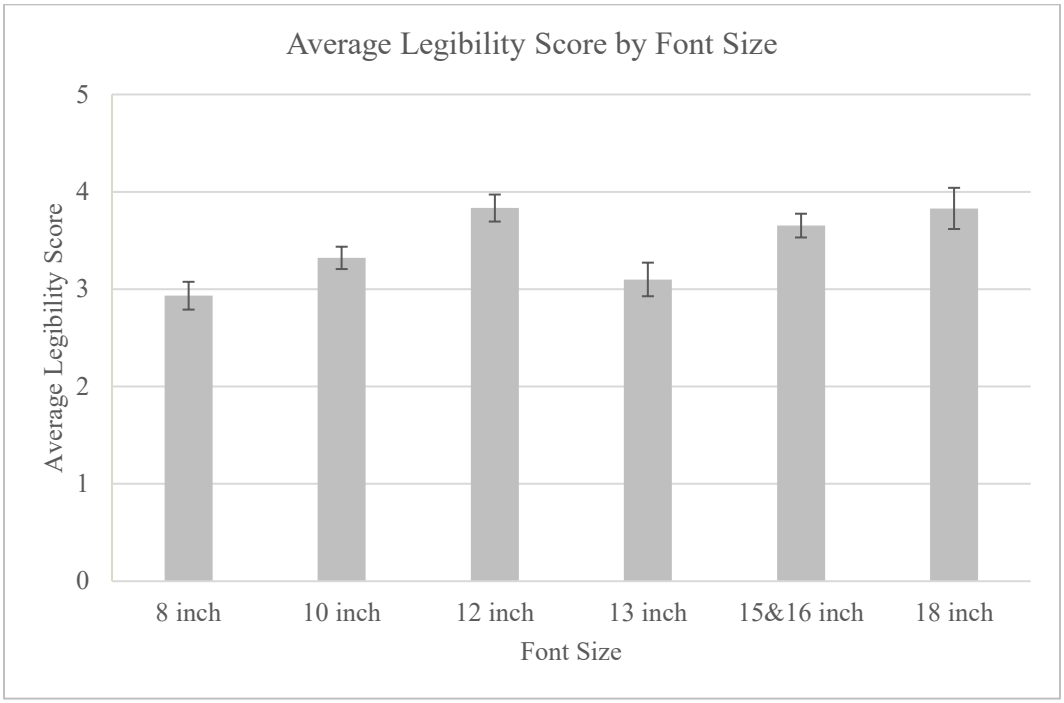

Figure 31. Graph. Average legibility score for each of the seven font sizes present on target signs. Error bars represent the standard error.

Visually similar font sizes were categorized as either small, medium, or large for analysis. The 8- and 10-inch fonts became the small category, the 12- and 13-inch fonts became the medium category, and any font 15-inches or bigger was considered large. The mean legibility score for

small category fonts was 3.17, medium was 3.49, and large was the most legible with a mean score of 3.70, as shown in Figure 32.

Figure 32. Graph. Average legibility score by font size category. Error bars represent the standard error.

Legibility

Legibility was the dependent variable constructed during the data preparation. The research team examined each picture taken during data collection to determine if a sign was present or not in the image. Images were captured at 200, 400, and 500 ft from the target sign structures. Due to road configuration and vehicle orientation, some signage was too far out of the view of the vehicle's camera to be captured, especially at 200 ft. Data reduction used the scale in Table 17 to assign legibility scores to the sign characters in each image. Legibility score was assessed for all font sizes in each sign image, and legibility score was recorded as a single data point representing all characters for each font size. Some images contained multiple signs located on either the side of the road or on overhead gantries at the target sign location. Table 17 gives the legibility score scale and a brief description of the criteria used to determine the scores.

Table 17. Legibility score scale used by researchers when evaluating sign images.

Legibility Score	Description
0	Cannot read sign
1	Difficult to read but the words can be guessed. Major issues with darkness, blurriness, and/or glare are present.
2	Somewhat difficult to read. The number of characters in each word can be distinguished, however some letters may require guessing. Some significant issues with glare, darkness, and/or blurriness exist.
3	Somewhat easy to read. The characters and letters within each word can be read. Some issues with glare, darkness, and or blurriness appear. The reader can distinguish differences in font size at this score.
4	Easy to read but obstructions due to glare, blurriness, and/or darkness may be present. All characters are clearly visible.
5	Very easy to read with no obstructions and all characters visible.

Legibility score data were reformatted for analysis so that instead of a discrete range, the legibility score was presented as a binary response. Each score was categorized as either illegible (0) or legible (1) based on the score descriptions in Table 18. Illegible signs were either completely unreadable or would not be reasonably expected to be read by machine vision technology due to glare, blurriness, or image quality. Legible signs were expected to be read by machine vision technology and contained varying levels of glare and blurriness but in much smaller amounts than illegible images. To account for image-to-image variability, the research team selected multiple images for consideration at each upstream distance (200, 400, and 500 ft). When the primary image quality was low, or the target sign structure was missing, the research team considered multiple pictures. Overall, 70% of sign characters scored were judged as legible, though this number was significantly different when comparing daytime to nighttime. The research team expects that routine refocusing of the machine vision camera would improve the image quality and subsequently sign character legibility. This should be a consideration for ongoing maintenance of future vehicles.

Table 18. Legibility category key for binary variable assignment.

Legibility Category	Description	Count
Illegible	Any sign assigned a score of 0, 1, 2	371
Legible	Any sign assigned a score of 3, 4, 5	886

Machine Vision Legibility

Machine vision analysis used the MATLAB OCR[59] function to evaluate all sign images for text recognition. Video was captured throughout the data collection effort using a forward-facing camera mounted on the experimental vehicle. Data reductionists extracted two images captured as close as possible to 200 ft, 400 ft, and 500 ft from each sign location. Pairs of images were reviewed to confirm that at least one contained the target sign structure. Images were then processed using the MATLAB OCR function, which outputs the words read by the machine vision algorithm. A data reductionist reviewed these results to evaluate the accuracy.

Based on the MATLAB OCR output, the project team attempted to calculate a legibility score (i.e., percentage of characters read correctly) for each sign; however, the results indicated low accuracy of character recognition. OCR results contained largely letters and symbols that were

not present on the target sign structure. Subsequently, the research team sought to process the sign images to improve the accuracy of the OCR function by using image binarization, which was available in MATLAB. Sign images were processed using the “greaythresh” and “imbinarize” functions to attempt to separate the background of the image from the text elements in the foreground. Additionally, the research team specified that the scene was natural using the LayoutAnalysis option. The processed images were again run through the OCR function; however, the performance was similar to pre-processing.

MATLAB suggests that images where the text is not visible after binarization may suffer from non-uniform lighting. Furthermore, the OCR function available in MATLAB, and used in this analysis, performs best for computer vision applications such as license plate reading and document analysis. These applications typically use images with a uniform-colored background and legend color. Daytime sign images captured during this research did not fit the mold of images typically analyzed using MATLAB’s OCR function. Daytime images frequently had high visual clutter levels with many other sources of text, including commercial signage and other vehicles. Additionally, nighttime images suffered from contrast issues where the dark background also included poorly illuminated text.

CHAPTER 5. DATA ANALYSIS

SIGN LOCATION

Linear regression modeling was used to evaluate the effect of sign location and font size on the legibility of sign characters. The model contained sign location and font size (category) as main effects and included the interaction between them. The response variable for this analysis was legibility score. The data were sorted and split by day and night to evaluate mean legibility score for day and night separately. The overall chi-square goodness of fit test results and their associated *p*-values are shown in Table 19. *P*-values ≤ 0.05 indicated significant difference in mean legibility was found between at least one pair of factor levels.

For both models, the null hypothesis tested was "*the size of characters and location of roadway signage (overhead versus side of the road) does not change the mean legibility score of sign characters*." Rejection of the null hypothesis indicated a statistically significant difference in mean legibility score between at least two factor levels. The chi-square goodness of fit test for both models found the main effect of sign location to be statistically significant. Font size (categorical) and the interaction between font size and sign location were not significant during either time of day. Post hoc analyses focused on the factor-level differences in legibility score between overhead and side of road signage. To account for multiple comparisons, *p*-value adjustments were done using Tukey's method to keep the familywise error rate at 0.05.

Table 19. Generalized linear modeling goodness-of-fit chi-squared results for legibility score by sign location, font size, and time of day.

Type 3 Tests of Fixed Effects					
Time of Day	**Effect**	**Num DF**	**Den DF**	***F*-value**	***P*-value**
Day	Sign Location (SL)	1	1041	3.9	0.05
	Font Size (FS)	2	1041	2.04	0.13
	SL*FS	2	1041	1.97	0.14
Night	SL	1	204	27.66	<.0001
	FS	2	204	1.14	0.32
	SL*FS	2	204	0.32	0.73

The model interaction term was not significant; however, the research team suspected that mean legibility may differ within each font size category. Therefore, post hoc analysis was informed by conducting a test of the simple effects. Table 20 displays results from the test of effect slices, which assess the differences of the least-squares means within each font size category (small, medium, and large). Testing significance (*p*-value less than 0.05) indicated a difference in legibility score between overhead and roadside signage within each font size category. Results showed that, during the day, there was significant difference in mean legibility score between small letters located on overhead and roadside signage. At night, effect slice testing found significant difference in mean legibility score between all font size categories. Subsequent results are presented for sign location independent of font size and separately for all font size categories.

Table 20. Tests of effect slices at all factor levels of font size (category) for the influence of sign location by time of day.

Time of Day	Effect	Font Size	Num DF	Den DF	*F*-value	*P*-value
Day	Sign Location*Font Size	Large	1	1041	1.68	0.196
		Medium	1	1041	0.1	0.756
		Small	1	1041	7.01	0.008
Night		Large	1	204	14.01	0.0002
		Medium	1	204	4	0.047
		Small	1	204	13.97	0.0002

Least squares means model estimates for legibility score by sign location are shown in Table 21, for day and night. During the daytime, sign legibility increased by 8.7% when characters were on overhead signage (4.33) compared to roadside signage (3.98). Although overhead signage was judged as more legible, on average, daytime sign characters, independent of font size, were found to be legible and easy to read, regardless of sign location.

At night, sign legibility increased by 428% when located on overhead signage (2.23) rather than roadside signage (0.55). Of note is that nighttime images of roadside signage frequently contained motion blur, which contributed to the poor legibility ratings. Additionally, the legibility scores for overhead nighttime sign characters were poor, with the mean score approaching illegibility (score less than 2). Overall, nighttime sign characters were difficult to read or barely legible. Although the research team expected differences in legibility by time of day, these results are confounded by the limitations of the image capturing technology used in this effort.

Table 21. Least Squares means table for legibility score by sign location, time of day, and font size.

Least Squares Means Table				
Font Size	Time of Day	Sign Location	Mean Estimate	Standard Error
ALL	Day	Overhead	4.33	0.17
		Side	3.98	0.06
	Night	Overhead	2.23	0.30
		Side	0.52	0.12

Figure 33 visualizes the mean legibility score for all sign location, font size, and time of day factor level combinations. For sign characters viewed on daytime images, no significant difference was found between the mean legibility score of overhead and roadside signage for medium- and large-sized fonts. Small fonts located on overhead signage viewed during the day (4.23 score) were found to be significantly more legible (20%) than small fonts on roadside signage during the day (3.53 score). Overall, fonts on signage viewed during the day were rated as being at least somewhat easy to read. Although there were some obstructions due to glare and blurriness, generally all characters were visible.

Significant difference in mean legibility score between sign locations at night was found for all within-font size comparisons. Small font mean legibility increased by 393% when located on overhead signage (2.6 score) compared to roadside signage (0.66 score) when viewed at night.

Similarly, medium-sized font legibility increased by 464% when located on overhead signage (1.67 score) compared to roadside signage (0.36 score) when viewed at night. Additionally, large font legibility increased by 440% when located on overhead signage (2.42 score) compared to roadside signage (0.55 score) when viewed at night. While significant differences between sign locations were found for all font sizes at night, their legibility scores would all be classified as illegible or difficult to read.

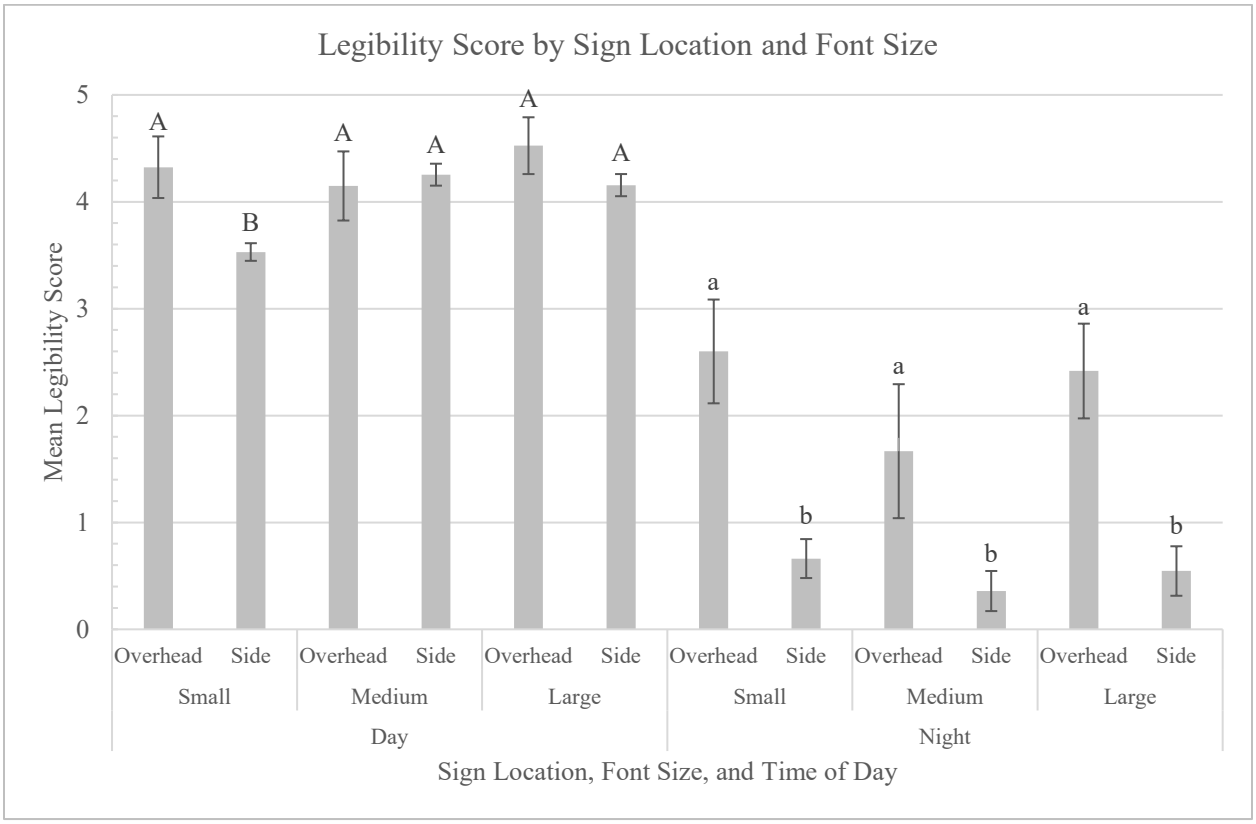

Figure 33. Graph. Mean legibility score by sign location and font size. Error bars represent standard error. Difference in capital letters indicates post hoc significance for daytime images. Difference in lower case letters indicates post hoc significance for nighttime images.

VIEW DISTANCE

Linear regression modeling was used to assess the influence of font size (category) and view distance on the legibility score of sign characters. Models were fit using legibility score as the response variable with view distance and font size as the categorical independent variables. Modeling also included the two-way interaction term. The data were evaluated for mean legibility score by the time of day. Post hoc analysis was done using a difference of least squares means procedure, and *p*-value adjustments were done using Tukey's method to keep the familywise error rate at 0.05. The overall chi-square goodness of fit results, by time of day, are shown in Table 22.

For both models the null hypothesis stated, *"mean legibility score is equal for all combinations of view distance and font size."* Rejection of the null hypothesis indicated a difference in mean

legibility score between two of the font size and view distance treatment combinations. Goodness of fit testing indicated that the interaction between view distance and font size was not significant for any of the factor-level combinations at either time of day. For nighttime images, the main effect of view distance was significant, and for daytime images font size (categorical) was found to be significant.

Table 22. Generalized linear modeling results for legibility score by font size, view distance and time of day.

Type 3 Tests of Fixed Effects					
Time of Day	**Effect**	**Num DF**	**Den DF**	***F*-value**	***P*-value**
Day	View Distance (VD)	2	1038	0.08	0.92
	Font Size (FS)	2	1038	9.96	<.0001
	VD*FS	4	1038	1.63	0.16
Night	VD	2	201	6.55	0.002
	FS	2	201	1.23	0.30
	VD*FS	4	201	1.05	0.38

Both models' interaction terms were not significant; however, the research team suspected mean legibility may differ between each font size based on view distance. As a result, post hoc analysis was informed by conducting a test of the simple effects. Table 23 displays the effect slice testing results, which assess the differences of the least-squares means within each font size category (small, medium, and large). Testing significance (*p*-value less than 0.05) indicated a difference in mean legibility score between at least two view distances for large font size letters at night. Analysis results are presented for view distance independent of font size and separately for all font size categories.

Table 23. Tests of effect slices at all factor levels of font size (category) for the influence of sign location by time of day.

Tests of Effect Slices						
Effect	**Time of Day**	**Distance**	**Num DF**	**Den DF**	***F*-value**	***P*-value**
View Distance*Font Size	Day	200	2	1038	0.99	0.37
		400	2	1038	3.57	0.029
		500	2	1038	16.89	<.0001
	Night	200	2	201	0.35	0.71
		400	2	201	0.67	0.51
		500	2	201	3.07	0.048

Post hoc analysis of the main effect view distance during day and night revealed a significant difference in mean legibility between sign characters viewed from 500 ft and both 200 and 400 ft. Nighttime mean legibility at 500 ft (1.22) saw an improvement of 658% and 248% over small (0.19) and medium (0.49) characters, respectively, as shown in Figure 34. However, no significant difference in legibility score was present between any font size and view distance factor combinations during the day. Overall, daytime legibility scores were not impacted by the differences in view distance tested in this study and, on average, daytime sign characters were judged to be easy to read. Conversely, nighttime sign characters were difficult to read across all view distances. Nighttime images were judged to be difficult to read at all distances and had consistent issues with blurriness, darkness, and glare. Camera technologies used in this effort

performed well during the daytime at all distances. In contrast, the system struggled to capture legible sign characters at night, from all distances.

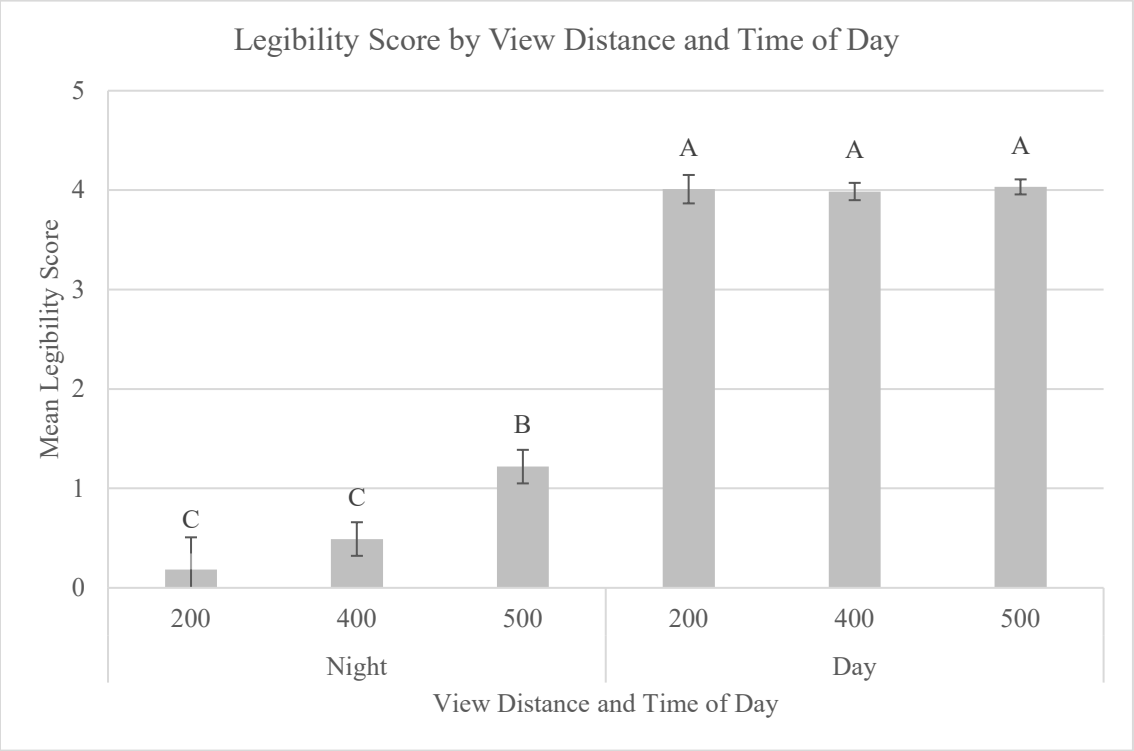

Figure 34. Graph. Mean legibility score by view distance and time of day. Error bars represent standard error. Difference in capital letters indicates post hoc significance.

Subsequent analysis was informed by simple effects tests and assessed difference in mean legibility between font size categories at all experimental differences. Significant difference in mean legibility score was found at the 500 ft distance during day and night, and at 400 ft during the day (Figure 35). From 500 ft, during the day, mean legibility score for font size large (4.38) was 27% higher than small font size characters (3.45). Similarly, from 500 ft, during the day, mean legibility score for font size medium (4.27) was 23% higher than small font size characters. The same pattern was true from 400 ft, during the day, where mean legibility score for font size large (4.07) was 10% higher than small font size characters (3.68). Also, from 400 ft, during the day, mean legibility score for font size medium (4.2) was 14% higher than small font size characters. Overall, mean daytime scores varied from 3.4 to 4.4 and were scored as easy to read at all view distances. Large and medium font size characters did not experience a drop off in legibility as view distance increased; however, small characters saw a steady decrease in legibility as view distance increased.

Nighttime legibility scores were below 2 for all font size and view distance combinations and were generally not legible. The sample size of nighttime images from 200 ft and 400 ft with visible sign characters was small, and therefore meaningful view distance comparisons were not possible. However, effect slice testing indicated significant difference at 500 ft where large (1.79) sign characters had mean legibility scores that were 57% and 246% higher than small (1.14) and medium (0.73) sign characters, respectively.

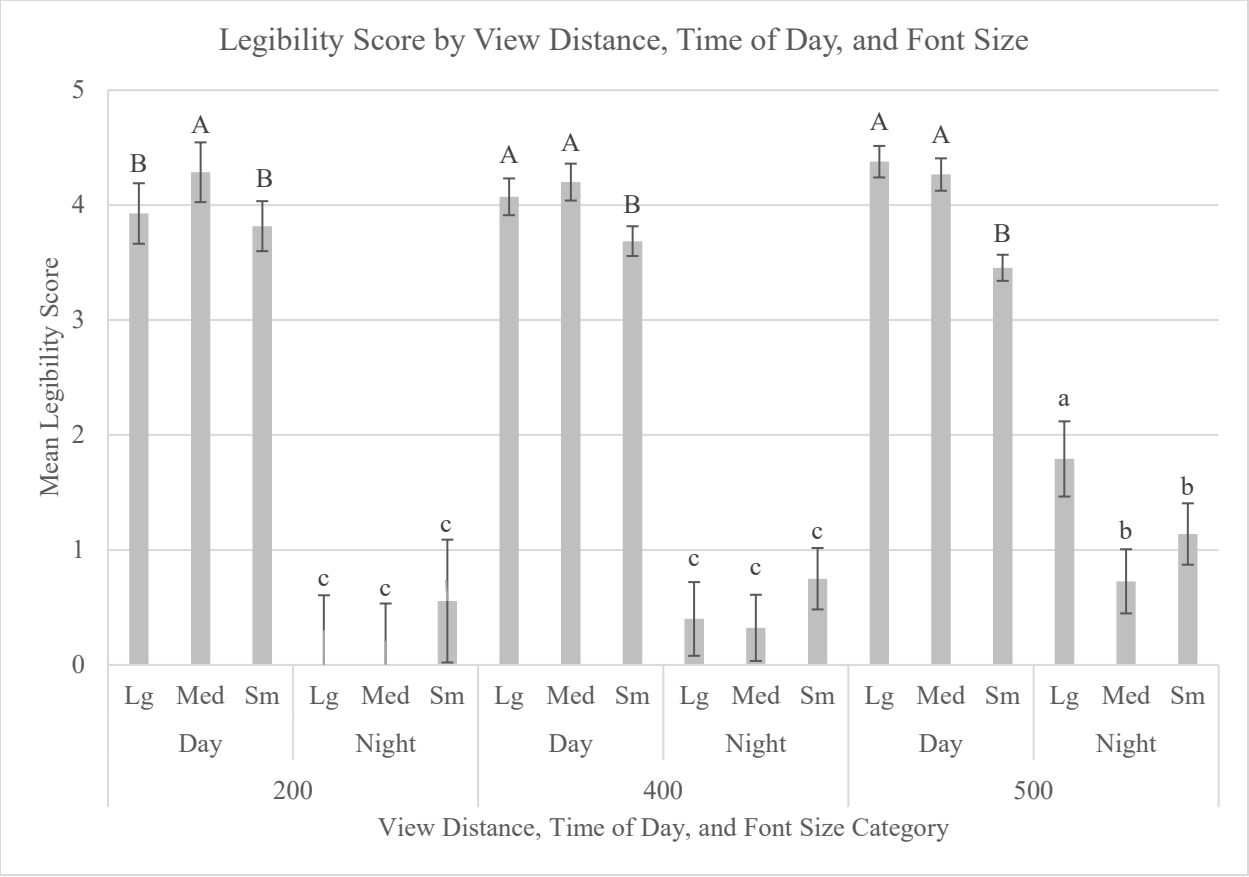

Figure 35. Graph. Mean legibility score by view distance, time of day, and font size category. Error bars represent standard error. Difference in capital letters indicates post hoc significance for daytime images. Difference in lower case letters indicates post hoc significance for nighttime images.

SIGN COLOR

Data collection efforts sought to select a representative sample of sign structures present along each experimental route. However, during data reduction it became apparent that some color schemes were only captured in a small number of images. To ensure the accuracy of mean legibility model estimates, the research team only included sign color, font size, and time of day factor level combinations that had a sample size of eight or more. In total, 43 legibility ratings were excluded from analysis. The color schemes present in sign images, during the day, used blue, brown, and green backgrounds with white legend text in addition to white and yellow backgrounds with black legend text. Nighttime images contained signage using a green background with white legend in addition to white and yellow backgrounds with black legend text.

After data processing, the remaining data (n = 1,214) were analyzed using linear regression modeling to evaluate the effect of sign color and font size on the legibility of sign characters. Models contained sign color and font size category as main effects. The two-way interaction between sign color and font size was also included. The overall chi-square goodness of fit test

results are summarized in Table 24. For both models the null hypothesis tested was *"all combinations of sign color and font size have equal mean legibility score."* Rejection of the null hypothesis at *p*-values less than 0.05 indicated a significant difference in mean legibility score between two of the font size and color scheme combinations.

For daytime sign images, the overall chi-square goodness of fit test found statistical significance for font size, sign color, and the interaction between them. For nighttime sign images, there was no statistical significance found for any of the model terms. Post hoc analysis was done using a difference of least squares means procedure and focused on the daytime differences in legibility score for the main effect of sign color and the interaction between sign color and font size.

Table 24. Linear modeling results for daytime legibility score by sign color and font size.

Type 3 Tests of Fixed Effects					
Time of Day	**Effect**	**Num DF**	**Den DF**	***F*-value**	***P*-value**
Day	Sign Color (SC)	5	1031	3.05	0.005
	Font Size (FS)	2	1031	20.77	<.0001
	SC*FS	8	1031	3.55	0.0005
Night	SC	2	161	2.19	0.115
	FS	2	161	2.53	0.083
	SC*FS	1	161	2.13	0.146

Analysis of the main effect of sign color found a significant difference in mean legibility score between signage using a yellow background and white legend color scheme and signage using blue or brown background with a white legend color (Figure 36). Sign images with a blue background and white legend (4.49) experienced an increase in legibility of 28% compared to signage with a yellow background and black legend (3.51). Similarly, signage with a brown background and white legend (4.15) saw an increase in legibility of 18% compared to signage with a yellow background and black legend. Overall, daytime mean legibility was judged as easy to read for all color schemes except for yellow background with black legend (somewhat easy to read).

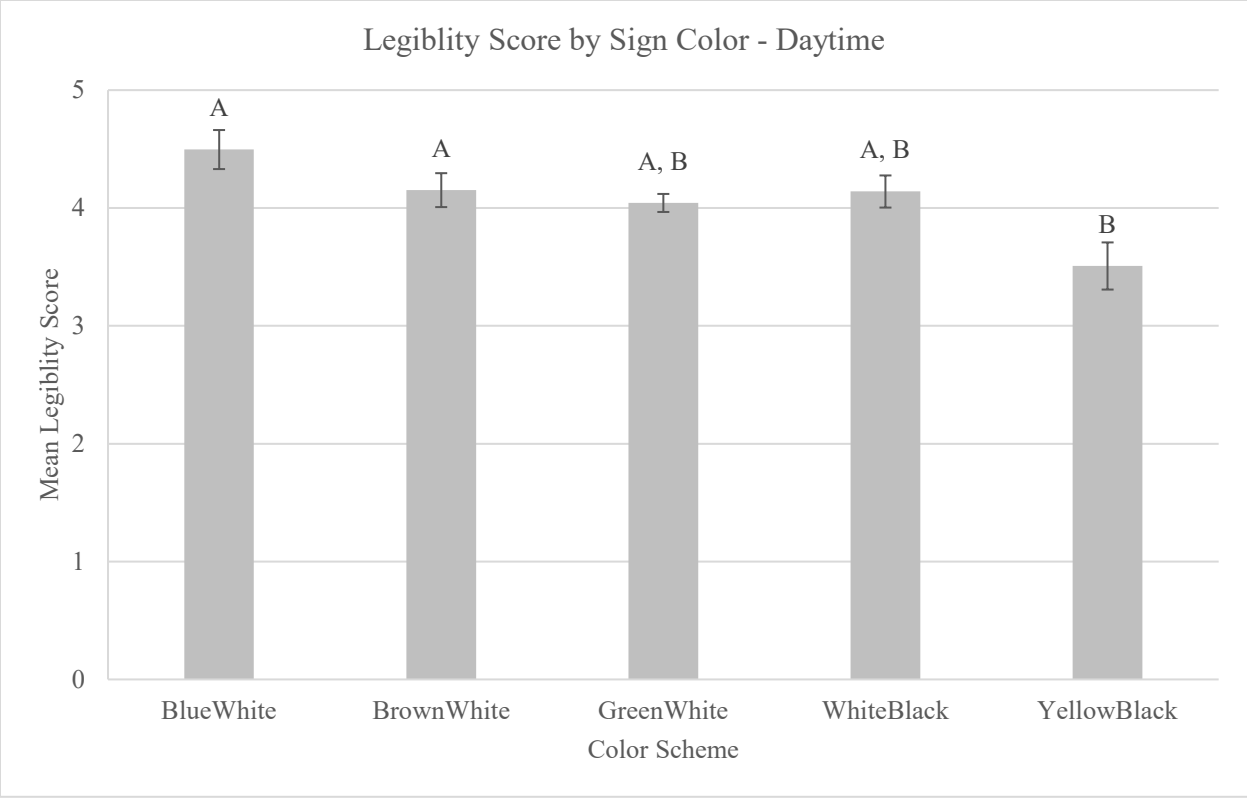

Figure 36. Graph. Legibility score by sign color during the daytime. Error bars denote standard error. Difference in capital letters indicates post hoc significance.

Pairwise comparisons for all factor levels resulted in very few statistically significant results. This was attributed to the large number of pairwise comparisons made in the interaction model (105 comparisons). For a more targeted follow-up analysis, the research team tested for significant difference of the simple effects. Table 25 displays the significance of effect slice testing results, which assess the differences of the least-squares means within each font size category (small, medium, and large). Testing significance (*p*-value less than 0.05) indicated a difference in mean legibility score between at least two sign color schemes for all font sizes at night. Further analysis results are presented for sign color by font size category.

Table 25. Tests of effect slices at all factor levels of font size (category) for the influence of sign location by time of day.

Tests of Effect Slices					
Effect	**Font Size**	**Num DF**	**Den DF**	***F*-value**	***P*-value**
Sign Color*Font Size	Large	4	1031	2.4	0.048
	Medium	4	1031	3.4	0.009
	Small	4	1031	7.43	<.0001

Figure 37 visualizes the mean legibility score estimates obtained during modeling. Large characters appearing in images of signs with blue background and white letters (4.91) were significantly more legible (23.1%) than those with green background and white legend (3.98)

during the day. No other significant difference was present between sign color schemes for large characters. The research team notes that the yellow background with black legend signage had the lowest scored mean legibility for large characters and suspect that an increased sample size would have resulted in significant difference.

Medium characters appearing on signage with blue background and white legend (5.00) were found to have significantly higher (33%) mean legibility scores than medium characters on signage with a yellow background and black legend (3.75) during the day. Similarly, medium characters appearing on signage with white background with black legend (4.83) were found to have significantly higher (29%) mean legibility scores than medium characters on signage with a yellow background and black legend during the day.

Small characters appearing on signage with brown background and white legend (4.14) significantly increased legibility by 30% and 43%, respectively, compared to characters on signs with white (3.19) or yellow (2.88) backgrounds and black legends. In addition, small characters appearing on signage with green background and white legend (3.91) significantly increased legibility by 23% and 36%, respectively, compared to characters on signs with white or yellow backgrounds and black legends.

Across all font sizes and sign colors, the characters on daytime images were all rated at least somewhat easy to read (Table 17). Signage with yellow legend color and black lettering was scored as being the least legible across all character sizes. No significant difference in mean legibility score was found between any sign color schemes for any font size at night. Moreover, all nighttime sign character mean legibility scores would be classified as illegible or difficult to read.

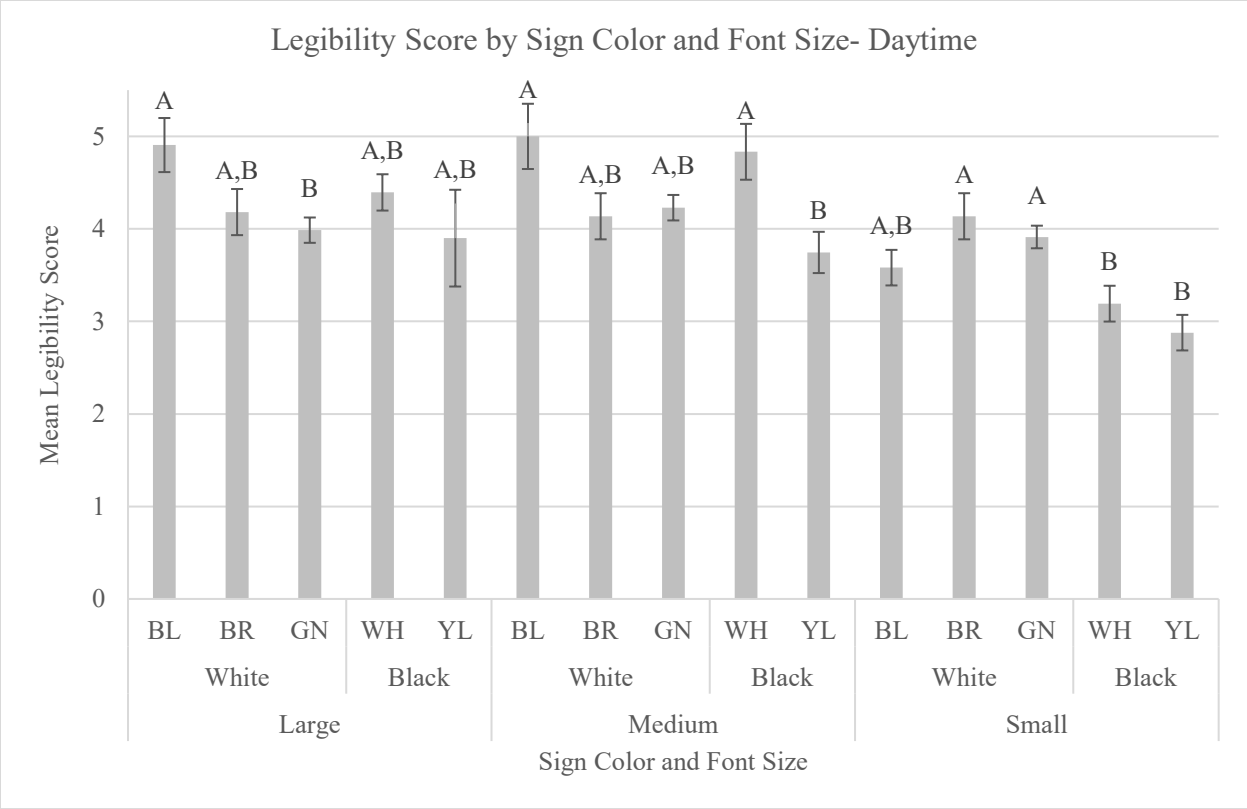

Figure 37. Graph. Legibility score by font size and sign color during the daytime. Error bars represent standard error. Difference in capital letters indicates post hoc significance within font size category. Color names assigned using Midmark color abbreviation chart.(67)

FONT SIZE

The research team used linear regression modeling to assess the influence of font size on the legibility of sign characters. Font size was assessed for two variable types. The first evaluation looked at the differences between all of the font sizes present on the target sign structures, and the second used the font size categories that were developed by the research team (small, medium, and large). Both modeling efforts used legibility score as the dependent variable and font size as the categorical independent variable. Data were evaluated for mean legibility score at day and night. Post hoc analysis was done using a difference of least squares means procedure, and *p*-value adjustments were done using Tukey's method to keep the familywise error rate at 0.05.

For both modeling efforts the null hypothesis tested was *"mean legibility scores are equal for all font size factor levels."* Rejection of the null hypothesis indicated a difference in mean legibility score between at least two of the font size treatment combinations. The chi-square goodness of fit test results are shown in Table 26. Results suggested significant difference in mean legibility rating during the day but no significant difference at night. Subsequent analysis sought to investigate the differences in daytime mean legibility by font size.

Table 26. Linear regression modeling results for legibility score by font size and time of day.

Type 3 Tests of Fixed Effects					
Time of Day	**Effect**	**Num DF**	**Den DF**	***F*-value**	***P*-value**
Day	Font Size	5	1041	9.65	<.0001
Night	Font Size	5	204	0.94	0.45

Figure 38 summarizes mean legibility rating for all font sizes by time of day. Pairwise comparison results revealed significant difference in daytime mean legibility score between 8-inch (3.33) font characters and all other font sizes, except for 10-inch (3.74). Enlarging the font size to 12-inch (4.41), 13-inch (4.02), 15-inch (4.14), and 18-inch (4.42) from 8 inches resulted in an increase of 32%, 21%, 24%, and 33% in mean legibility rating, respectively. A significant difference in mean legibility was also found between 10-inch letters and both the 12- and 18-inch font sizes. Mean legibility increased by 18% when signage contained 12- and 18-inch font sizes, compared to 10-inch font sized characters. There were no significant differences between any of the font sizes at night.

Overall, daytime mean legibility score estimations varied between 3.33 and 4.42. The 8- and 10-inch characters were rated between somewhat easy to read and easy to read, which was significantly less legible than the larger sized characters. Nighttime mean legibility score estimations varied between 0.36 and 1, which is, on average, well below the threshold for legibility (score of 2). Researchers note that night images suffered from visual distortions likely due to the influence of headlamp glare. In addition, the roadway was frequently very dark at night and, in the absence of illumination from headlamps, the target signs were often missing from the images. As a result, all nighttime mean legibility scores were significantly lower than daytime ones for every font size.

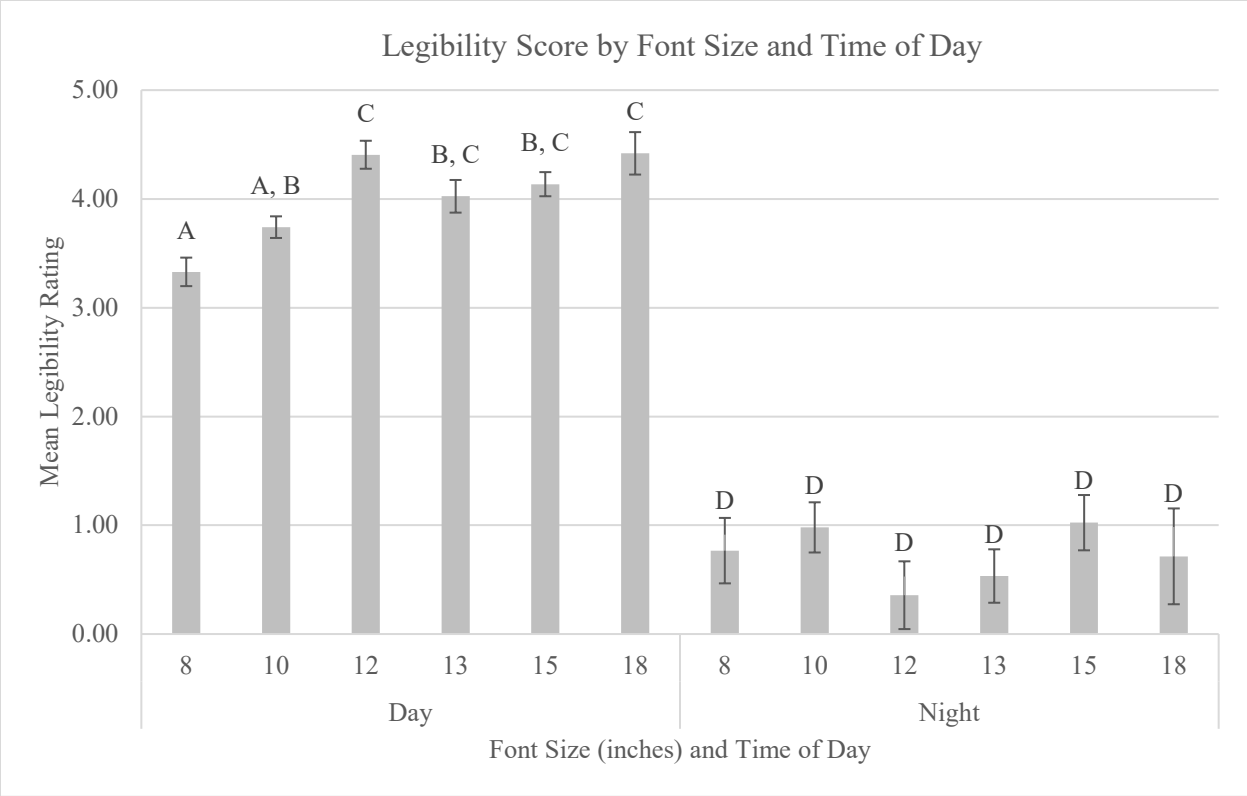

Figure 38. Graph. Mean legibility score for font size by time of day. Error bars represent standard error. Difference in capital letters indicates post hoc significance.

Font size category was assessed for difference in mean legibility for the category bins determined by the research team during data reduction. Linear regression modeling was used to estimate the mean legibility rating for small, medium, and large font sign characters. The chi-square goodness of fit test results, as shown in Table 27, indicated that significant difference in mean legibility rating was present between font size categories during the day, but not at night. Subsequent analysis sought to investigate the differences in daytime mean legibility by font size.

Table 27. Linear regression modeling results for legibility score by font size category and time of day.

Type 3 Tests of Fixed Effects					
Time of Day	**Effect**	**Num DF**	**Den DF**	***F*-value**	***P*-value**
Day	Font Size	2	1044	18.19	<.0001
Night	Font Size	2	207	1.84	0.16

Figure 39 summarizes mean legibility rating for all font size categories by time of day. Pairwise comparison results revealed significant difference in daytime mean legibility score between small (3.6), medium (4.24), and large (4.20) sign characters. Sign characters that were medium and large sized saw an increase in mean legibility score of 18% and 17%, respectively, compared to small. Nighttime sign characters were judged, on average, to be either unreadable or difficult to read regardless of font size category.

Overall, daytime sign character font size category looked to have a positive relationship with legibility rating; however, there was no visual performance increase between the medium- and large-size fonts. Daytime legibility scores were, on average, easy to read for medium and large characters and somewhat easy to read for small characters.

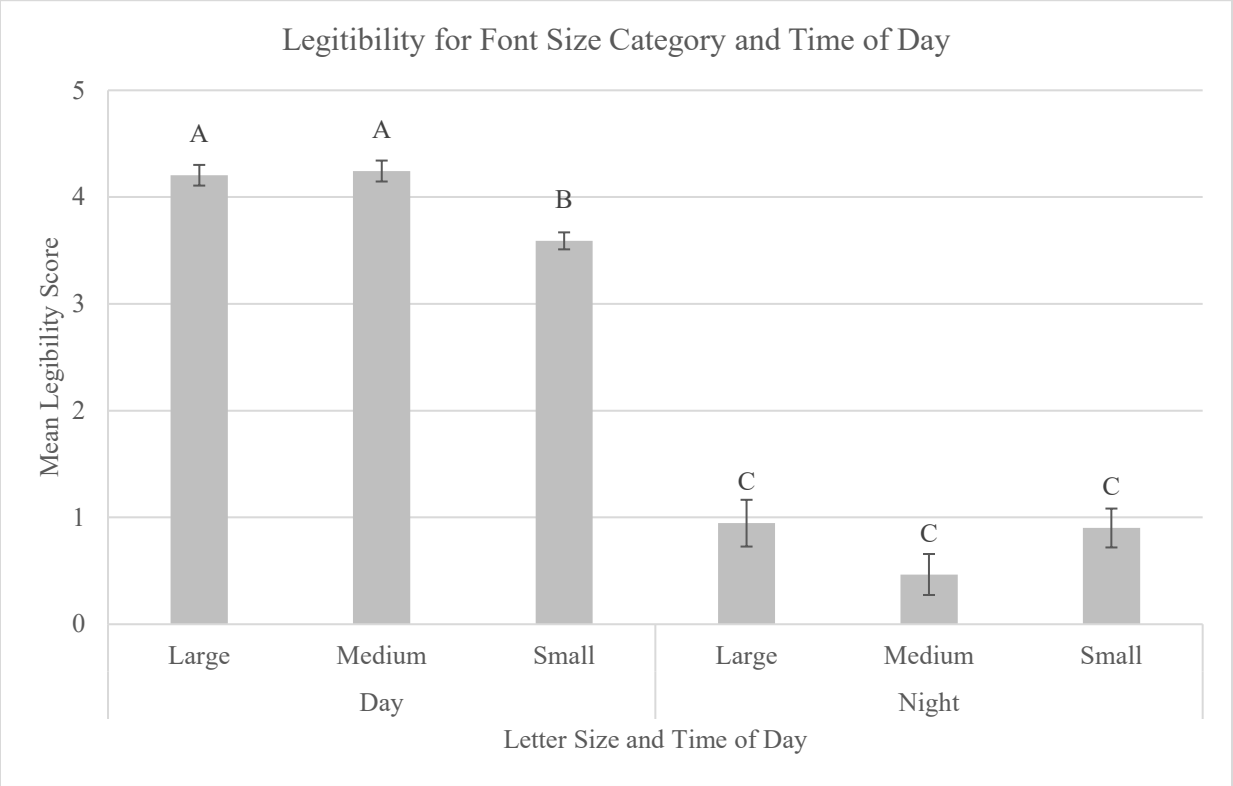

Figure 39. Chart. Mean legibility score for font size category by time of day. Error bars represent standard error. Difference in capital letters indicates post hoc significance.

SUN POSITION

To address the question, *"does the probability/odds of being legible significantly change as the position of the sun changes,"* researchers created a data subset containing only measurements marked as daytime. The resulting data were analyzed using a logistic regression procedure. Logistic regression modeling sought to estimate the likelihood of sign characters being legible. All statistical modeling was done in SAS, and results are reported in terms of odds ratios and the probability of being categorized as legible. The response variable for this analysis was a binary categorical variable indicating if the sign characters were legible or not. Table 18 summarizes the legibility response levels. The sample size for the daytime data set included 1,047 sign legibility measurements.

The horizontal component of sun position was referred to as the sun orientation. Modeling sought to determine if changes in the horizontal position of the sun had an impact on the odds of being legible. Horizontal sun position was categorized into three groups: front, side, and behind, as illustrated in Figure 40. All sun orientation categories were relative to the direction of travel of the experimental vehicle at a given target sign structure location.

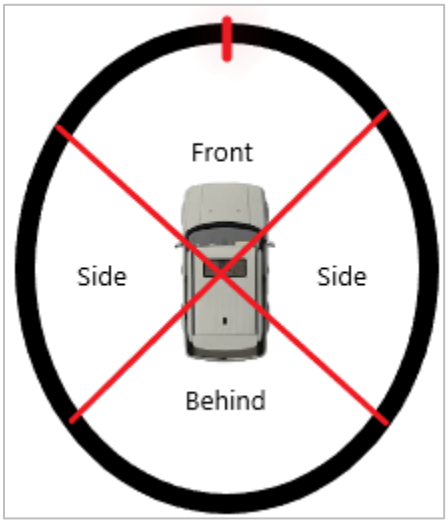

Figure 40. Diagram. Visualization of the sun orientation categories.

The vertical component of sun position was named sun elevation. Sun elevation measurements lower than 30 degrees were categorized as low in the sky, and any measurements over 30 degrees were tagged as high in the sky, as shown in Figure 41. Any data where the sun elevation was less than -6 degrees were classified as night and excluded from the analysis.

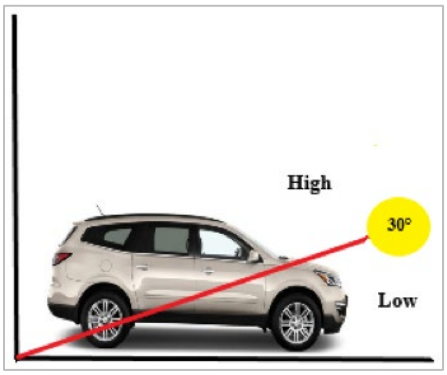

Figure 41. Diagram. Sun elevation variable cutoff between the high and low categories.

To assess the overall influence of the location of the sun, relative to the direction of travel, the research team combined the sun orientation and elevation into one measure of the sun's position. Sun position was assigned for each of the six factor-level combinations of sun orientation and sun elevation (Table 28). The reference level for modeling was chosen to be a sun position of high and side as the research team expected this position to have a high rate of legibility. Results for the sun position analysis are reported in terms of odds ratios compared to the reference position and the probability of legibility at each sun position.

Table 28. Factor-level combinations of sun position.

Sun Elevation	Sun Orientation	Sun Position	Count
Low	Side	Low Side	335
	Front	Low Front	194
	Behind	Low Behind	354
High	Side	High Side	186
	Front	High Front	160
	Behind	High Behind	28

Researchers fit a logistic regression model containing the main effect of sun position. The overall chi-square goodness of fit test gave a Walden ratio chi-square statistic of 59.86, which resulted in a *p*-value of < 0.001 (Table 29). Modeling results indicated that at least one sun position was leading to significantly different odds of sign characters being legible, when compared to the reference level. Post hoc analysis focused on significant differences in odds of being legible between the six factor levels of sun position.

Table 29. Type 3 analysis of effects results for interaction between sun elevation and sun orientation.

Type 3 Analysis of Effects			
Effect	**DF**	**Wald Chi-Square**	***P*-value**
Sun Position	5	59.8618	<.0001

Table 30 gives the maximum likelihood estimates for the comparisons between all sun positions with the reference position set as the sun being high in the sky and on the side of the research vehicle. When compared to the reference level, three of the sun positions were found to significantly reduce the odds of sign characters being legible, and two were found to increase the odds of legibility.

Table 30. Analysis of maximum likelihood estimates for comparisons using the side high sun position as reference.

Analysis of Maximum Likelihood Estimates Table							
Parameter	**Factor Level**	**DF**	**Estimate**	**Standard Error**	**Wald Chi-Square**	***P*-value**	**Exp(Est)**
Intercept		1	2.48	0.24	104.80	<.0001	11.98
Sun Position	High Behind	1	0.08	0.65	0.02	0.90	1.09
Sun Position	High Front	1	2.59	0.85	9.16	0.00	13.27
Sun Position	Low Behind	1	-1.70	0.27	40.75	<.0001	0.18
Sun Position	Low Front	1	-1.89	0.27	47.56	<.0001	0.15
Sun Position	Low Side	1	-1.12	0.28	16.33	<.0001	0.33

Odds ratio estimates were computed in and provided by SAS. The odds ratio estimates for all sun position factor-level comparisons are shown in Table 31. Results showed that when the sun was located in front of the vehicle, rather than on the side, and high in the sky the odds of the target sign being legible increased by a factor of 2.6. When the sun was measured as being low in the sky, the odds of legibility were significantly reduced regardless of horizontal sun orientation. Additionally, when the sun was located behind the experimental vehicle and high in the sky, the

odds of being legible were reduced by a factor of 0.08, compared to the reference level (side and high). Sun position high and behind the vehicle had the lowest amount of available data, and the Walden confidence limits included 1, indicating no significant difference in odds.

Table 31. Odds ratio estimates comparing the side condition to behind and front.

Odds Ratio Estimates				
Effect	**Reference**	**Point Estimate**	**95% Wald Confidence Limits**	
High Behind	High Side	0.14	0.02	1.05
High Front	High Side	1.73	0.16	19.24
Low Behind	High Side	0.02	0.01	0.10
Low Front	High Side	0.02	0.01	0.08
Low Side	High Side	0.04	0.01	0.18

SAS also provided a classification percentage estimate of target sign characters being legible for each factor level of sun position. Figure 42 gives the average estimated probability to be classified as legible for each of the sun position factor levels. Sign characters captured while the sun was high in the sky were found to have a very high chance of being legible, regardless of the orientation of the sun. In contrast, when the sun was low in the sky, the probability of being found legible was significantly lower for all sun orientations. While the sun was located behind or in front of the vehicle and low in the sky, the probability of being legible was reduced to 68.70% and 64.44%, respectively. Odds ratios suggested a significant reduction in the odds of being found legible for all low-in-the-sky sun positions, and this notion is supported by the classification percentage data.

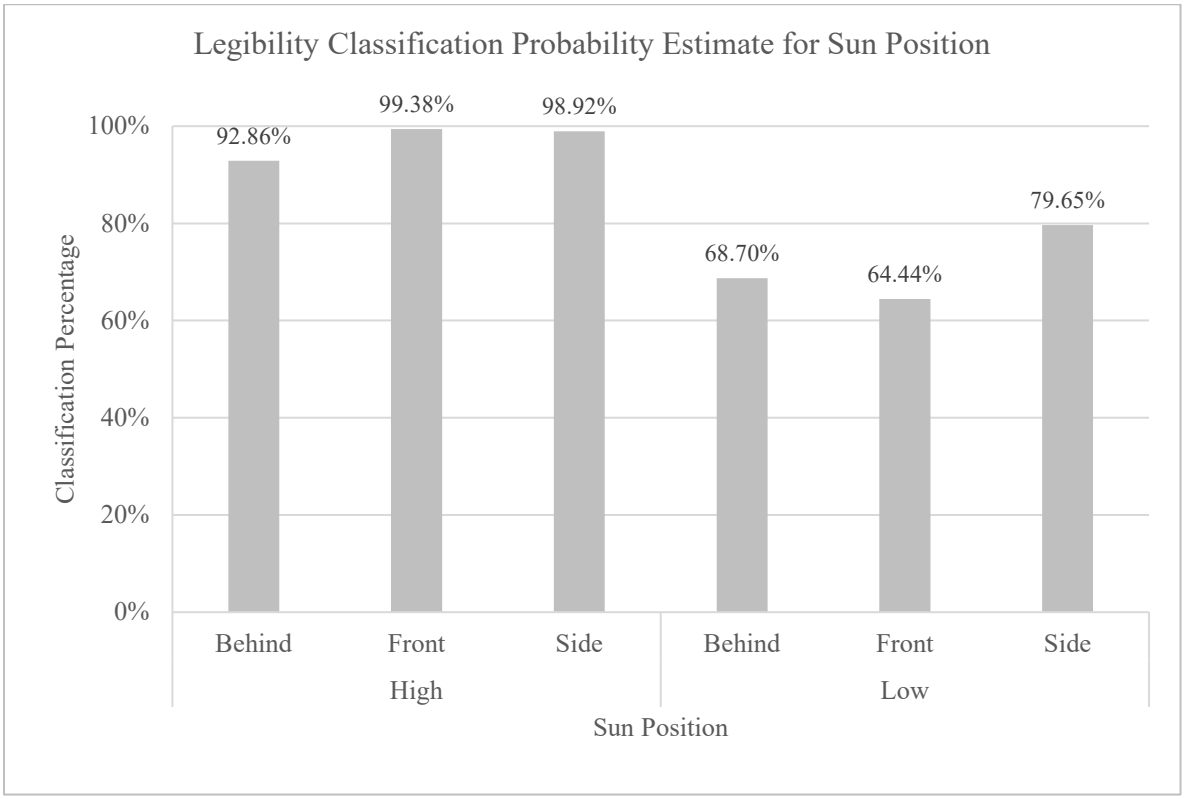

Figure 42. Graph. Classification probability of being legible by sun position.

In addition to the legibility odds analysis, the research team also conducted a mean legibility score analysis of sun position. Linear regression modeling was used to evaluate the effect of sun position and font size on the legibility of sign characters. The model contained sun position and font size (category) as main effects and included the interaction between them. The response variable for this analysis was legibility score. The overall chi-square goodness of fit testing results are shown in Table 32. *P*-values ≤ 0.05 indicate that significant difference in mean legibility was found between at least one pair factor levels.

Table 32. Linear regression modeling results for legibility score using sun position and font size by time of day.

Type 3 Tests of Fixed Effects				
Effect	**Num DF**	**Den DF**	***F*-value**	***P*-value**
Font Size (FS)	2	1239	2.5	0.08
Sun Position (SP)	5	1239	59.16	<.0001
FS*SP	10	1239	0.32	0.98

For both models the null hypothesis tested was *"Mean legibility score is equal for all font size and sun position variable level combinations."* Rejection of the null hypothesis indicated a statistically significant difference in mean legibility score between at least two factor levels. The chi-square goodness of fit test found the main effect of sun position to be statistically significant. Font size (categorical) and the interaction between font size and sun position were not statistically significant. Post hoc analyses focused on the significant differences in legibility score between sun positions. To account for multiple comparisons, *p*-value adjustments were done using Tukey's method to keep the familywise error rate at 0.05.

Pairwise comparisons revealed no significant difference in mean legibility score between any of the positions when the sun was high in the sky (Figure 43). Whenever the sun was high in the sky and behind (4.78), in front (4.85), or on the side (4.82), legibility score was judged as easy to read. Positions where the sun was low in the sky were all rated significantly lower for mean legibility score compared to high-in-the-sky positions. When the sun was low in the sky and positioned in front (3.29) of the vehicle, mean legibility increased by 21% and 19% compared to behind (2.73) and side positions (2.77), respectively. Overall, during the day, when the sun was high in the sky, researchers would expect a high rate of legibility for all of the sign characters captured with similar camera technology, regardless of horizontal sun position. When the sun was low in the sky, researchers would expect lower rates of legibility.

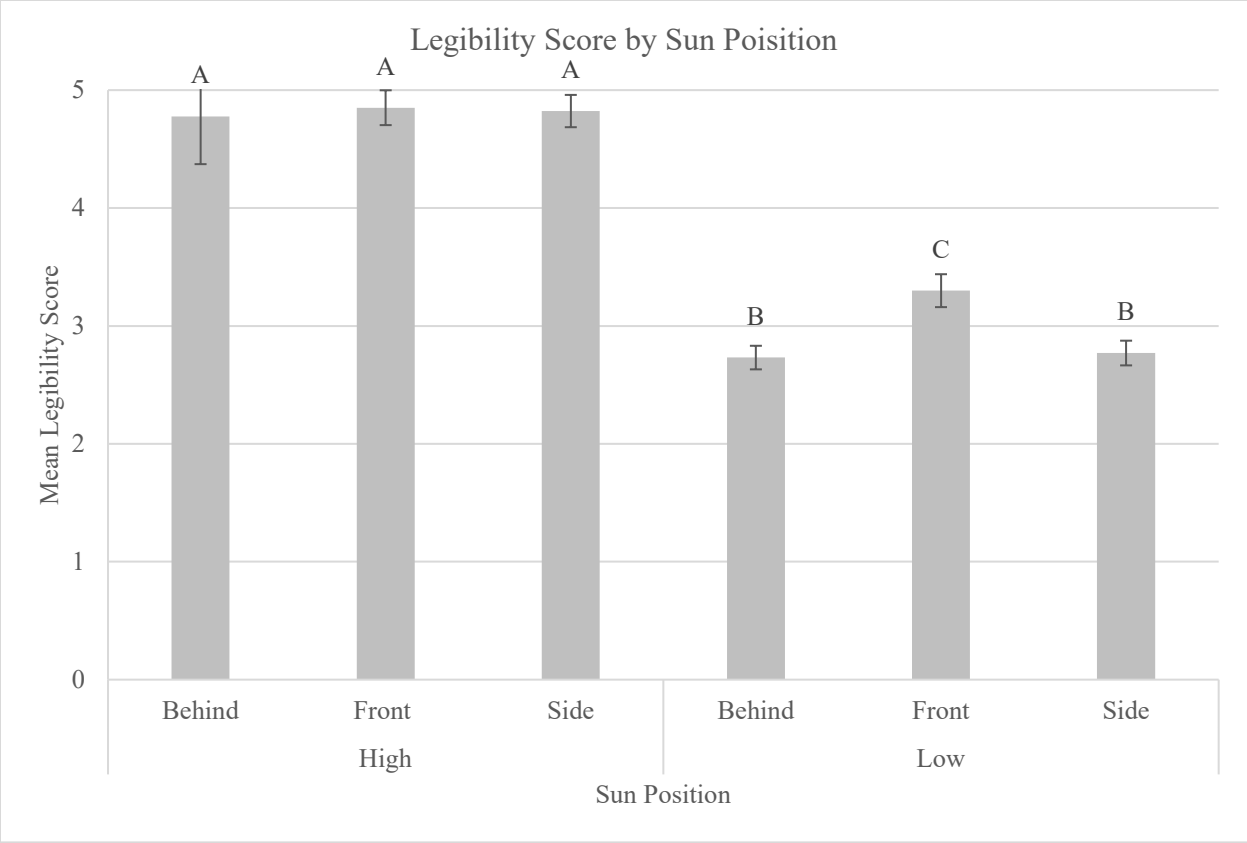

Figure 43. Graph. Legibility score by sun position and font size. Error bars denote standard error. Difference in capital letters indicates post hoc significance.

ILLUMINATION

To address the question *"does the probability of being legible change as ambient light levels change,"* logistic regression modeling was used to estimate the likelihood of sign characters being legible when taking into consideration environmental light level. All statistical modeling was done in SAS, and the results are reported in terms of odds ratios and the probability of being legible. The sample size for the data set included 1,257 sign legibility measurements.

A logistic regression model was fit using the main effect of illumination level (night, overcast, sunny, and very sunny) for all font sizes. The chi-square goodness of fit testing resulted in *p*-values smaller than 0.001 for all font sizes, as shown in Table 33, which indicated significant difference in legibility odds between at least two illumination categories for all of the font sizes.

Post hoc analyses assessed the influence that changing the levels of illumination had on the odds of sign characters being legible. The research team did not manipulate or influence the lighting conditions; rather they were all naturally encountered on data collection trips. The reference level for illumination was chosen to be the sunny level for comparisons.

Table 33. Type 3 analysis of effects for legibility by font size and illumination.

Type 3 Analysis of Effects				
Font Size	**Effect**	**DF**	**Wald Chi-Square**	***p*-value**
Large	Illumination Category	3	60.29	<.0001
Medium	Illumination Category	3	100.93	<.0001
Small	Illumination Category	3	123.90	<.0001

Table 34 presents the maximum likelihood estimates and model parameter estimates. Across all font sizes, the sign images captured at night or on overcast days were found to significantly decrease the odds of sign characters being found legible when compared to signs captured on sunny days. In contrast, the very sunny condition was found to increase the odds of sign character legibility at all font sizes.

Table 34. Analysis of maximum likelihood estimates for font size using sunny as the reference level.

Analysis of Maximum Likelihood Estimates							
Font Size	**Parameter**	**DF**	**Estimate**	**Standard Error**	**Wald Chi-Square**	***P*-value**	**Exp(Est)**
Large	Intercept	1	1.79	0.29	37.09	<.0001	5.98
	Night	1	-2.55	0.33	58.56	<.0001	0.08
	Overcast	1	-0.83	0.36	5.24	0.02	0.44
	Very Sunny	1	3.38	0.77	19.35	<.0001	29.25
Medium	Intercept	1	1.48	0.24	36.88	<.0001	4.40
	Night	1	-3.12	0.31	100.20	<.0001	0.04
	Overcast	1	-0.79	0.33	5.68	0.02	0.45
	Very Sunny	1	2.99	0.56	28.61	<.0001	19.88
Small	Intercept	1	0.48	0.11	18.81	<.0001	1.62
	Night	1	-1.72	0.20	77.31	<.0001	0.18
	Overcast	1	-0.41	0.19	4.80	0.03	0.66
	Very Sunny	1	1.89	0.20	86.82	<.0001	6.61

Odds ratio estimates were computed in and provided by SAS. The odds ratios for all illumination levels for all three front sizes are summarized in Table 35. Odds ratio confidence limits that do not contain 1 are significant at a 5% significance level, and all odds ratio results showed significant influence on the odds of being found legible. Sign characters viewed on very sunny trips were found to increase the legibility odds of sign characters, when compared to sunny days, by a factor of 29.2, 7.95, and 5.2 for large, medium, and small characters, respectively. Conversely sign characters viewed at night were found to reduce the odds of legibility by a factor of 0.08 (large), 0.02 (medium), and 0.14 (small), and characters viewed on overcast days reduced the odds of legibility by a factor of 0.52 (large), 0.18 (medium), and 0.43 (large). Overall, odds ratio estimates showed that, as the illumination level increased, the odds of sign characters being found legible increased significantly.

Table 35. Odds ratio estimates for all font size and illumination comparisons.

Odds Ratio Estimates				
Font Size	**Illumination Comparison**	**Point Estimate**	**95% Wald Confidence Limits**	
Large	Night vs Sunny	0.08	0.03	0.22
	Overcast vs Sunny	0.43	0.14	1.33
	Very Sunny vs Sunny	29.15	3.29	258.15
Medium	Night vs Sunny	0.02	0.01	0.06
	Overcast vs Sunny	0.18	0.06	0.60
	Very Sunny vs Sunny	7.95	1.41	44.84
Small	Night vs Sunny	0.14	0.08	0.26
	Overcast vs Sunny	0.52	0.29	0.93
	Very Sunny vs Sunny	5.20	2.81	9.63

SAS also provided the classification percentage estimate of being legible for all factor-level combinations of font size and illumination. Figure 44 gives the average probability of being found legible for each of the font size and illumination category combinations. Sign characters viewed on very sunny days were estimated to be legible over 90% of the time regardless of font size, with large and medium characters expected to be legible 99 out of 100 times. Conversely, across all font sizes, sign characters viewed at night were expected to be legible at a low rate for large (31.9%), medium (16.33%), and small (22.5%) font sizes. Overall, sign characters viewed at night were estimated to be legible at a significantly lower rate than any of the daytime conditions across all font sizes.

Logistic regression modeling results indicated that the odds of being legible decreased as illumination level was reduced, and this notion is supported by the legibility classification data (Figure 44), which showed increasing probability of being found legible for all three of the font size categories. In general, a reduction in font size and illumination level had negative impacts on the odds of sign characters being legible. However, small characters on sunny and overcast days saw noticeably larger decreases in legibility when compared to medium- and large-size letters. In addition, at night both the medium and small letters were found legible at a significantly lower rate than large letters.

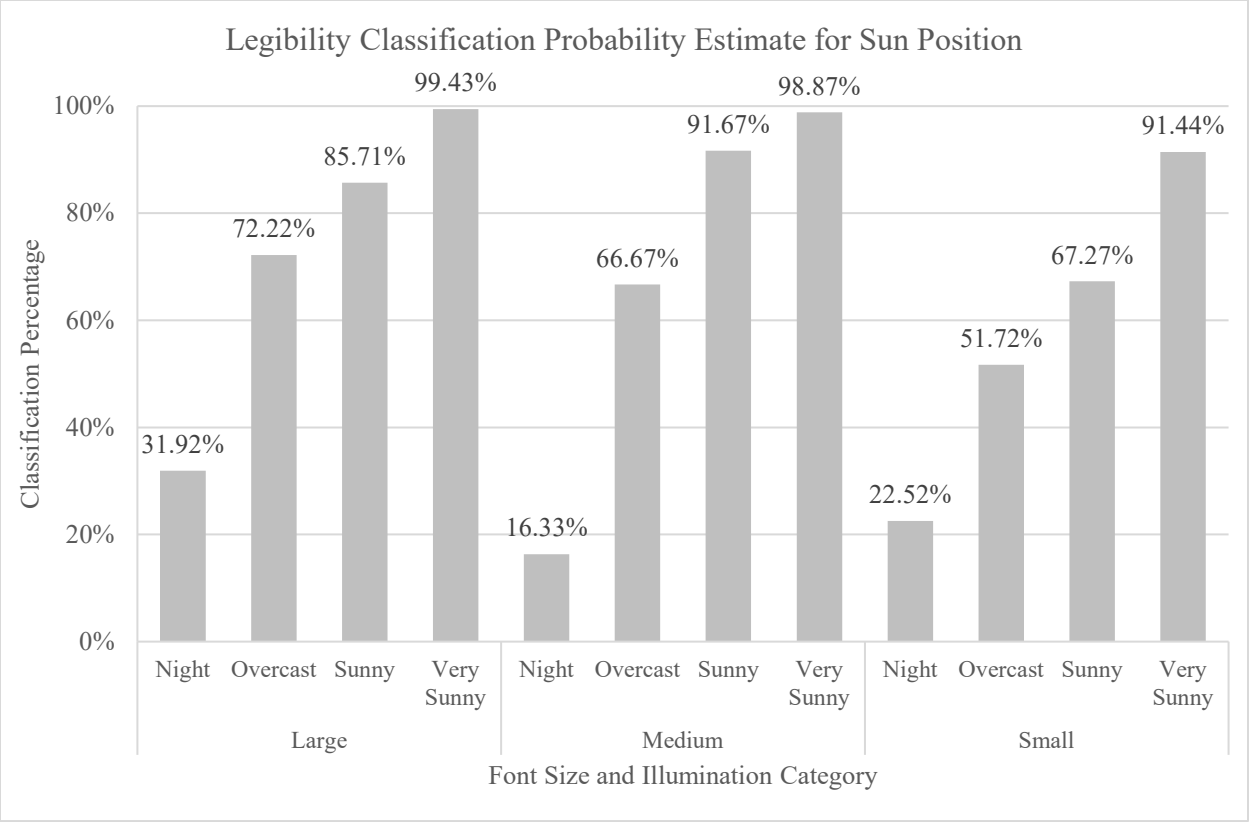

Figure 44. Graph. Probability of legibility by font size for all illumination factor levels.

To supplement the legibility odds analysis, linear regression modeling was used to evaluate the influence of sun position and font size on the legibility of sign characters. The model contained sun position and font size (category) as main effects and included the interaction between them. The response variable for this analysis was legibility score. The overall chi-square goodness of fit testing results are shown in Table 36. *P*-values ≤ 0.05 indicated a significant difference in mean legibility was found between at least one pair factor levels.

For both models the null hypothesis tested was *"Mean legibility score is equal for all font size and illumination category variable level combinations."* Rejection of the null hypothesis indicated a statistically significant difference in mean legibility score between at least two factor levels. The chi-square goodness of fit test found the main effect of sun position to be statistically significant, while font size (categorical) and the interaction between font size and sun position were not significant. Post hoc analyses focused on the significant differences in legibility score between sun position and font size factor interaction factor levels. To account for multiple comparisons, *p*-value adjustments were done using Tukey's method to keep the familywise error rate at 0.05.

Table 36. Linear regression modeling results for legibility score using illumination category and font size by time of day.

Type 3 Tests of Fixed Effects				
Effect	**Num DF**	**Den DF**	***F*-value**	***P*-value**
Font Size (FS)	2	1245	18.85	<.0001
Illumination Category (IC)	3	1245	433.06	<.0001
FS*IC	6	1245	4.54	0.0001

Pairwise comparisons for all factor levels resulted in quite a few statistically significant results; however, researchers were primarily interested in the difference in mean legibility between illuminations levels at each font size. For a more targeted follow-up analysis, the research team tested for significant difference of the simple effects. Table 37 shows the significance of effect slice testing results, which assess the differences of the least-squares means within each font size category (small, medium, and large). Testing significance (*p*-value less than 0.05) indicated a difference in mean legibility score between at least two illumination levels for all font sizes. Subsequent results are presented for significant difference in mean legibility score between illumination categories by font size category.

Table 37. Tests of effect slices at all factor levels of font size (category) for the influence of sign location by time of day.

Tests of Effect Slices					
Effect	**Font Size**	**Num DF**	**Den DF**	***F*-value**	***P*-value**
Font Size * Illumination Category	Large	3	1245	120.17	<.0001
	Medium	3	1245	180.85	<.0001
	Small	3	1245	141.84	<.0001

Figure 45 visualizes the mean legibility score estimates obtained during modeling. Large characters appearing in images of signs on very sunny days (4.91) were significantly more legible than all other light levels. Mean legibility score increased by 21%, 43%, and 242% when comparing sign character legibility on very sunny days to sunny (4.05), overcast (3.43), and nighttime (1.43), respectively.

A significant difference in medium character mean legibility score was observed when comparing very sunny (4.81) and sunny (4.52) days to overcast (3.31) and night (0.69). There was no significant difference between sunny and very sunny mean legibility scores. Medium character mean legibility score increased significantly when comparing any of the daytime conditions to night; however, there was also a large increase comparing sunny days to overcast.

Small characters appearing on signage on very sunny days (4.41) were significantly more legible than on days that were sunny (3.30) or overcast (2.60), and at night (1.03). For small characters all comparisons were significantly different, with mean legibility score increasing as the illumination level increased. Small characters were rated the least legible for all daytime conditions.

Across all font sizes on very sunny days, sign characters were judged to be easy to read. The research team expects legibility to increase as the font size and illumination are increased.

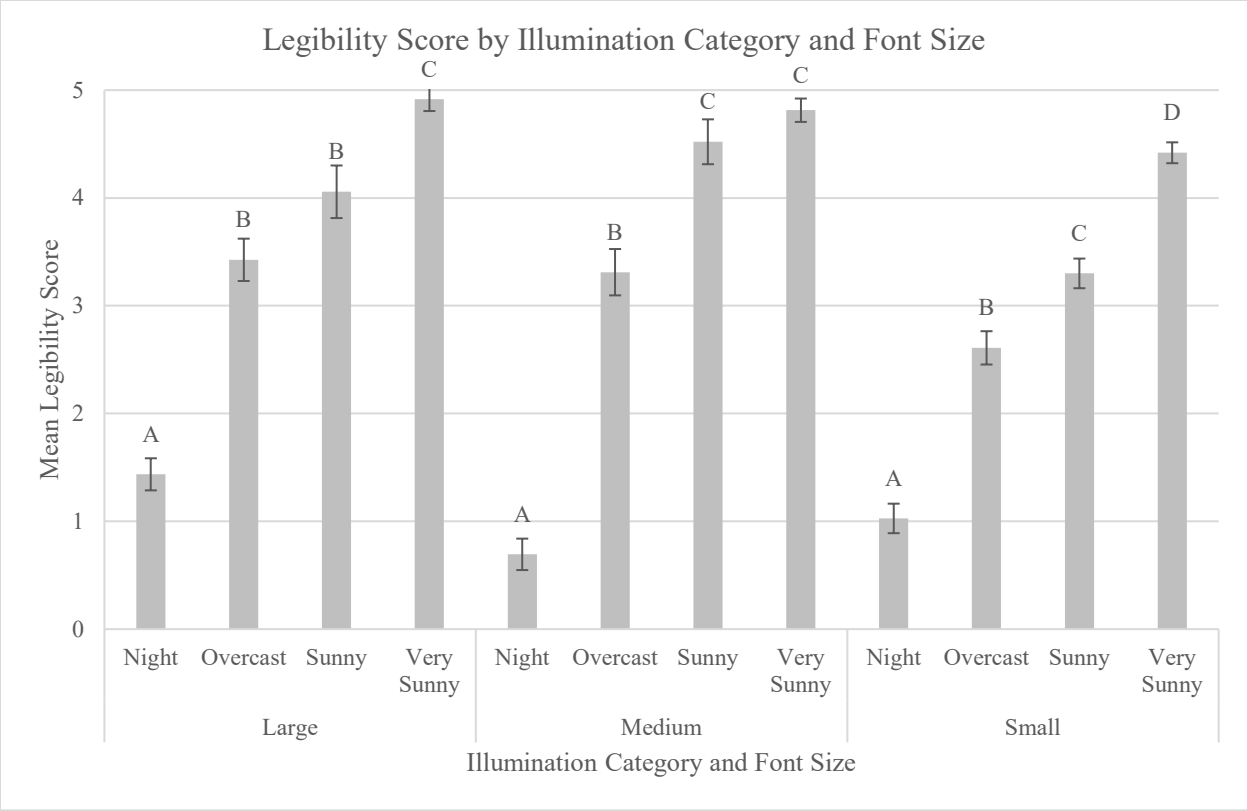

Figure 45. Graph. Legibility score by sun positions and font size. Error bars denote standard error. Difference in capital letters indicates post hoc significance.

CHAPTER 6. DISCUSSION, CONCLUSION, AND RECOMMENDATION

DISCUSSION

Location

Roadway sign location was studied at two levels (roadside, overhead) in this research. Overall, characters on overhead signage during the daytime were scored as *easy to read*, and characters on roadside signage were scored between *somewhat easy to read* and *easy to read*.

During the daytime, large and medium characters on roadside signs were scored as *easy to read*; however, small characters were scored significantly lower as *somewhat easy to read.* Small characters on roadside signage were 16% less legible than large and 15% less legible than medium characters on roadside signage, in addition to being 19% less legible than small characters on overhead signage. Viewing angle rate of change on vehicle approach is suspected to have contributed to the reduction in legibility of small characters on roadside signage. Roadside signage using at least 12-inch font sizes for all characters is expected to be significantly more legible for vehicle vision systems.

Issues with nighttime images resulted in a much smaller sample size to assess legibility, especially for roadside signage. Sign structures without illumination from headlamps or lighting infrastructure were absent from images. The nighttime images of roadside signage were rated, on average, as *illegible*. Whereas the nighttime images of overhead signage were rated as ranging from *difficult* to *easy to read*. With a more comprehensive sample of nighttime images for analysis, stronger conclusions about nighttime sign location could be made.

Results showed a significant drop in legibility for all sign characters at night, regardless of location, and indicated that sign characters smaller than 12 inches are significantly less visible on roadside signage during the day. Motion blur, picture quality, and camera angle of view all negatively impacted the legibility of nighttime images. In addition, legibility scores of sign characters located on roadside signage were negatively impacted by the low amount of headlamp light striking the signage as the experimental vehicle passed by. Due to vehicle headlamps being the primary source of sign illumination at night, the legibility scores of roadside sign characters suffered. Well-developed machine vision algorithms would be expected to identify most of the daytime sign characters regardless of sign location; however, nighttime sign characters are expected to be significantly less legible, especially for roadside signage. Employing camera technologies more advanced than those available to the research team would also help to improve small font size and nighttime sign character legibility.

View Distance

View distance was studied at three levels: 500 ft, 400 ft, and 200 ft, which correspond to travel times of approximately 5 s, 4 s, and 2 s, respectively, at highway speeds (65 mph).

Independent of view distance, during the daytime sign characters were scored as legible and *easy to read* from all distances. Although daytime sign character legibility was consistently good as distance increased, the research team expects that there is a point where legibility will decline during the day. However, that inflection point did not occur at distances shorter than 500 ft. For

nighttime images, independent of font size, legibility increased with view distance, which can be attributed to the retroreflectivity of the signage. Researchers noted that at night all sign characters were scored, on average, as illegible regardless of view distance.

For sign characters appearing in daytime images, from 500 ft, large-size characters were significantly more legible than medium (27%) and small (23%) characters. The same pattern was true from 400 ft, where large- (10%) and medium-size (14%) characters were significantly more legible than small font characters. Similarly, at night, large sign characters were significantly more legible than medium and small sign characters; however, nighttime legibility was scored, on average, below 2 for all font size and view distance combinations and was generally not legible. The sample size of nighttime images from 200 ft and 400 ft with visible sign characters was small, and not well represented in the data set.

Overall, daytime sign character legibility was scored *as easy to read* at all view distances. Large and medium font characters did not experience a drop off in legibility as view distance increased; however, small characters saw a steady decrease in legibility as view distance increased. In general, sign characters were legible during the day at all three experimental distances (200, 400, and 500 ft), with small characters becoming less legible as view distance increased.

Using similar camera technology, the research team expects well-developed machine vision algorithms to read most daytime characters up to 500 ft, independent of character size. However, nighttime sign characters are expected to have a much lower rate of legibility. Well-developed machine vision algorithms would not be expected to recognize many, or any, sign characters viewed during the night, from 400 ft and 500 ft.

Nighttime sign characters increased in legibility with view distance, which was not in line with expectations. Researchers suspect that, from longer distances, the angle of approach was such that experimental vehicle headlamps were able to illuminate the signage while they were still in the camera's field of view. Pictures taken from 500 ft were captured from a "head-on" angle while the signage was more illuminated, which positively contributed to legibility. In contrast, motion blur, angle of capture, and the optics of retroreflectivity all detracted from sign character legibility in images captured from 400 and 200 ft. The research team notes that retroreflective material on signage is designed to reflect light directly back at its source, which in this case would be the experimental vehicle's headlamps. Therefore, the legibility of sign characters may be negatively impacted by using a camera which is not directed along the line of illumination.

Color

Sign color scheme was studied at five levels: blue, green, and brown backgrounds with white legends in addition to yellow and white backgrounds with black legend text. Only one sign structure had signage with a black background and white legend text, and this condition was excluded due to low sample size. Analysis only considered sign color, font size, and time of day factor level combinations that had a sample size of eight or more, which excluded 43 legibility ratings. Daytime sign images contained five color schemes, and nighttime sign images contained two color schemes.

For daytime images, sign characters on a blue background with a white legend were found to be 8% more legible than any other color scheme, while yellow signage using a black legend was significantly less legible than all other color schemes. Yellow signage with a black legend appeared on the side of the road at a high rate (96%) and was typically found on advisory signage alerting drivers to changes in speed limit, roadway conditions, and lane use changes. These types of signage used only small and medium characters, which may have contributed to the significantly lower legibility rating. Independent of font size, daytime mean legibility was judged as *easy to read* for all color schemes except for yellow background with black legend (*somewhat easy to read*).

Three color schemes experienced a notable decrease in legibility as font size decreased; however, sign characters on brown and green signage with white legend text were not found to have a drop-off in daytime legibility. Additionally, brown signs with white characters were found to be the most legible from the farthest distance studied (500 ft). Results suggest that signage with a high number of units of information will be most legible using green or brown background color and a white legend color; however, brown background signage has restricted use and is only found in Virginia on supplemental guide signs used to indicate recreational, historical, or cultural landmarks. Large and medium characters on blue signage with white legend were rated as the most legible; however, legibility was reduced for small characters, which may be due to the lower contrast that the blue background color had with the blue daytime sky.

For daytime sign images, the research team would expect a well-developed machine vision algorithm to identify most, if not all, sign characters for all color schemes except for yellow background and black legend, independent of font size. For the yellow and black color scheme, a well-developed machine vision algorithm would be expected to identify sign characters at a decreased rate compared to other sign color schemes. No significant difference in mean legibility score was found between any sign color schemes for any font size at night. Moreover, all nighttime sign character mean legibility scores would be classified as illegible or difficult to read. At night, researchers expect very few or none of the characters to be readable by machine vision algorithms when using similar camera technology.

Font Size

Font size was evaluated for the individual character font sizes (8, 10, 12, 13, 15, 16, and 18 inches) and also the sizes grouped as categories (small, medium, and large), with results showing significant difference in legibility rating during the day but no significant difference at night.

Daytime legibility by font size varied, on average, between *somewhat easy to read* and *very easy to read*. The research team expects a well-developed machine vision algorithm to recognize the majority of 8- and 10-inch characters, and most, if not all, characters of font size 12 inches or larger. Overall, increasing the font size is expected to correspond with an increase in accuracy of vehicle vision systems; however, this benefit appears to plateau around 12 inches. Legibility was similar for all sign characters 12 inches or larger, suggesting that using a 12-inch font size would be sufficient for daytime sign legibility, and that other considerations can be made on when to increase font sizes beyond 12 inches.

Nighttime legibility by font size, on average, varied between being not readable and difficult to read. Characters were difficult to decipher and often could not be identified by machine vision algorithms or human data reductionists. Overall, sign characters in nighttime images would be categorized as illegible. Well-developed machine vision algorithms would not be expected to recognize any characters on signage at night with images captured using similar camera technologies. The research team notes that night images suffered from blurriness, glare, and insufficient lighting. Pictures were frequently very dark at night and, in the absence of illumination from headlamps, the target signs were frequently missing from the images. As a result, nighttime mean legibility scores were significantly lower than daytime ones for every font size.

The lack of significant difference in legibility between sign character sizes at night was in conflict with what the research team expected. Future research efforts would be expected to show differences in nighttime legibility based on font size, especially at large distances. Insufficient nighttime data prevented this research effort from drawing strong conclusions about nighttime sign character legibility. However, the research team can conclude that better image capture technologies would be needed to produce images that would reasonably be expected to be identified by vehicle vision systems. The REIMS used in this research performed well during the daytime for all font sizes.

Sun Position

Sun position was evaluated for the combined influence of the location of the sun's vertical and horizontal positions, relative to the direction of travel of the experimental vehicle. The research team assessed sun position for its influence on the odds of sign characters being legible and on the mean legibility score of sign characters. Both analyses were in agreement: when the sun was positioned high in the sky, independent of horizontal position, legibility improved compared to when the sun was low in the sky.

Sign characters had the greatest probability of being legible when the sun was located on the side of the vehicle. When the sun was located behind or in front of the experimental vehicle and low in the sky, the probability of being legible and mean legibility rating decreased. Sign characters when the sun was high in the sky were judged, on average, to be *very easy to read* regardless of the horizontal position of the sun. When the sun was low in the sky, mean legibility was lowest when the sun was behind or on the side of the experimental vehicle. Mean legibility significantly decreased for all sun positions when the sun was low in the sky.

Overall, when the sun was high in the sky legibility increased. Analysis results showed that the sun being behind the vehicle and low in the sky decreased legibility odds. When the sun was low and behind the experimental vehicle, its light may have been interacting with the sign surface, causing increased glare or inconsistent illumination. While the sun was low in the sky and in front the vehicle, its light was shining directly into the camera equipment and causing windshield glare, which may have contributed to the lower odds of legibility. Overall, changing the sun's position relative to the direction of travel influenced the odds of sign characters being legible.

Illumination

Naturalistic illumination level was captured during data collection using the VTTI-developed REIMS. Continuous illuminance measurements, in lux, were categorized into four factor levels; very sunny, sunny, overcast, or nighttime. Modeling indicated the odds of being legible had a positive relationship with illumination level. Across all font sizes, the probability of being found legible increased as daytime light levels increased. Nighttime illumination levels were significantly lower than daytime, and sign characters viewed at night were found to be legible at a significantly lower rate than any of the daytime conditions across all font sizes.

Probability estimates indicated that changes in illumination were having a similar influence on legibility, independent of font size, for all levels except for on sunny days. Compared to lower illumination levels, on sunny days the difference in legibility between medium and small characters was increased, suggesting a legibility plateau may exist. Increases of font size beyond 12 inches on sunny or very sunny days were not found to significantly increase legibility. In general, reducing font size and illumination level had a negative impact on the odds of sign characters being legible; however, small- and medium-sized characters on overcast days saw markedly large decreases in legibility when compared to sunny days. As character size decreased, the influence of illumination on legibility was amplified. Increasing font size in areas frequently impacted by lower illumination levels will give the best chance for sign characters to be found legible by well-developed machine vision algorithms.

Overall, the odds and mean legibility of sign characters significantly decreased at night. At night, legibility score was found to be similar for medium and small font sizes; however, sign characters with a large font size did show a significant increase in legibility. Vehicle vision systems are expected to struggle to identify sign characters in images captured by similar camera technology at night illumination levels. Poorly lit or low-light environments should consider using at least a 15-inch font size to increase the odds of legibility for vehicle vision systems.

On very sunny days, for all font sizes, sign characters were judged to be *easy to read*. The research team expects that, on very sunny days, well-developed machine vision algorithms would identify nearly all, if not all, sign characters captured with similar camera technology. Similarly, well-developed machine vision algorithms would be expected to identify most, if not all, of the medium and large font size characters on sunny days, but smaller characters at a lower rate. On overcast days, the research team would expect a well-developed machine vision algorithm to identify a majority of medium and large sign characters but struggle with identifying small sign characters. The research team surmised that on overcast days and at night the illuminance levels may not provide enough visual information for vehicle vision systems to identify sign characters at high levels of certainty.

LIMITATIONS & GAPS IN RESEARCH

Several areas were intended to be looked at during analysis with the experimental data but there was not robust enough information to perform a meaningful analysis. These variables are discussed briefly below in the limitations and gaps in the research section.

Temperature and Humidity

Temperature and humidity were captured during data collection, as summarized in Chapter 4, and visualized to assess any effects of clustering on legibility score; essentially, was there any influence of temperature and humidity together on legibility score. Graphical analyses did not show any clustering effect when considering temperature, humidity, and legibility score. In practice, the temperature and humidity were consistent across trips as the experimental vehicle only drove for brief periods during dusk and dawn. Furthermore, the research team lacked a reliable way to tell if the sign surface was impacted by condensation or distortions due to the temperature and humidity. Therefore, these variables were summarized but not used as factors in the analysis.

Visibility

Visibility was captured by the VTTI REIMS data collection system and processed to isolate the conditions at each sign location as the experimental vehicle passed. Modeling efforts did not produce usable results due to low replication. Results indicated that not enough data were collected in hazy or foggy conditions to compare legibility against those collected on clear days. The data collection team self-reported that hazy or foggy conditions were not encountered near any of the sign structures. Planning data collection efforts to occur during periods of haze or fog would result in a more robust data set.

CONCLUSIONS

- Blue and brown signage with white legend text, which commonly appear on supplemental guide signage, provided the best chance of sign character legibility during the daytime. These color schemes have restricted use cases, and consideration should be given to moving vehicle vision system information onto signage with dark background and white legend text, especially for small letters.
- Sign characters were easy to read during the day at all three experimental distances (200, 400, and 500 ft), with small characters becoming less legible as view distance increased. Nighttime data suggested that increasing font size would help vehicle vision systems identify sign characters at 500 ft.
- Daytime legibility did decrease as light levels decreased. On sunny or very sunny days, sign characters appeared universally easy to read; however, once the illumination level became overcast, legibility issues with sign images arose. Sign images captured at nighttime illumination levels had very poor legibility results. Vehicle vision systems will struggle to read sign images present in areas with low illumination levels or at night, using similar camera technologies.
- Font size increases correspond to an increase in legibility rating and the odds of being legible. Daytime legibility plateaus around a 12-inch letter size, and font sizes beyond 12-inches were found to offer no improvement in the expected legibility of sign characters for vehicle vision systems.
- Sign characters on overhead signage were found to be more legible and are expected to be identified at a higher rate by vehicle vision systems. Systems not designed for

high-speed image capture will struggle to read roadside signage at highway speeds. In addition, overhead signage may suffer from less dynamic visual obstruction, as only very tall vehicles would obscure them but heavy traffic flow was found to frequently block camera vision for roadside signage.

- Data collection efforts found that vehicle vision systems should use a high-quality camera capable of taking pictures at night without motion blur. Experimental images suffered from unexpected quality issues that impacted nighttime legibility assessments. Systems only earmarked for daytime sign character recognition would perform well with similar camera technologies used in this report.

RECOMMENDATIONS

- Conduct controlled testing using a variety of capable and established machine vision tools to assess the visibility needs of roadway signage. Studying the most common sign locations and types would help to standardize lighting practice for automated vehicle technologies.
- Subsequent research should consider the stroke width of the sign characters in addition to the font size.
- Sign image quality was limited by the image capturing technologies used in the data collection. Future data collection efforts should look to employ a high-sensitivity camera that allows for high shutter speed images and performs at low lighting levels. Consideration should be given to vehicle speed, as this may be a limiting factor for shutter speed. In addition, cameras must be able to capture the full range of sign locations, whether vertically or horizontally offset.
- Future research should look to assess the influence of weather conditions. This effort was limited by the naturalistic approach of the study and did not encounter much inclement weather. Additionally, further investigations should consider conditions where dew and condensation are evident on the sign surface.
- Future research efforts should look to study the influence of sun position under more controlled conditions. Sun position analyses were limited by the naturalistic approach of this study. Additional research should look to identify problematic sun positions and consider if lighting design needs should adapt.
- Future research should evaluate sign lighting needs for machine vision applications. This study was limited by the practical implementation of signage by the MUTCD. Consideration of alternative sign character sizes, sign locations, and color schemes could lend insight into the lighting needs of sign machine vision.

REFERENCES

1. Sivak, M. (1996). The information that drivers use: is it indeed 90% visual?. *Perception*, *25*(9), 1081-1089.

2. Federal Highway Administration. (2009). *Manual on uniform traffic control devices* (MUTCD). Washington DC: Unites States Department of Transportation (USDOT).

3. Federal Highway Administration. (2023, Nov. 16). *Standard highway signs*. http://mutcd.fhwa.dot.gov/ser-shs_millennium_eng.htm.

4. Office of Transportation Operations, Federal Highway Administration. (2018, Dec. 14). *Report on highway guide sign fonts*. https://mutcd.fhwa.dot.gov/resources/interim_approval/ia5rptcongress/index.htm.

5. Federal Highway Administration. (2020, March 20). *United States road symbol signs*. https://mutcd.fhwa.dot.gov/services/publications/fhwaop02084/index.htm.

6. ASTM. (2019, July 10). *D4956, Standard specification for retroreflective sheeting for traffic control*.

7. Montebello, D., & Schroeder, J. (2000). *Cost effectiveness of traffic sign materials* (No. MN/RC-2000-12).

8. Persaud, B. N., Lyon, C., Eccles, K., Lefler, N., & Amjadi, R. (2010). Safety evaluation of increasing retroreflectivity of STOP signs. *Accident Reconstruction Journal*, *20*(1), 47-54.

9. McGee, H. W. (2010). *Maintenance of signs and sign supports: A guide for local roads maintenance personnel* (No. FHWA-SA-09-025).

10. Khalilikhah, M., Fu, G., Heaslip, K., & Carlson, P. (2018). Analysis of in-service traffic sign visual condition: Tree-based model for mobile LiDAR and digital photolog data. *Journal of Transportation Engineering, Part A*: *Systems*, *144*(6), 04018017.

11. Khalilikhah, M., Heaslip, K., & Louisell, C. (2015, January). Analysis of the effects of coarse particulate matter (PM10) on traffic sign retroreflectivity. In *TRB 94th Annual Meeting Compendium of Papers* (pp. 11-15).

12. Khalilikhah, M., & Heaslip, K. (2016). Analysis of factors temporarily impacting traffic sign readability. *International Journal of Transportation Science and Technology*, *5*(2), 60-67.

13. Brimley, B., & Carlson, P. J. (2013). The current state of research on the long-term deterioration of traffic signs. In *Transportation Research Board 92nd Annual Meeting* (Vol. 2, No. 3).

14. American Association of State Highway and Transportation Officials. (2018, October). *Roadway lighting design guide, seventh edition*.

15. Khalilikhah, M., & Heaslip, K. (2016). The effects of damage on sign visibility: An assist in traffic sign replacement. *Journal of Traffic and Transportation Engineering*, *3*(6), 571-581.

16. Opiela, K. S., & Andersen, C. K. (2007, April). *Maintaining traffic sign retroreflectivity: Impacts on state and local agencies* (Report No. FHWA-HRT-07-042). Turner-Fairbank Highway Research Center, Federal Highway Administration.

17. Khalilikhah, M., Heaslip, K. (2016). Analysis of factors temporarily impacting traffic sign readability. *International Journal of Transportation Science and Technology, 5*, 60-67.

18. Munehiro, K., Tokunaga, R. A., Asano, M., & Hagiwara, T. (2005). Effect of time and foggy conditions on subjective visibility: Evaluation of retroreflective traffic control devices. *Transportation Research Record*, *1911*(1), 85-104.

19. Hildebrand, E. (2003). Reductions in traffic sign retroreflectivity caused by frost and dew. *Transportation Research Record: Journal of the Transportation Research Board,* (1844), 79-84.

20. National Weather Service. (n.d.) *What causes frost?*. https://www.weather.gov/arx/why_frost. Accessed 05/23/2021.

21. Haby, J. *The forecasting of dew*. Weather.gov. https://www.weather.gov/source/zhu/ZHU_Training_Page/fog_stuff/Dew_Frost/Dew_Frost.htm. Accessed 05/23/2021.

22. Hooper, K .G., & McGee, H. W. (1983). Driver perception-reaction time: Are revisions to current specification values in order? *Transportation Research Record 904*, 21-30.

23. Salvucci, D .D., & Liu, A. (2002). The time course of a lane change: Driver control and eye-movement behavior. *Transportation Research Part F, 5*, 123-132.

24. McGee, H. W. (1979). Decision sight distance for highway design and traffic control requirements. *Transportation Research Record, 736*, 11-13.

25. American Association of State Highway and Transportation Officials. (2018). *A policy on geometric design of highways and streets* (7th Edition).

26. National Highway Transportation Safety Administration. (n.d.) *Automated vehicles for safety*. https://www.nhtsa.gov/technology-innovation/automated-vehicles-safety#resources. Accessed 08/12/2020.

27. Qayyum, A., Usama, M., Qadir, J., & Al-Fuqaha, A. (2020). Securing connected & autonomous vehicles: Challenges posed by adversarial machine learning and the way forward. *IEEE Communications Surveys & Tutorials, 22*(2), 998-1026.

28. Kockelman, K. et al. (2017, March). *An assessment of autonomous vehicles: traffic impacts and infrastructure needs – Final report* (Report No. FHWA/TX-17/0-6847-1). University of Texas at Austin, March.

29. Zhou, L., & Deng, Z. (2014, October). LIDAR and vision-based real-time traffic sign detection and recognition algorithm for intelligent vehicle. In *2014 IEEE 17th International Conference on Intelligent Transportation Systems (ITSC)* (pp. 578-583). IEEE.

30. Riveiro, B., Díaz-Vilariño, L., Conde-Carnero, B., Soilán, M., & Arias, P. (2016). Automatic segmentation and shape-based classification of retro-reflective traffic signs from mobile LiDAR data. *IEEE Journal of Selected Topics in Applied Earth Observations and Remote Sensing*, *9*(1), 295-303.

31. Beyerer, J., León, F. P., & Frese, C. (2015). *Machine vision: Automated visual inspection: Theory, practice and applications*. Springer.

32. Charge-coupled Device. (n.d.). In *Wikipedia*. http://en.wikipedia.org/wiki/Charge_coupled_device#Basics_of_operation. Accessed 02/12/2021.

33. Complementary metal-oxide-semiconductor. (n.d.) In *Wikipedia.*https://en.wikipedia.org/wiki/CMOS. Accessed 02/12/2021.

34. Escalera S., Baró X., Pujol O., Vitrià J., & Radeva P. (2011). Background on traffic sign detection and recognition. In *Traffic-Sign Recognition Systems*. Springer Briefs in Computer Science. Springer, London.

35. Ritter, W., Stein, F., & Janssen, R. (1995). Traffic sign recognition using colour information. *Mathematical and Computer Modelling*, *22*(4-7), 149-161.

36. Bahlmann, C., Zhu, Y., Ramesh, V., Pellkofer, M., & Koehler, T. (2005, June). A system for traffic sign detection, tracking, and recognition using color, shape, and motion information. In *IEEE Proceedings. Intelligent Vehicles Symposium, 2005* (pp. 255-260). IEEE.

37. Shi, J. H., & Lin, H. Y. (2017, June). A vision system for traffic sign detection and recognition. In *2017 IEEE 26th International Symposium on Industrial Electronics (ISIE)* (pp. 1596-1601). IEEE.

38. Piccioli, G., De Micheli, E., Parodi, P., & Campani, M. (1996). Robust method for road sign detection and recognition. *Image and Vision Computing*, *14*(3), 209-223.

39. Zadeh, M. M., Kasvand, T., & Suen, C. Y. (1998, January). Localization and recognition of traffic signs for automated vehicle control systems. In *Intelligent Transportation Systems* (Vol. 3207, pp. 272-283). International Society for Optics and Photonics.

40. Fleyeh, H., & Davami, E. (2011). Eigen-based traffic sign recognition. *IET Intelligent Transport Systems*, *5*(3), 190-196.

41. Shustanov, A., & Yakimov, P. (2017). CNN design for real-time traffic sign recognition. *Procedia Engineering*, *201*, 718-725.

42. Ciresan, D., Meier, U., Masci, J., & Schmidhuber, J. (2012). Multi-column deep neural network for traffic sign classification. *Neural Networks*, *32*, 333-338.

43. Stallkamp, J., Schlipsing, M., Salmen, J., & Igel, C. (2012). Man vs. computer: Benchmarking machine learning algorithms for traffic sign recognition. *Neural Networks*, *32*, 323-332.

44. Mathias, M., Timofte, R., Benenson, R., & Van Gool, L. (2013, August). Traffic sign recognition—How far are we from the solution? In *The 2013 International Joint Conference on Neural Networks (IJCNN),* (pp. 1-8). IEEE.

45. Larsson, F., & Felsberg, M. (2011). Using Fourier descriptors and spatial models for traffic sign recognition**.** In *Proceedings of the 17th Scandinavian Conference on Image Analysis, SCIA 2011* (pp. 238-249).

46. Shustanov, A., & Yakimov, P. (2017). CNN design for real-time traffic sign recognition. *Procedia Engineering, 201*, 718-725.

47. Zoria, S. (2020, Jan. 7). Smart cities: A new look at the autonomous-vehicle infrastructure. *Iotforall.com*. https://www.iotforall.com/autonomous-vehicle-infrastructure/. Accessed 08/12/2020.

48. Agashe, N., & Chapman, S. (2019). Traffic signs in the evolving world of autonomous vehicles [White paper]. Avery Dennison Reflective Solution. https://reflectives.averydennison.com/content/dam/averydennison/reflective-responsive/documents/english/white-papers/traffic-signs-evolving-world-autonomous-vehicles.pdf. Accessed 08/12/2020.

49. Boateng, R. A., Zhang, X., Park, H., &. Smith, B. L. (2019, May). *Providing traffic control device information in a connected and automated vehicle environment* (Report No. VTRC 19-R19). University of Virginia.

50. Boateng, R. A., Zhang, X., Park, H., &. Smith, B. L. (2019, May). *Providing traffic control device information in a connected and automated vehicle environment* (Report No. VTRC 19-R19). University of Virginia.

51. Gibbons, R. B., Meyer, J., & Edwards, C. J. (2018, January). *Development of a mobile measurement system for roadway lighting* (Report #18-UR-062). National Surface Transportation Safety Center for Excellence, Virginia Tech Transportation Institute.

52. Konica Minolta, Inc. *Light meters*. (n.d.) https://sensing.konicaminolta.asia/wp-content/uploads/2017/08/T-10-and-T-10M-Illuminance-Meters.pdf. Accessed 05/23/2021.

53. Li, Y., Bhagavathula, R., Terry, T. N., Gibbons, R. B., & Medina, A.(2020, June). *Safety benefits and best practices for intersection lighting* (Report No. FHWA/VTRC 20-R31). Virginia Tech Transportation Institute.

54. Audio Video Supply. (2021). *Point Grey: GRAS-20S4M-C specifications*. https://www.avsupply.com/ITM/29778/GRAS-20S4M-C.html. Accessed 05/23/2021.

55. Audio Video Supply. (2021). *Point Grey: FL2G-13S2C-C specifications*. https://www.avsupply.com/ITM/29759/FL2G-13S2C-C.html. Accessed 05/23/2021.

56. Ocean Optics Inc. (2006). *HR4000 and HR4000CG-UV-NIR series high-resolution fiber optic spectrometers HR4000 / HR4000CG-UV-NIR installation and operation manual* (Document # 210-00000-000-02-1006). https://www.usna.edu/Users/physics/vanhoy/_files/SP425/LabDocs/Ocean%20Optics%202000/SpectraSuite/070131_1347%20R/documentation/Spectrometers%20and%20Software/hr4000.pdf. Accessed 05/23/2021.

57. Cleware. (n.d.). *Data-sheet USB humidity*. https://www.cleware-shop.de/WebRoot/Store17/Shops/63698188/5038/A1A2/A062/554E/6246/C0A8/2971/BBA1/USB-Humidity_EN.pdf. Accessed 05/23/2021.

58. Livox Lidar. (2020, September). *Livox Horizon user manual*, *v1.2*. https://terra-1-g.djicdn.com/65c028cd298f4669a7f0e40e50ba1131/Download/update/Livox%20Horizon%20user%20manual%20v1.2.pdf. Accessed 05/25/2021.

59. MathWorks. (2021). *Optical character recognition (OCR)*. https://www.mathworks.com/help/vision/optical-character-recognition-ocr.html?s_tid=CRUX_lftnav. Accessed 05/23/2021.

60. *Tesseract OCR.* (n.d.) Google Open Source. https://opensource.google/projects/tesseract. Accessed 05/23/2021.

61. *Tesseract Open Source OCR Engine*. (n.d.) GitHub. https://github.com/tesseract-ocr/tesseract. Accessed 05/24/2021.

62. Tesseract (Software). In *Wikipedia*. https://en.wikipedia.org/wiki/Tesseract_(software). Accessed 05/24/2021.

63. Global Monitoring Laboratory, National Oceanic and Atmospheric Administration. (n.d.) *Solar calculation details*. https://gml.noaa.gov/grad/solcalc/calcdetails.html. Accessed 05/24/2021

64. Sabatini, R. (2013, March). *New techniques for laser beam atmospheric extinction measurements from manned and unmanned aerospace vehicles*. Accessed Jul 16 2022. https://www.researchgate.net/publication/257909928_New_techniques_for_laser_beam_atmospheric_extinction_measurements_from_manned_and_unmanned_aerospace_vehicles/figures?lo=1

65. Virginia Department of Transportation. (2009). *Virginia supplement to the 2009 MUTCD – Revision 1*. https://www.virginiadot.org/business/resources/TED/final_MUTCD/2013_sup/Revision_1_Part_2_Signs.pdf

66. American Meteorological Society. (2023). Accessed 5/23/2021. https://graphical.weather.gov/definitions/defineSfcVisibility.html#:~:text=Visibility%20is%20a%20measure%20of,%2C%20a%20known%2C%20preferably%20unfocused%2C

67. Midmark. (n.d.). *Technical library - Color abbreviation chart*. https://technicallibrary.midmark.com/Global/Global-GB-00003.htm

68. Qiu, W., & Li, X-J. (2019). A novel method for predicting and mapping the occurrence of sun glare using Google Street View. *Transportation Research Part C: Emerging Technologies*, *106*, 132-144.